The influence of demographic rates on stand structure in old-growth forests

Rebecca Charlotte Banbury Morgan

University of Leeds

School of Geography

Submitted in accordance with the requirements for the degree of Doctor of Philosophy

June 2023

The candidate confirms that the work submitted is their own and that appropriate credit has been given where reference has been made to the work of others.

Acknowledgements

Completing this thesis would not have been possible without the support, encouragement, and involvement of a great many people.

First, I would like to thank my supervisor, Tim, whose enthusiasm for the project kept me motivated throughout. Tim - thankyou for your support and kindness in helping me navigate this process, for sharing your expertise and helping me become a better scientist, and for always being ready to get excited about cool-looking figures.

I was lucky to work with Roel Brienen and Manuel Gloor in developing Chapters 3 and 4. I am very grateful for the ideas and knowledge they both shared with me, and their willingness to have endless meetings discussing the finer details of the modelling framework. I have so much enjoyed working with you both!

Thankyou also to Oliver Phillips and David Galbraith, whose input never failed to improve my work and offer a different perspective on my findings. It has been a privilege to work with so many brilliant people and to benefit from such a range of advice, ideas, and support.

My thesis is based on data collected from two forest inventory networks: the RAINFOR/ForestPlots network and the Quebec provincial forest inventory network. My research would have been completely impossible without the generous people who shared this data with me. I'm hugely grateful to the hundreds of people involved in collecting and managing the data contained in the RAINFOR network, and to everyone who gave me feedback and shared ideas on Chapters 2 and 4. Thankyou also to Louis Duchesne, who shared the forest inventory data from Quebec, and whose help has been so valuable in developing Chapter 3.

Throughout my time in Leeds I've been supported by friends both in and out of the department, who have made the journey much more fun and kept me sane and smiling. Thanks in particular to Pete, who was my first PhD pal; Andy (and Laika), for the running company and distractions from writing; and Taylor, who made me go outside and climb a lot more in the last six months of this than I otherwise would have. Biggest thanks to Sam and Seb, who helped me through some pretty rough patches last year with love, affection, and mockery, and to Annika, for her light and love. To Sam again, for being the best.

Finally, to my family, for everything. Doing a PhD during a pandemic was a strange experience, and I only really got through it thanks to you. Alice, you are sunshine, and lockdown would have sucked without you. Mum and Dad - thankyou for being there every step of the way with me, for your patience and understanding, and for teaching me the importance of occasionally sacking it all off and running away to the woods.

Abstract

Forests store significant quantities of carbon in their aboveground biomass, and represent the majority of the terrestrial carbon sink. Globally, increases in mortality rates are driving declines in this carbon sink; however projections of future changes are poorly constrained as we lack an understanding of the mechanisms of change. A better understanding of the links between demographic rates, forest stem size distributions, and aboveground biomass is needed to predict forest responses to changes in demographic rates. This thesis uses analysis of forest inventory data and a simulation modelling approach to extend our understanding of relationships between demographic rates and forest stand structure. In Chapter 2, I analyse structural variation in Amazonian forests, and show that relationships between demographic rates and stand structure vary with forest type, climate, and soils. Variation in mortality rates shapes stand structure in warm, wet forests with stable soils, but stand structure in dry and montane forests is more strongly shaped by variation in growth rates. In Chapter 3, I develop a novel individual-based simulation approach, using forest inventory and tree ring data from four bioclimatic domains in Quebec. This approach demonstrates the importance of demographic rates in determining forest structure, and provides a methodology which is applicable to many permanent sample plot networks. In Chapter 4, I apply this simulation approach to plot data from Amazonia, to analyse forest resilience to increases in mortality rates. For a given percentage increase in mortality rate, forests with lower baseline demographic rates show greater declines in basal area and longer recovery times than forests with higher baseline demographic rates. This thesis clarifies relationships between demographic rates and stand structure, and provides a novel simulation method with which to better

understand how stand structure and forest biomass may respond to changes in demographic rates.

Contents

List of Figures

List of Tables

Abbreviations

AGB - Aboveground biomass

AIC - Akaike information criterion

ANOVA - Analysis of variance

BA - Basal area

BCI - Barro Colorado Island

BS - Brazilian Shield

CO_2 - Carbon dioxide

DBH - Diameter at breast height

DGVM - Dynamic global vegetation model

EC - East-Central Amazon

ForestGEO - Forest Global Earth Observatory

GS - Guiana Shield

ha - hectare

KS - Kolmogorov-Smirnov

MAP - Mean annual precipitation

MAT - Mean annual temperature

MRNF - Ministere des Ressources Naturelles et des Forets; Ministry for Natural Resources and Forests

PC - Principal component

PCA - Principal component analysis

Q1 - 25% quantile

Q3 - 75% quantile

PSP - Permanent sample plot

RAINFOR - Red Amazónica de Inventarios Forestales; the Amazon Forest Inventory Network

SSD - Stem size distribution

WD - Wood density

Chapter 1: Introduction

Globally, forests store an estimated 861 Pg of carbon, and represent the vast majority of the terrestrial carbon sink (Pan et al., 2011). Tropical forests dominate this sink, with evidence from plot networks across the tropics identifying that the carbon sink in tropical forests is significant and long term (Phillips et al., 1998; Baker et al., 2004a; Lewis et al., 2009; Gloor et al., 2012). However, the strength of this sink, and the rate of aboveground biomass (AGB) accumulation, is decreasing (Brienen et al., 2015; Qie et al., 2017), and it is likely that the peak of the carbon sink has already passed (Hubau et al., 2020). Though extrapolation from current trends suggests that, in Amazonia, the sink may decline to zero by 2035 (Hubau et al., 2020), there is significant uncertainty in these projections, a result of poor mechanistic understanding of the observed changes (Friend et al., 2014).

Changes in forest AGB are determined by the net balance of recruitment, growth and mortality (Pan et al., 2013). Increases in growth promote accumulation of AGB, while increases in mortality drive AGB losses. Long-term studies of the Amazonian carbon sink have found that declines in the rate of AGB accumulation across Amazonian forests are associated with increasing stem mortality across the region (Brienen et al., 2015). Productivity has increased across Amazonia during the same period, but has been insufficient to offset the significant rise in mortality (Brienen et al., 2015). Linking these trends with observations of environmental change, such as increasing temperatures and more frequent droughts, has enabled researchers to generate projections of long term declines in AGB under climate change (Hubau et al., 2020).

While analyses such as these offer some insight into possible future trends in forest structure, there are significant limitations to this type of approach. Correlating

changes in environmental conditions with trends in AGB bypasses a mechanistic understanding of how these changes develop, resulting in estimates that are not constrained or contextualised by an understanding of forest dynamics and processes. For example, forest AGB is closely linked to the stand structure of the forest (Baraloto et al., 2011), and in particular the relative abundance of large stems (Lindenmayer and Laurance, 2017), which in turn is associated with stand-level growth and mortality rates (Muller-Landau et al., 2006a). These relationships are unlikely to be linear, meaning that structural responses to changes in stand structure may be challenging to predict from linear extrapolation. This suggests that an improved understanding of the links between demographic rates, stem size distributions, stand structure, and biomass, would be of great value in improving our understanding of forest responses to changes in demographic rates.

The aim of this thesis is to gain a better mechanistic understanding of the way that demographic rates structure stem size distributions in natural forests, and to explore the implications of this for future forest trajectories under global change. I focus particularly on the forests of tropical South America, using plot census data from long-term permanent sample plots from the ForestPlots network.

In Chapter 1, I review the controls on forest structure and biomass, with a focus on the relationship between demographic rates and forest structure. I use Amazonian forests as a case study to explore the complex relationships between demographic rates, stand structure, species composition, and environmental variation. In Chapter 2, I use inventory data from the ForestPlots network to explore how the stand structure of Amazonian forests is controlled by variation in demographic rates, and mediated by variation in forest type, climate, and soils. In Chapter 3, I move away from the tropics and develop an individual-based simu-

lation of forest stand structure, using tree ring and plot inventory data from an extensive sample plot network in Quebec. Finally, in Chapter 4, I apply this simulation approach to data from 19 Amazonian forests, to compare intrinsic variation in forest structural resilience to increases in mortality rates.

The first two sections of this literature review establish current knowledge regarding the components of forest structure, their co-variation with AGB in natural forests, and the demographic controls on forest structural parameters. In the third section, I consider how demographic rates are changing in forests globally, and the implications for forest carbon source-sink dynamics. In section four, I review approaches to modelling forest stand structure and explore the potential of simulation approaches to improve our understanding of forest structural responses to changes in demographic rates. In section five, I introduce Amazonian forests as a study system for exploring these research questions. In section six, I discuss the key methodological approaches employed in my analyses, and finally, in section seven, I provide an outline of the rest of the thesis.

1.1 Forest structure and aboveground biomass

Accurately predicting forest biomass responses to global change demands a detailed understanding of forest dynamics and function. Here, I first describe the components of AGB in natural forests, before considering the key processes which shape them.

Within a forest, the majority of aboveground biomass is stored in the woody stems of trees (Anderson-Teixeira et al., 2021). The biomass contained in an individual tree stem can be estimated using measurements of diameter at breast height (DBH) and tree allometry equations (Chave et al., 2014), meaning that census in-

formation on stem sizes and frequencies can offer relatively simple approximations of the biomass storage and carbon dynamics of individual forest stands (Phillips et al., 1998; Anderson-Teixeira et al., 2015). AGB is therefore well-explained by the parameters describing the physical attributes of a forest, such as basal area, stem size distributions, stem frequencies, and mean stem height (Baraloto et al., 2011; de Paula et al., 2011; Rödig et al., 2018) (Figure 1.1). Basal area in particular is strongly positively associated with AGB (Baker et al., 2004a; Muller-Landau et al., 2021), and has been found to explain up to 85% of variation in AGB across large climatic gradients (Álvarez-Dávila et al., 2017), and so can be employed as a reasonable proxy for AGB in analyses.

At an individual stem level, biomass and basal area do not scale linearly with tree DBH, and instead increase disproportionately in the largest stems (Chave et al., 2005), with one study of Panamanian forests finding that, despite having low stem densities in comparison to smaller stems, stems $\geq$ 50cm DBH account for 59% of stand AGB (Meakem et al., 2018). As a result, although large trees make up a small proportion of the total stems in a stand, their relative abundance is particularly important in determining stand AGB (Lindenmayer and Laurance, 2017): at the plot scale, the presence of large trees is strongly associated with higher stand-level AGB stocks (Nascimento and Laurance, 2004). Similarly, any loss of large trees from a stand results in a disproportionate decrease in AGB (Poorter et al., 2017). The largest trees also dominate carbon cycling dynamics, with stems $\geq$ 50cm DBH contributing 45% of woody productivity (Fauset et al., 2015; Meakem et al., 2018), meaning that stand structure is also closely related to forest function, and changes in stand structure are expected to have downstream effects on overall carbon fluxes and forest productivity.

The non-linear relationship between biomass and tree size points to the importance of considering AGB in terms of stem size distributions. Different forests could theoretically store similar quantities of AGB, but support distinct stem size distributions and frequencies, meaning that they might have different rates of AGB change under global change scenarios.

Species composition of forest stands also influences AGB, primarily through its role in shaping patterns of wood density (Figure 1.1). Wood density is an important predictor in determining AGB, both at an individual- and a stand-level (Baker et al., 2004b; Chave et al., 2005), as higher wood density values are associated with higher AGB. Wood density is an important functional trait, and correlates negatively with growth and mortality (Chave et al., 2005), such that different functional groups are associated with different wood densities. Fast-growing, early-successional species tend to have lower average wood densities (Nascimento and Laurance, 2004), while slower-growing, shade-tolerant species typically have higher wood densities (Ter Steege et al., 2006; Camac et al., 2018). Stem allometries, or the scaling relationships between stem diameter and stem height, also vary among species (Chave et al., 2005), resulting in regional variation in biomass stocks being driven in part by variation in height-diameter relationships between forest communities (Feldpausch et al., 2011). Furthermore, stem allometries and architectural properties are linked back to wood density - lower wood density is associated with higher efficiency in attaining greater stem heights (Iida et al., 2012).

Differences in species composition among forests can therefore result in significant variation in community level wood density and stand allometries, affecting AGB at the stand level and shaping regional patterns of AGB stocks (Baker

et al., 2004b). As a result, species composition may be an important mediator in the relationships between stand structure, demographic rates, and AGB: shifts in species composition as a result of environmental change have the potential to generate feedbacks to constrain or exacerbate other forest responses. For example, this is seen on forest edges, where, following fragmentation, increases in mortality rates are associated with the loss of canopy trees and shifts in species composition towards early-successional, fast-growing species (Laurance et al., 2006, 2018). This compositional shift further elevates stand demographic rates (Laurance et al., 2011), ultimately maintaining forests in an early successional state and limiting the re-establishment of large trees (Tabarelli et al., 2008).

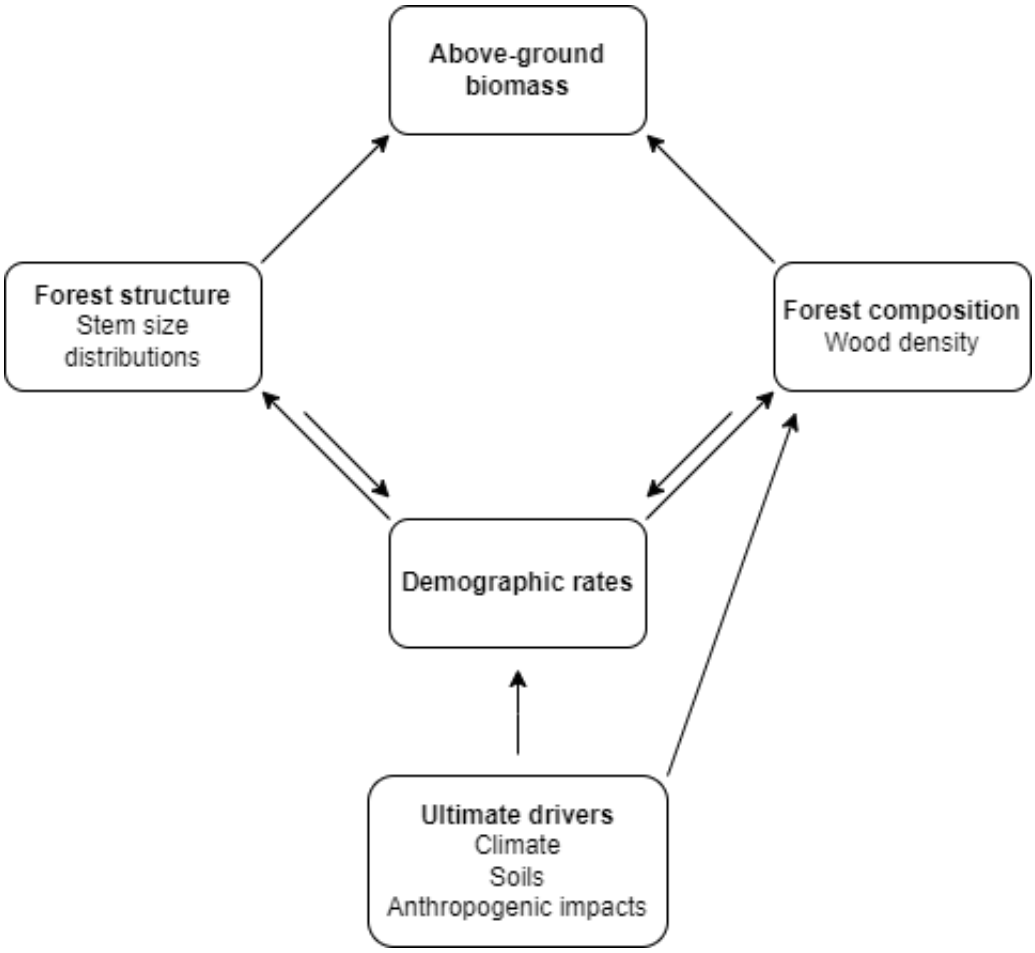

Figure 1.1: A conceptual framework illustrating the links between environmental drivers, demographic rates, forest structure, forest composition, and aboveground biomass.

1.2 Demographic controls on forest structure

In natural forests, stem numbers are typically highest in the smallest size classes and decrease with increasing size. Across large latitudinal gradients and diverse forest types, stem size distributions are observed to be highly consistent, showing a strong right skew, with a high frequency of small stems, and a long tail of larger stems. As a result, a linearly scaling relationship between frequency and stem size

was hypothesised, as predicted by metabolic scaling theory (Enquist and Niklas, 2001) (Figure 1.2).

Scaling relationships between body mass and resource use are widely observed across plants and animals. The ubiquity of these relationships in natural systems suggests that they are an important factor in shaping energy flows and population densities across ecosystems, and ultimately in structuring ecological communities (Enquist et al., 1998; Schramski et al., 2015). In forest communities, observations of consistent size distributions across forest indicated that size distributions were indeed shaped by energy flows and metabolic factors universal across forest sites, which drive consistent rates of self-thinning of stems as a result of competition for light (Enquist and Niklas, 2001). Application of metabolic scaling theory to forest ecosystems predicted that stem frequency and stem size should scale linearly, with the stem number scaling as the -2 power of stem diameter (Enquist and Niklas, 2001). However, subsequent research has shown that stem size distributions vary among forests and species (Coomes et al., 2003; Kohyama et al., 2015). Although stem size distributions tend to show a declining trend, the skewness of this relationship varies, with species showing stem size distributions ranging from exponential decline to close to unimodal (Bin et al., 2012; Lima et al., 2016). Evidence from field sites shows that metabolic scaling theory tends to over-predict the numbers of the largest and - to a lesser extent - smallest trees (Muller-Landau et al., 2006b; Farrior et al., 2016).

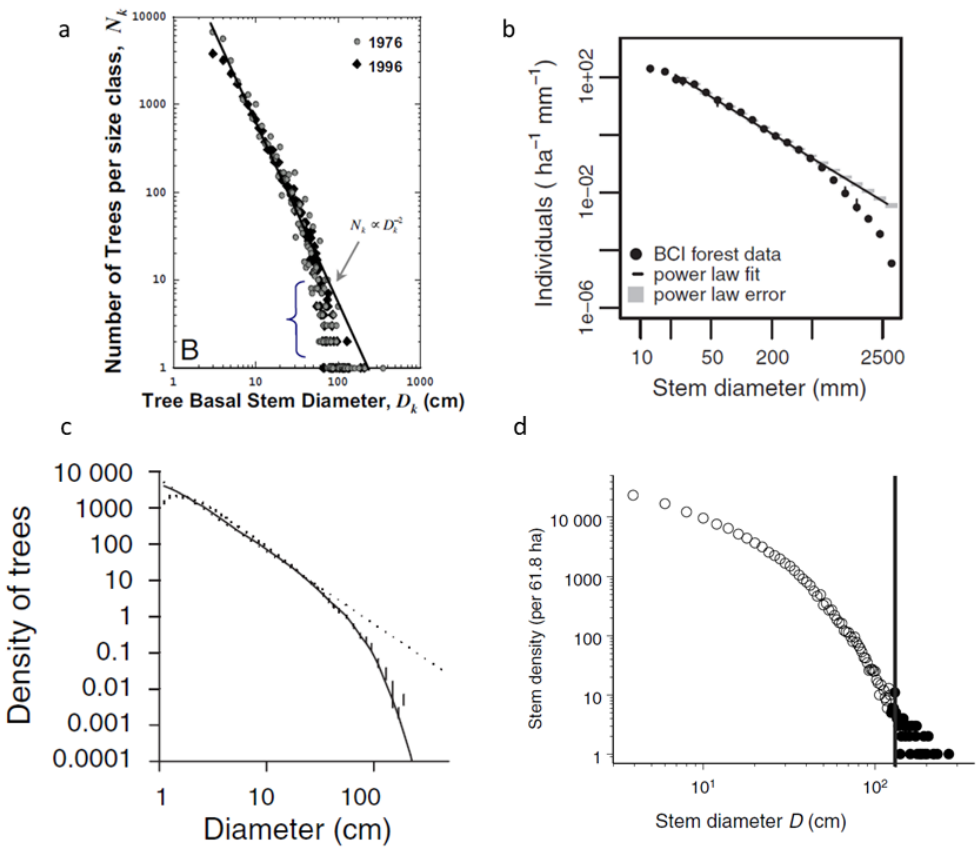

Figure 1.2: Figures to show the size distributions of stems for (a) the 16-ha tropical deciduous forest at San Emilio, Guanacaste, Costa Rica (Enquist and Niklas, 2009); (b) the 50-ha tropical forest at Barro Colorado Island, Panama (Farrior et al. 2016); (c) the 50-ha tropical forest at Pasoh Forest Reserve, Malaysia (Muller-Landau et al. 2006); and (d) pooled data for 1546 temperate forest plots in New Zealand (Coomes et al. 2003). Distributions are plotted on a log-log scale, with a line plotted to show the scaling distribution predicted by metabolic scaling theory, with the exception of plot (d). This illustrates both the consistency of stem size distributions across diverse forest types, and the consistent deviations from power-law predictions in the smallest and largest stem size classes.

The consistency with which stem size distributions deviate from the predictions of metabolic scaling theory is informative in understanding the controls on stem size distributions. Generally, stems in the mid-size classes fit closely to a power-law distribution, but deviate at the tails of the distribution (Enquist et al., 2009, Muller-Landau et al. (2006a); Farrior et al., 2016). This is most likely because

of the different factors which drive mortality at different stem sizes: competition strongly structures trees in the understorey, resulting in these stems fitting more closely to a power-law distribution (Enquist et al., 2009); however different drivers of mortality have a stronger influence over large canopy trees. External mortality drivers, such as drought stress, lightning strikes, and wind throws disproportionately affect the largest trees in a stand (Bennett et al., 2015; Gora and Esquivel-Muelbert, 2021), resulting in lower stem numbers in these size classes than is predicted by metabolic scaling theory. Furthermore, the mortality dynamics of the largest trees structure the size distributions of trees in the understorey, as the canopy gaps generated by large tree mortality control light availability in the understorey, and therefore influence recruitment and growth of the smaller size classes (Farrior et al., 2016). This implies the largest trees have important controls over the overall stand structure, and so changes in the demographic rates of these stems may have downstream effects on the size distribution of the entire stand. As a result, consideration of how mortality rates and drivers vary within stands may help to resolve the issues with metabolic scaling theory (Enquist et al., 2009).

An alternative approach to understanding controls on stem size distributions is demographic equilibrium theory (Coomes et al., 2003; Kohyama et al., 2003; Muller-Landau et al., 2006b; Kohyama et al., 2015), which suggests that size distributions are the result of the variation between and balance of growth and mortality within a stand. This is intuitive, as rates of recruitment, growth and mortality will determine how stems enter, move through, and leave the stand, shaping stem numbers and size distributions. Stem mortality rates appear to have a particularly strong influence on stand structure, with lower stem mortality rates associated with higher stand AGB (van der Sande et al., 2017; Johnson et al., 2016). Lower

mortality rates mean that stems survive longer, and so, broadly speaking, are more likely to survive to larger sizes, resulting in a higher proportion of large trees within a stand (Malhi et al., 2015). In contrast, high mortality rates reduce stem survivorship, resulting in a stand structure with a higher relative frequency of small stems.

Demographic equilibrium theory suggests an important role of size-dependency of demographic rates in shaping stand structure (Muller-Landau et al., 2006a; Kohyama et al., 2015). Typically, demographic rates are not uniform across size classes; mortality and relative growth rates are usually highest in the smallest stem size classes, and decrease with increasing stem size (Coomes et al., 2003; Rüger et al., 2011; Iida et al., 2014a; Johnson et al., 2018). Demographic rates in natural forests do not scale linearly with size (Coomes et al., 2003; Muller-Landau et al., 2006b; Coomes and Allen, 2007). Instead, demographic functions tend towards non-linearity, with individuals showing differences in demographic rates at different sizes, in response to changes in environmental and competitive pressures experienced across different size classes (Rüger et al., 2011; Anderson-Teixeira et al., 2015). This indicates that demographic rate functions are not inherent to a species, but are also determined by context; for example, small trees may show high mortality as a result of competitive suppression by larger trees, rather than as an intrinsic result of small size (Coomes et al., 2003). Demographic functions vary among species at a given site (Kohyama et al., 2015), and between sites (Muller-Landau et al., 2006a), a result of differences in environmental and climatic conditions modifying mortality and growth rates (Coomes et al., 2003; Stephenson et al., 2011; Lima et al., 2016), which will act to generate variation in stand structure among sites.

Size-dependent variation in demographic rates may also be important in shaping stand structure under environmental change. Large trees tend to have low background mortality rates in comparison to smaller individuals (Stephenson et al., 2011; Thomas et al., 2013), and so may be disproportionately vulnerable to increases in mortality rates. The relative influence of different drivers of mortality also varies across stem size: mortality in smaller trees is dominated by biotic factors, such as competition, herbivory, and disease, while mortality in larger trees is dominated by abiotic factors, including drought stress, lightning strikes, and wind throws (Bennett et al., 2015; Gora and Esquivel-Muelbert, 2021). As a result, larger trees may be more vulnerable to increases in mortality as a result of extrinsic drivers of environmental change than small trees. Because large tree frequencies exert important controls on understory stem frequencies (Farrior et al., 2016), increases in the mortality rates of canopy trees could potentially resulting in large cascading changes to stand structure.

Demographic rates also vary with life-history traits. Traits associated with shade-tolerance and longer lifespans, such as high wood density and higher seed volumes, are associated with lower growth and mortality rates (Poorter et al., 2008; Rüger et al., 2012), leading to divergence in demographic rates across functional groups (Rüger et al., 2020). Growth rates also show variation with adult stature, with species with higher maximum stem height showing higher growth rates than smaller species (Poorter et al., 2008; Rüger et al., 2012). Interestingly, these associations show size-dependency. For example, the effect of wood density appears to vary with stem size; species with low wood density show fast growth rates which decline at large stem sizes, while species with higher wood density grow slowly, but show increasing growth rates with size (Rüger et al., 2012). Similarly, the association between demographic rates and architectural traits, such as maximum

stem size, are strongest at small stem diameters and in the understorey (Iida et al., 2014b). This suggests an important effect of community composition in determining demographic rates, such that stand structure is interdependent with stand composition.

1.3 Demographic rate change in tropical forests

Global climate change is currently exposing forests worldwide to unprecedented environmental stressors, which are already driving directional changes in forest dynamics and functioning (Hubau et al., 2020). In old-growth, intact forests, which have not experienced any direct anthropogenic disturbances (e.g. timber extraction or stand clearance), the primary drivers of change are a result of increases in atmospheric CO_2, and include rising temperatures, declines in precipitation, increased frequencies of drought, and CO_2 fertilisation (Malhi et al., 2014), with the combination of drought and high temperatures being of particular significance (Allen et al., 2015; Millar and Stephenson, 2015). These drivers are altering demographic rates globally; increases in mortality rates have been recorded across a range of forest ecosystems (Van Mantgem et al., 2009; Peng et al., 2011; Allen et al., 2015), with significant implications for forest productivity, biomass stocks, and carbon sink dynamics at a global level (Millar and Stephenson, 2015).

Across a number of regions, there is increasing evidence of declines in the carbon sink capacity of intact forests (Qie et al., 2017; Hubau et al., 2020). Disentangling the demographic drivers of this is complex. Increasing frequency and severity of drought events have driven declines in forest productivity and growth rates, coupled with increases in mortality (Phillips et al., 2009; Zhao and Running, 2010; Feldpausch et al., 2016). These impacts can last for several years following

the peak of the drought (Phillips et al., 2010; Doughty et al., 2015), suggesting that frequent repeated droughts could drive directional change in forest dynamics. Declines in growth have also been linked to increases in temperature (Hubau et al., 2020), which are likely to increase tree stress and exacerbate the effects of water limitation.

The effect of CO_2 fertilisation has been theorised to counteract the negative impacts of water and heat stress, as elevated CO_2 levels increase growth rates and forest biomass (Terrer et al., 2019). There is evidence that there have been positive effects of CO_2 on productivity across large areas of forests (Hubau et al., 2020); however, the implications of this for forest structure and biomass are not straightforward. CO_2 fertilisation has been associated with a global increase in stem turnover rates in forests, as demographic rate feedbacks mean that increases in growth lead to subsequent increases in mortality rates (Yu et al., 2019; Brienen et al., 2020). This link may offset the benefits of any increase in growth or productivity, and reduce the carbon sink capacity of old-growth forests (Brienen et al., 2015, 2020; Hubau et al., 2020). There is already evidence for this from across the tropics, where increases in productivity over the past few decades have been lagged by increases in mortality, resulting in steady declines in the tropical forest carbon sink; ultimately the carbon sink of these forests is projected to decline to zero as these changes propagate through the forests (Brienen et al., 2015; Hubau et al., 2020).

The complexity of demographic rate change in response to this range of environmental drivers makes projecting forest trajectories into the future challenging. While it is relatively straightforward to extrapolate correlative associations between demographic rate change and biomass change, generating predictions based

solely on extrapolation of historic trends is of limited utility in complex systems, where there are likely to be non-linear responses and feedback effects at play. Here, an approach based on understanding the mechanisms of change - i.e. based on knowledge of how demographic rates influence stand structure and biomass - will allow greater accuracy and flexibility in predicting forest responses under a range of future change scenarios.

1.4 Approaches to simulating forest structure

While observational data are of great value for understanding current forest structure, dynamics and composition, and describing historic responses to change, there are limitations to this type of analysis. Descriptive studies of relationships between forest structure and demographic rates can help to provide insights into controls on natural forests, but without a mechanistic understanding of the relationships, these approaches are limited in their ability to extrapolate relationships to accurately predict forest structure under demographic rate change (Muller-Landau et al., 2006b). Here, simulation approaches are of great value. Models can be calibrated and validated with observational data from field studies, and then used to test theories and make predictions, allowing consideration of forest dynamics over much longer time-scales than is possible from observational studies alone.

The first models of forest dynamics were developed for forest management in order to better estimate timber yields and generate increased timber production (Shifley et al., 2017; Shugart et al., 2018). As a result, models of growth and productivity were important, and so early modelling approaches were focussed on understanding overall stand growth and stand structure (e.g. Moser and Hall,

1969; Burkhart, 1971; Bailey and Dell, 1972; Vanclay, 1989). As the availability of forest inventory data increased, so too did the complexity of models, incorporating information on recruitment and mortality, and moving away from modelling managed forestry systems to simulation of dynamics in natural old-growth forests, where structural complexity and species richness is much higher (Shifley et al., 2017). The inclusion of a wider range of demographic processes led to the development of individual-based approaches, where the growth and survival of individual trees within a stand were modelled (e.g. Newnham, 1964; Lieberman et al., 1985), and scaled up to model stand-level dynamics (Botkin et al., 2010; Pacala et al., 1993, 1996).

Many subsequent models were based on core assumptions of forest dynamics which are used to determine how the model functions, with the most common being gap formation and succession (Pacala et al., 1996; Maréchaux and Chave, 2017). Forests are assumed to consist of multiple of small patches experiencing patch clearance and succession, and individual trees within these patches are modelled, with varying degrees of complexity included (Bugmann, 2001; Shugart et al., 2018). This allows recruitment, growth, and mortality of trees to be simulated in a spatially explicit way, such that model results can be validated against observed forest stands in order to test hypotheses about controls on forest dynamics and structure (e.g. Busing, 1991; Kohyama, 1992). Increased complexity can be incorporated by including information on plant physiology and representation of processes such as photosynthetic production and resource allocation (Fauset et al., 2019).

Within these modelling approaches, there are a range of different methods to model mortality and recruitment processes. Early forestry-driven approaches

typically used "thinning" approaches, which predicted a rate at which trees were thinned through competition (Shugart et al., 2018). However, as models increased in complexity, so too did approaches to understanding demographic rates, leading to development of species-specific mortality and recruitment sub-models within the larger stand-level models (Pacala et al., 1996). Increasingly, functions were used to reflect the dependency of mortality, seed production, and recruitment on factors such as species life-history traits, previous stem growth, and stem size (Pacala et al., 1996; Maréchaux and Chave, 2017; Shugart et al., 2018). Where models are spatially explicit, the influence of light availability and stem density can be incorporated into mortality functions, and extrinsic mortality through random stand disturbances included at a constant rate (Shifley et al., 2017). Similarly, recruitment can be modelled as spatially explicit, with elevated recruitment rates occuring in response to gap-creating mortality (Bugmann, 2001).

While initially forest models were largely applied in temperate regions, individual-based modelling approaches are increasingly being developed for application to tropical forests (e.g. Chave, 1999; Fischer et al., 2016; Maréchaux and Chave, 2017). There are inherent challenges to this due to the high species diversity and structural complexity of tropical forests (Fischer et al., 2016). Despite this, models are increasingly able to accurately simulate forest dynamics, structural parameters, and biomass (Rödig et al., 2017; Rüger et al., 2020), in part due to the rapid advances in computing power which have enabled development of sophisticated modelling approaches. This has quickly established the utility of individual-based modelling approaches in developing and testing ecological theory (e.g. Kohyama, 1993; Morin et al., 2011; Farrior et al., 2016), and suggest huge potential for simulations to be used to explore potential impacts on stand structure under different types of environmental change. Already, studies have used individual-based mod-

els to project the long-term impacts of different logging strategies on forest structure and community composition (Kohler and Huth, 2004; Rüger et al., 2008). In addition, dynamic global vegetation models (DGVMs), which are widely used to simulate large-scale vegetation responses to climate change, are increasingly recognising the importance of incorporating an individual-based approach within the broader modelling framework (e.g. Moorcroft et al., 2001; Sato et al., 2007)

Individual-based models can be highly data-intensive, and often demand specific data inputs, such as data on plant functional traits (Rüger et al., 2020), resource use and competition (Chave, 1999), crown position (Farrior et al., 2016), or photosynthetic rate (Fauset et al., 2019), which may not be readily available for all sites. This can make scaling up these models across wider regions a challenge, with studies relying on extrapolation of data from a limited number of sites or broad ecological assumptions to generate summary parameters (e.g. Rödig et al., 2017). In addition, inclusion of a range of complex processes can make models less well-suited to testing how simple demographic processes affect long-term forest structure and biomass.

Simpler individual-based approaches, which are less heavily process-driven, could bypass these limitations to enable models to be applied across a wide range of sites with less reliance on parameter generalisations and assumptions. By putting a greater focus on demographic processes, this type of approach could also facilitate mechanistic analysis of the relationship between demographic rates and forest structure. One example of this is in the development of simple stochastic growth simulations, which generate simulated trajectories of individual stem growth by repeated random sampling of annual growth steps from forest inventory growth increment data (Lieberman and Lieberman, 1985; Lieberman et al., 1985). This

approach has been subsequently adapted to estimate tree ages in mixed-age and multi-species stands (Baker, 2003), and to use growth increments estimated from tree cores as input data (Brienen et al., 2006). This type of approach is simple, requires minimal data input, and uses observed growth data, and so offer a strong foundation for developing a widely-applicable individual-based model to explore links between demographic rates and forest structure.

1.5 Forests in Amazonia and Quebec

1.5.1 Describing spatial variation in Amazonian forest characteristics

The tropical forests of the Amazon Basin constitute one of the most significant areas of intact forest globally: 75% of the Brazilian Amazon is over 1km from a forest edge, compared with a global average of 30% (Haddad et al., 2015). Amazonia contributes significantly to global ecosystem production (Zhao and Running, 2010) and as a result represents a significant carbon sink (Pan et al., 2011; Phillips et al., 2017). However, the region is also undergoing rapid change, with increasing threats from drought, fire, deforestation, and rising temperatures compounding to drive significant shifts in forest composition and function (Malhi et al., 2014; Aragão et al., 2014). As a result, understanding outcomes for Amazonian forests under environmental change is of critical importance (Aragão et al., 2014). In addition to being a globally significant ecosystem, Amazonian forests are highly structurally, functionally, and compositionally diverse, making them a useful study system within which to explore links between demographic rates and stand structure.

Across the Amazon Basin, forest dynamics and structure vary in a broad east-west gradient. Forest biomass stocks and measures of stand basal area are highest

in the north-eastern Amazon (Malhi et al., 2006; Quesada et al., 2012), which is at least partially a result of higher frequencies of large, tall trees in these forests (Feldpausch et al., 2012). This is associated with a gradient in forest dynamics, with stem turnover rates lowest in the the north-east and increasing towards the south-west of the basin (Quesada et al., 2012); the reverse trend is seen in woody residence times (Galbraith et al., 2013). As such, there are negative correlations at both local and regional scales between forest dynamism (e.g. stand demographic rates and rates of turnover), and stand biomass (Johnson et al., 2016; Vilanova et al., 2018). Functional trait composition also varies across this gradient. Species with lower wood densities are more abundant in the western Amazon than in the eastern Amazon (Baker et al., 2004a; Keeling and Phillips, 2007). As wood density is negatively correlated with both mortality and growth rate (Poorter et al., 2008; Chave et al., 2009; Fauset et al., 2019), there are likely to be feedback effects between forest demographic rates and species composition, which may act to constrain forest traits across this gradient.

Some of the intrinsic variation in Amazonian forests may be explained by variation in climate and soils. Soil physical condition is associated with variation in turnover rates and wood density; lower soil stability, shallower soil depth and steeper topography are all related to faster turnover times, as structural instability increases vulnerability to disturbance and reduces tree lifespans (Quesada et al., 2012). This in turn favours species with lower wood densities and faster growth (Poorter et al., 2008), creating feedback effects in stand dynamics. Water availability also has an influence on forest structure and dynamics. Lower water availability is associated with higher rates of turnover and lower biomass (Quesada et al., 2012; Vilanova et al., 2018), and has also been shown to decrease tree height relative to DBH (Feldpausch et al., 2011), with implications for forest

structure.

1.5.2 Environmental change in Amazonian forests

Environmental change is driving shifts in forest dynamics across Amazonia, which are consistent with the changes observed across tropical regions more broadly. Demographic rates are increasing across the Amazon (Brienen et al., 2015), with increases in productivity and growth linked to CO_2 fertilisation effects, and increases in mortality rates linked to rising temperatures and an increase in the frequency and severity of droughts (Hubau et al., 2020). This suggests a combination of long-term chronic increases in demographic rates coupled with transient climate events driving short-term pulses of elevated mortality (Phillips et al., 2009; Jiménez-Muñoz et al., 2016). There is already evidence that these changes are altering the composition of Amazonian forests (Chave et al., 2008; Esquivel-Muelbert et al., 2019); associated impacts on forest structure are expected.

The spatial heterogeneity in forest dynamics, structure, and composition across Amazonia, as well as the associated environmental variation in climate and soils, may result in potentially significant differences in forest responses and resilience to environmental change and demographic rate increases. Forests on the south-western edge of the Amazon Basin may be closer to their environmental limits and so vulnerable to increases in drought; however the higher dynamism of these forests may help their recovery from perturbations. Similarly, forests in the north-east may be more buffered from environmental impacts, but vulnerable to significant declines in biomass if mortality rates of large trees increase. An improved understanding of the current links between demographic rates and stand structure in the context of these forests will enable better predictions of forest responses

and resilience to future environmental change.

1.5.3 Forests of Quebec

Forests in Quebec stretch across a huge latitudinal range, from temperate forests dominated by a mix of hardwood deciduous species, to low-diversity boreal forests at the highest latitudes, with the majority of the forest ecosystem located within the boreal region (Ministère des Ressources naturelles et des Forêts (MRNF), 2022). These forests have been comprehensively classified, according to a system based on vegetation communities and climate which broadly classifies ecological domains along a latitudinal gradient from south-to-north (Grondin et al., 2023). This classification system forms the basis for guiding forest management; while classifications are based on the characteristics of natural old-growth forests, the majority of Quebec's forests are managed for resource extraction, with around 1% of the total area of managed forests harvested annually (, MFFP). As a result, many landscapes in Quebec are dominated by relatively young forest stands, with implications for stand structure and composition (Boucher et al., 2009).

Environmental change is driving significant shifts in the structure and functioning of Quebec's forests (Duchesne and Ouimet, 2008). In addition to the impact of logging, there are increasing effects from climate change, forest fires, and insect outbreaks (Duchesne and Ouimet, 2008). Climate projections indicate increased temperatures and elevated risk of forest fires in Quebec (van Bellen et al., 2010; Ameray et al., 2023). As fire regimes are important in shaping stand structure and composition (Bergeron, 2000), changes in the frequency and intensity of fires is likely to drive shifts in ecosystem function and composition (van Bellen et al., 2010). These changes are likely to be exacerbated by shifts in species' distribu-

tions, leading to novel distributions of forest ecosystems (Ameray et al., 2023). Finally, insect outbreaks are an important control on boreal forest ecosystems. Cycles of insect outbreaks occur naturally across the forests of Quebec, driving significant defoliation, mortality, and reductions in growth rate of surviving trees (Cooke and Lorenzetti, 2006; Navarro et al., 2018), with long-term implications for forest structure and function. It is unclear how these dynamics will interact with climate change and changing mortality regimes to shape the future of Quebec's forests.

1.6 Methodological approach

My thesis aims to improve our understanding of the links between demographic rates and forest structure in old-growth forests both under current conditions, and under conditions which may drive changes in demographic rates. The focus of this study is on Amazonian forests because of their unique global importance. Because the objective of this thesis is to consider the mechanisms by which forest stands are structured, an individual-based approach is used, which examines the individual dynamics of stems comprising forest stands. As such, this research is centred around forest census data, which contains both detailed stand-level information as well as information on individual stem recruitment, growth, and mortality.

Data generated from the establishment and ongoing monitoring of long-term forest permanent sample plots (PSPs) are fundamental for studying forest ecosystems. Plot networks first started to be developed in the 1970s and have expanded rapidly since; PSP databases now contain decades of data on forest structure, function, and composition across local, national, and international scales (ForestPlots.net

et al., 2021). Exact methodologies for forest plot censuses vary according to the objectives of the network. Typically census protocols aim to generate a representative census of the stems composing a forest stand by mapping and tagging stems within the plot area. Diameter at breast height (DBH) measurements of the stems are recorded, and the stems are identified to species level if possible. For an individual census, this provides information on the stand structure, size distribution, aboveground biomass stocks, and species composition of the plot, while over multiple censuses it becomes possible to calculate stand demographic rates, biomass productivity, and structural and compositional change. These datasets serve many purposes, including providing a baseline measure of forest dynamics, enabling the testing of ecological theory, and capturing changes in forests through time.

Observational analyses can only progress our understanding so far, especially when considering the decadal-scale time-frames over which forest structure develops and responds to environmental change. I therefore also make use of individual-based modelling approaches, in order to extend our understanding of structural dynamics over longer time periods, and enable testing of forest responses to change. Forest inventory data is well-suited to use in the development and validation of modelling approaches (e.g. Farrior et al., 2016; Rüger et al., 2020), and, as plot networks expand spatially, increasingly offer the opportunity to apply these simulations over larger scales (e.g. Rödig et al., 2017).

When building and calibrating simulations, validation of outputs across multiple data streams is important to ensure robustness (Fischer et al., 2019), meaning that, to employ this approach in my thesis, additional data beyond plot inventory data is necessary. This data could come from a range of sources, including

remote sensing data (Fischer et al., 2019), data from functional trait databases (Maréchaux and Chave, 2017), or tree ring data (Brienen et al., 2020). Of these, tree ring data are best suited to application in an individual-based approach, as they provide measurements of the annual growth of individual stems over the lifetime of the tree (Babst et al., 2014). In addition, they complement forest inventory datasets, by providing growth measurements over much longer periods than are available from forest census data, with tree ring growth sequences often extending over several centuries (Babst et al., 2014). As a result, it is possible to derive novel information on stem and stand age, growth trajectories of individual trees, and historic variation in growth rates (Baker, 2003; Brienen et al., 2006), offering a different temporal dimension to plot data.

However, tree ring data are not available for all species or forest ecosystems. Well-defined tree rings are formed in seasonal environments, where intra-annual variation in growth rates results in temporal variability in the formation of woody cell structures, leading to the formation of tree rings (Babst et al., 2014). Because of this, tree ring data from the tropics is limited. Some tropical species in regions with a degree of seasonality (for example, tropical forests with distinct wet and dry seasons) have been shown to form annual growth rings (Brienen and Zuidema, 2006), but for most of Amazonia, there is a lack of readily available tree ring data, making acquisition of long-term data on the growth trajectories of Amazonian trees a challenge (Vieira et al., 2005). Further, as tropical tree ring data is not available for all species, any datasets which do exist are not representative of the complete community, and so are of limited utility in combination with inventory data.

1.6.1 Assessment of the datasets used

My thesis makes use of two large-scale, long-term datasets: firstly, the South American RAINFOR plot network; and secondly the Quebec provincial forest inventory. In this section I introduce these datasets and their role in my thesis, and assess their strengths and limitations.

The RAINFOR database, managed within the larger pan-tropical ForestPlots database (Malhi et al., 2002; ForestPlots.net et al., 2021), represents hundreds of plots across tropical South America, and forms the primary data source for my thesis. It was initiated as a network in 2000, and now contains census data for 593 plots, 427 of which have had multiple censuses conducted (ForestPlots.net et al., 2021). Most plots are ~1ha in size. The sites in the RAINFOR database encompass a broad range of environmental conditions across Amazonia. Lowland Amazonian rainforest can be classified into four biogeographic regions based on the soil substrate: the Guiana Shield, the East-Central Amazon, the Western Amazon, and the Brazilian Shield (Feldpausch et al., 2011). There are meaningful differences between the forests of these regions, with significant regional variation in species composition, AGB stocks, and demographic rates, making them useful classifications in analyses of Amazonian forests (Ter Steege et al., 2006; Feldpausch et al., 2012; Johnson et al., 2016). The forests of the Guiana Shield are particularly distinct, showing high biomass stocks and high frequencies of large tall trees (Feldpausch et al., 2012; Johnson et al., 2016). All four regions are well-represented in the RAINFOR database. Forest types outside of lowland moist tropical forest are also increasingly well-represented, including dry forests (Moonlight et al., 2020), and montane forest (Malhi et al., 2017). The diversity of plots in the database therefore allows for rigorous testing of relationships across

environmental gradients, enabling analyses of the ways in which climate, soils, and forest type mediate forest structure.

Censuses of plots within the RAINFOR network follow a standardised measuring protocol (Phillips et al., 2021). All stems $\geq$ 10cm DBH (measured at 1.3m height) are given a unique tag number. Stem DBH and species identity are recorded for each stem, and additional information regarding stem condition (e.g. broken stem, fallen stem etc), stem status (alive or dead), point of measurement (if other than 1.3m height), whether the stem is part of a multi-stemmed individual, and mode of mortality (if applicable) is recorded via codes where relevant (Phillips et al., 2021). Plots are typically re-censused every 1 - 10 years, with most sites aiming for re-census every 5 years.

As tree ring data is unavailable for the RAINFOR dataset, I chose to additionally incorporate forest data from temperate and boreal regions. The PSP network of the Quebec provincial forest inventory program (Ministère des Forêts, 2016; Ministère des Ressources naturelles et des Forêts (MRNF), 2022) contains forest census data and randomly sampled tree ring data surveyed from the across the same set of plots, offering a detailed perspective in both time and space. The plot network extends over a broad bioclimatic gradient, representing six distinct forest types: (1) sugar maple-bitternut hickory; (2) sugar-maple-basswood; (3) sugar maple-yellow birch; (4) balsam fir-yellow birch; (5) balsam fir-white birch; (6) spruce-moss (Duchesne et al., 2019). This makes the dataset a strong complement to the RAINFOR data, as both encompass broad gradients in forest dynamics, structure, and composition, but in very different abiotic environments. The network was established in the 1970s, and contains ~100000 circular plots, with a radius of 11m (Duchesne et al., 2019). All stems $\geq$ 91mm DBH are uniquely

tagged, and their stem DBH and species identity are recorded (Ministère des Forêts, 2016). Of these, I used a subset of 10518 plots selected based on their disturbance history. Plots are re-censused approximately every 10 years.

There are challenges and limitations to working with forest inventory data. Data is vulnerable to human error, particularly as field teams are likely to be different at each census, and so it is harder to maintain long-term consistency. As a result, quality control is important to ensure consistency of diameter measurements between censuses: measurement errors can be corrected by comparing multiple measurements of the same tree over time, and interpolating to correct extremely anomalous measurements (Phillips et al., 1998). Additionally, information recorded about measurement technique, anomalies in tree structure, and post-field data management of anomalous measurements can all be used to minimise use of erroneous measurements in data analysis (Phillips et al., 2014; Ministère des Forêts, 2016).

Enabling robust analyses across such large-scale and diverse datasets is challenging. Plots may have experienced a wide range of conditions that could influence their structure and composition, including variation in disturbance history. Information in the dataset on stand age and/or forest maturity (where known), and the magnitude of recent disturbances - which may range from small natural disturbances up to much more significant stand-clearing disturbance, such as logging or burning - allows this to be accounted for in analyses. This is a particularly important consideration in working with the Quebec provincial forest inventory dataset, as many of the forests in Quebec are managed and have been subject to stand clearance or logging (Ministère des Forêts, 2016). In the case of this thesis, I focus on old-growth forests and select stands with minimal disturbance history,

in order to remove the effects of external disturbance on stand structure from my analyses. As a result, the final dataset consisted of 10518 plots.

Sample size is an important consideration, both spatially and temporally. Sampling errors are higher in smaller plots and across shorter or fewer census intervals (Baker et al., 2004a). In addition, smaller plots fail to fully capture large-scale disturbances, and so may underestimate mortality rates, and overestimate biomass accumulation rates (Chambers et al., 2013). Therefore, ensuring sample size sufficiency is important in designing robust analyses. The average plot size in both inventory datasets is small ($\leq$ 1ha); however, this is compensated for by the number of plots sampled, particularly in the Quebec forest inventory database, where my analyses aggregate data across bioclimatic regions. As a result, the plots represent a large area of forest sampled: a total of 477ha in Quebec, and 312ha in Amazonia. In using the RAINFOR data, I choose to exclude plots $\leq$ 0.8ha, unless they are being aggregated as part of a wider plot cluster. Additionally, analytical robustness may be improved by weighting plots within the analysis by census interval length and plot area, thus giving more weight to the more representative larger plots and longer sampling frames (Baker et al., 2004a).

In addition to the forest inventory data, tree core samples were used from a selection of the inventory plots in Quebec, with 5 trees randomly sampled within each selected plot (Duchesne et al., 2019). This provides a multi-species dataset of tree ring data, overlapping with the forest inventory data described above. Tree cores in this dataset were processed by first identifying rings using binocular magnification, and then measuring rings using the WinDendro image analysis system (Duchesne et al., 2019). As with plot data, quality control of tree ring data is important, as cores may be incomplete or inaccurately measured. In this

dataset, tree ring growth trajectories were summed to calculate a tree diameter estimate. These estimates were compared against the DBH of the stem measured in the field at the time of coring. Because bark thickness is variable, and not included in tree ring trajectories, direct comparison of the values is not possible, and so anomalous values were determined by setting confidence intervals around the trend line between the two values for each species (Caldwell, 2018).

1.6.2 Estimating demographic rates for analyses

There are a range of approaches used for estimating demographic rates from forest inventory data, each of which have advantages and disadvantages. As mortality rate estimates are central to my analytical approach, I outline the main approaches I use for mortality rate calculation here. Since my thesis takes an individual-based approach with a focus on stem size distributions, I use measures of the annual probability of stem mortality and annual stem increment growth, allowing me to directly relate these rates to the dynamics and frequencies of individual stems within the stand.

The simplest measure of mortality I use is a constant stand-level stem mortality rate, measured as the percentage of stems dying each year. This is calculated as the exponential mortality coefficient μ,

$$\mu = \frac{ln(n_0) - ln(n_0 - n_d)}{t} * 100$$

where n_0 is the number of stems at the start of the census interval, n_d is the number of stems that die in the census interval, and t is the census interval length (Lewis et al., 2004a). Mortality rate estimates are influenced by the census interval length, as within each census interval there are some trees which recruit

and die without being measured in either census. As a result, as census interval lengths increase, the mortality calculation will increasingly underestimate the true mortality rate (Lewis et al., 2004b). This effect can be corrected for quite simply, by using a correction of

$$\mu * t^{0.08}$$

, where μ is the rate estimate, and t is the census interval length (Lewis et al., 2004b). I apply this correction to all mortality rate estimates in this thesis.

Although stand-level mortality estimates are simple to calculate and provide a useful measure of the overall dynamics of the plot, in reality mortality rates are unlikely to be constant across individuals. Here, use of probability functions which describe within-stand variation in mortality are valuable. Site-specific mortality functions can be estimated from plot data using maximum likelihood methods (Kohyama et al., 2015; Camac et al., 2018), and the function then used to generate annual mortality probabilities for individual trees, dependent on their specific characteristics. In this thesis, I focus on two mortality probability functions: a function to describe size-dependent mortality, and a function to describe growth-dependent mortality. Size-dependent mortality has been widely observed in natural forests (Coomes et al., 2003; Muller-Landau et al., 2006b), a result of differences in mortality risk factors across size classes (Gora and Esquivel-Muelbert, 2021). Patterns of size-dependent mortality are known to vary between species, and can varying between declining, increasing, or a U-shaped pattern with increasing stem size (Iida et al., 2014a). Any size-dependent mortality function therefore needs to reflect this variability. I use the equation

$$M(x) = a \exp^{b(x)} x^c$$

where $M(x)$ is the instantaneous mortality rate ($year^{-1}$), x is the individual stem DBH, and a, b and c are plot-specific parameters (Iida et al., 2014a; Kohyama et al., 2015).

In addition, mortality may show growth-dependency, whereby low stem growth rates in previous years are associated with higher mortality risks (Kobe, 1996; Camac et al., 2018). Growth-dependent mortality has been observed to typically follow an exponential decline where the risk of mortality does not completely decline to zero (Kobe, 1996; Wyckoff and Clark, 2000). Here, I use the equation

$$M(x) = a \exp^{-b(x)} + c$$

where $M(x)$ is the instantaneous mortality rate ($year^{-1}$), x is the previous year's growth rate, and a, b and c are plot-specific parameters (Camac et al., 2018).

1.7 Thesis outline

In this thesis I use forest inventory data from two major plot networks to analyse relationships between demographic rates and stand structure in natural forests, and to assess the implications for forest responses to global change scenarios.

In Chapter 2, I use RAINFOR inventory data from across six major forest types across the Amazon to (1) characterise variation in forest structure across major environmental gradients; (2) test for relationships between demographic rates and forest structure; (3) analyse how these relationships are mediated by variation in climate, soils, and forest type. This provides a rigorous observational framework of relationships between forest structure and demographic dynamics across the Amazon.

In Chapter 3, I develop a novel individual-based simulation approach, using demographic data from the Quebec provincial forest inventory program. I use forest inventory data to build the simulation, and validate it with tree ring data from the same plot network. The simulation approach developed illustrates the importance of demographic rate control on forest stand structure, and provides a methodology which is widely applicable to permanent sample plot networks.

Finally, in Chapter 4, I apply the simulation approach developed in Chapter 3 to 19 Amazonian plot clusters, in order to analyse how forest structure in Amazonian forests may respond to mortality rate change. I calculate a set of response and recovery metrics to assess how forest response and recovery vary with baseline mortality rate, and determine the importance of intrinsic demographic rates in shaping forest responses to change.

Chapter 2: Climate-mediated variation in stem size distribution and demography across South American tropical forests

2.1 Abstract

Understanding how stem size distributions (SSDs) of forests are controlled by variation in growth and mortality rates is essential to predict future forest responses to global change. Here, I test how variation in SSDs is associated with stem demographic rates - specifically stem growth and mortality rates - across 242 permanent sample plots (PSPs), encompassing the full range of environmental conditions found in tropical South American forests. I show that the primary axis of variation in stand structure is related to the evenness of SSDs, from lower stand evenness (stands with a particularly high proportion of small trees), to higher stand evenness (stands with a greater proportion of mid- and large-sized trees). Across the whole dataset, I find a negative relationship between forest stand evenness and stem mortality rate, but also find that the relationships between SSDs and demographic rates vary with forest type, climate, and soil physical structure. Lower demographic rates are associated with higher stand evenness in the less dynamic forests of the Guiana Shield and East-Central Amazon, and in warm, wet forests with a stable soil structure. This pattern likely reflects the importance of variation in mortality rates in determining variation in SSDs in these high biomass, tall stature forests. However, this pattern is reversed in dry and montane forests, and forests on the Brazilian Shield, where higher demographic rates are associated with higher stand evenness, and a higher proportion of large stems. This suggests that variation in growth rates determines forest structure in

forests growing in more marginal environmental conditions, such as under drier and colder conditions, or on less stable soils. Our results highlight that the responses of forest structure to changes in growth and mortality rates as a result of global change will vary among tropical South American forests.

2.2 Introduction

Within a forest, the majority of aboveground biomass is stored in the woody stems of trees (Anderson-Teixeira et al., 2021). As such, parameters describing forest structure, such as basal area, stem size distributions, stem frequencies, and mean stem height (Baraloto et al., 2011; de Paula et al., 2011; Rödig et al., 2018) are strongly associated with stand AGB. Stem size distributions (SSDs) of forests, which describe the number of individual trees of different sizes, represent a key parameter linking variation in demographic rates with variation in aboveground biomass (AGB). SSDs are shaped by stem demographic rates - recruitment, growth, and mortality - which determine the rates at which stems are recruited into, move through, and are lost from the population (Lima et al., 2016). In turn, SSDs are closely linked to stand AGB, as a result of the key role of tree size in determining AGB stocks (Baraloto et al., 2011; Bastin et al., 2015). Understanding the controls on SSDs is therefore important as they mediate the link between demographic rates and stand AGB. It is well-documented that spatial variation in AGB in tropical South American forests is linked to variation in tree mortality rates (Johnson et al., 2016), and that there are close associations between changes in growth and mortality rates and changes in forest AGB (see e.g. Brienen et al., 2015; Hubau et al., 2020); however, we need to understand *how* variation in demographic rates drives variation in forest SSDs in order to predict

the potentially non-linear responses of forest structure to changing growth and mortality rates.

SSDs quantified using frequency distribution fits - most commonly the power-law and the Weibull distributions (Muller-Landau et al., 2006b; Coomes et al., 2003; Lima et al., 2016; Moore et al., 2020) - have a number of advantages for examining structural variation among forests. Firstly, they quantify structural variation over the full range of stem sizes, and so show greater sensitivity to structural variation than simple summary statistics, such as stem number and basal area. Secondly, these fits are linked to theoretical explanations of forest structure. For example, Enquist and Niklas (2001) proposed that SSDs are shaped by allometric scaling relations governing resource flows, such that stem frequencies scale closely with stem diameter in a power-law relationship (Enquist and Niklas, 2001). Indeed, the theory predicts that SSDs are so tightly governed by allometric scaling, that the power-law exponent (α) in steady state old growth forests will approximately equal -2 (Enquist and Niklas, 2001; Enquist et al., 2009). Subsequent studies have failed to find support for a universally close fit to a power-law, instead highlighting variation both in the slope of the size distribution, and in how well size distributions fit to a power-law, with the power-law consistently over-predicting numbers of large stems (Muller-Landau et al., 2006b; Coomes et al., 2003; Farrior et al., 2016). Instead, the Weibull distribution offers a better overall fit, in particular at large stem sizes, where the largest proportion of biomass is held (Muller-Landau et al., 2006b; Lima et al., 2016; Moore et al., 2020).

Stand structure - and ultimately biomass stocks - is in large part determined by stem demographic rates - specifically stem recruitment, growth, and mortality rates - which shape how stems enter, move through, and leave the population.

Our current understanding is that the strongest demographic influence on tropical forest stand structure is stem mortality rates, which are negatively associated with stand biomass (Johnson et al., 2016; van der Sande et al., 2017). High rates of mortality reduce survivorship and woody residence time and increase gap fractions (Dalagnol et al., 2021), reducing the numbers of large trees, and weighting stem size distributions towards smaller stems. In contrast, lower mortality rates and longer woody residence times are associated with a higher proportion of large trees and greater stand AGB, as stems survive through to the largest size classes (Malhi et al., 2015; Rödig et al., 2017).

However, it is unclear whether mortality would remain the primary control on stand structure under different environmental conditions. For example, there is evidence that both growth and mortality rates correlate with size distribution parameters across a small range of sites (Muller-Landau et al., 2006b). In addition, in early successional forests, growth is the most important factor shaping structural change, as growth is important in pushing individuals towards larger stem size classes (Rozendaal and Chazdon, 2015). We might therefore expect growth rates to be important in shaping stand structure in mature forests in marginal conditions where environmental factors such as low water availability or poor soil structure place constraints on the ability of individuals to reach the largest stem size classes. Here, fewer large stems may reduce light competition at smaller sizes, resulting in growth becoming a strong driver of stand structure.

Currently, studies of SSDs have tended to focus on only one or a few sites (Muller-Landau et al., 2006a,b; Farrior et al., 2016), or have not tested how stand structure varies between forest types and along environmental gradients (Moore et al., 2020). We therefore lack a comprehensive understanding of how stand structure

varies over large spatial scales. Amazonian forests encompass a wide range of environmental, structural, and demographic variation (see e.g. Baker et al., 2004a; Feldpausch et al., 2011; Quesada et al., 2012), including a wide range of variation in water availability - from moist through to seasonally dry tropical forests - and temperature - from lowland to high montane forests. As a result, they offer an ideal study system through which to explore variation in and demographic controls on stand structure.

Here, I use data from permanent sample plots (PSPs) across the ForestPlots network (Lopez-Gonzalez et al., 2009, 2011) to analyse variation in structural parameters and SSDs across a diversity of South American forests. I expand the focus of previous studies on single biomes (see e.g. Lima et al., 2016; Moore et al., 2020; Moonlight et al., 2020; Duque et al., 2021) to the full range of Amazonian and Andean forests, identifying six forest categories: moist lowland forest across four distinct biogeographic regions (Feldpausch et al., 2011), (1) the Brazilian Shield; (2) the Western Amazon, (3) the East-Central Amazon, (4) the Guiana Shield, alongside (5) montane forest and (6) dry forest. I first clarify and describe patterns of variation in SSDs across these forests, before analysing a) how this variation relates to variation in demographic rates across all forest plots; and b) how relationships between forest structure and demographic rates vary by forest classification, and with climate (temperature and precipitation) and soils.

2.3 Methods

All data was obtained from the ForestPlots database (Lopez-Gonzalez et al., 2009, 2011), and all analyses were conducted in R version 3.5.1 (R Core Team, 2020).

2.3.1 Plot selection and descriptive parameters

This analysis is focused on data from across the full environmental gradient of South American tropical forests, encompassing a wide range of climatic, structural and compositional variation. To simplify this variation,I classify forests into six South American forest categories: moist lowland forest across four distinct biogeographic regions, (1) the Brazilian Shield; (2) the Western Amazon, (3) the East-Central Amazon, (4) the Guiana Shield, defined according to Feldpausch et al. (2011), alongside (5) montane forest, defined as forest $\geq$ 1500m in elevation; and (6) dry forest, defined as forest with a dry season $\geq$ 5 months in length and mean annual precipitation $\leq$ 1500mm, following the classification by ForestPlots (Lopez-Gonzalez et al., 2009, 2011). Classification of lowland Amazonian forests by biogeographic region is well-supported, with the different regions showing sufficiently different dynamics to justify analysis in this way (Feldpausch et al., 2011; Johnson et al., 2016).

Only plots following the standard ForestPlots measurement protocol (all stems $\geq$ 10cm DBH recorded and measured at 1.3m) were included. Where stems <10cm DBH had been recorded, these stems were excluded from analysis. Plots were only included if they were identified as old-growth forest with no recent anthropogenic disturbance from burning, grazing, or logging. Plots which have experienced natural disturbances, such as drought or windthrow, were not excluded. Mixed forest and mono-dominant forest were included, but savannah, and palm-, liana-, and bamboo-dominated plots were excluded. Plots were included in this analysis if they were $\geq$ 0.8ha in size. Only plots with $\geq$ 2 censuses over a total minimum census interval of 3 years were included, in order to allow robust estimates of demographic rates to be calculated; in calculating structural parameters only

data from the most recent census of each plot was used. Plot locations are shown in Figure 2.1.

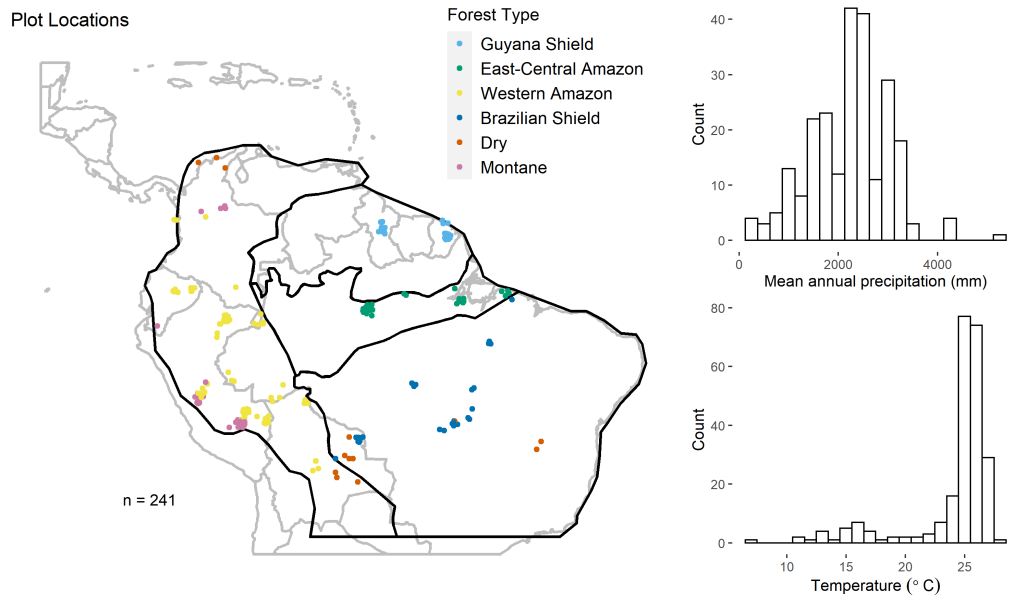

Figure 2.1: Clockwise plots show: a) Locations of plots (n = 241) used in analysis. Plots are coloured according to forest type, with outlines of biogeographic regions, as defined in Feldpausch et al. (2011) shown in black. Plot locations are offset slightly to improve visualisation of plots which are located close to each other. b) Histogram of mean annual precipitation values of plots included in analysis. c) Histogram of mean annual temperature values of plots included in analysis. Climate data is taken from WorldClim 2.1.

2.3.2 Calculating structural parameters and describing stem size distributions

Stem size distributions were fit to power-law and Weibull distributions. The power-law fit followed the equation $f(x) = x^{-\alpha}$, where α is the exponent parameter, and describes the slope of the power-law fit. Higher alpha parameter values suggest a steeper slope and a more skewed distribution (Figure 2.2). I set x_{min} equal to 100mm across all plots, such that the power-law was fit across the available size distribution for all plots. The transition point (mm) is used as an

estimate of the point at which the power-law fit begins to over-predict the number of large stems (see Farrior et al., 2016), and is calculated here as the size class at which the deviations of the observed fit from the expected power-law fit become negative.

A two-parameter Weibull distribution was used to fit to SSDs, with the equation

$$f(x) = \frac{\gamma}{\beta}\left(\frac{x}{\beta}\right)^{(\gamma-1)} \exp - \left(\frac{x}{\beta}\right)^{\gamma} \qquad \gamma, \beta > 0$$

where γ is the shape parameter, and β is the scale parameter. The scale parameter controls the evenness of the distribution, and so higher scale parameters indicate higher stand evenness, and a relatively higher proportion of large stems (Figure 2.2). The shape parameter controls the slope of the distribution, and is sensitive to the extremes of the distribution: lower shape parameters indicate a higher frequency of small stems, but also a larger maximum stem size.

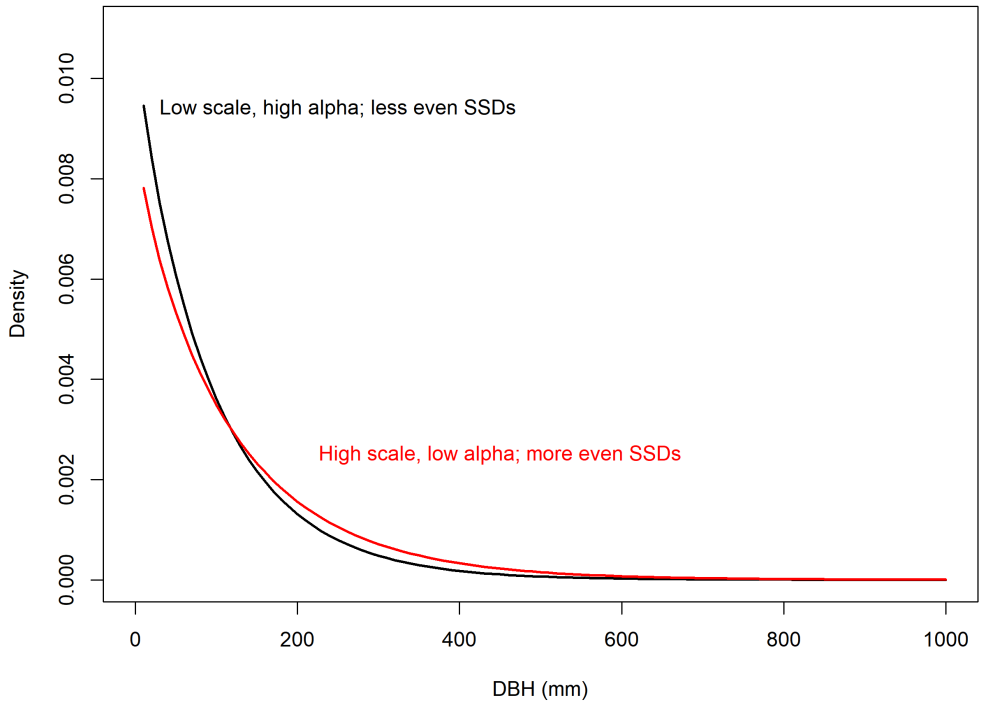

Figure 2.2: Illustration of the effect of variation in scale and alpha parameters on theoretical stem size density distributions, where each line shows a frequency distribution with different calculated scale and alpha parameters. In these simulations, shape parameter is constant at 0.95. For the black line, the scale parameter is 97 and the alpha parameter 2.7, giving a SSD with lower stand evenness skewed more heavily towards smaller stem sizes. For the red line, the scale parameter is 123, and the alpha parameter 2.4, giving a SSD with higher stand evenness, with a relatively higher proportion of large stems.

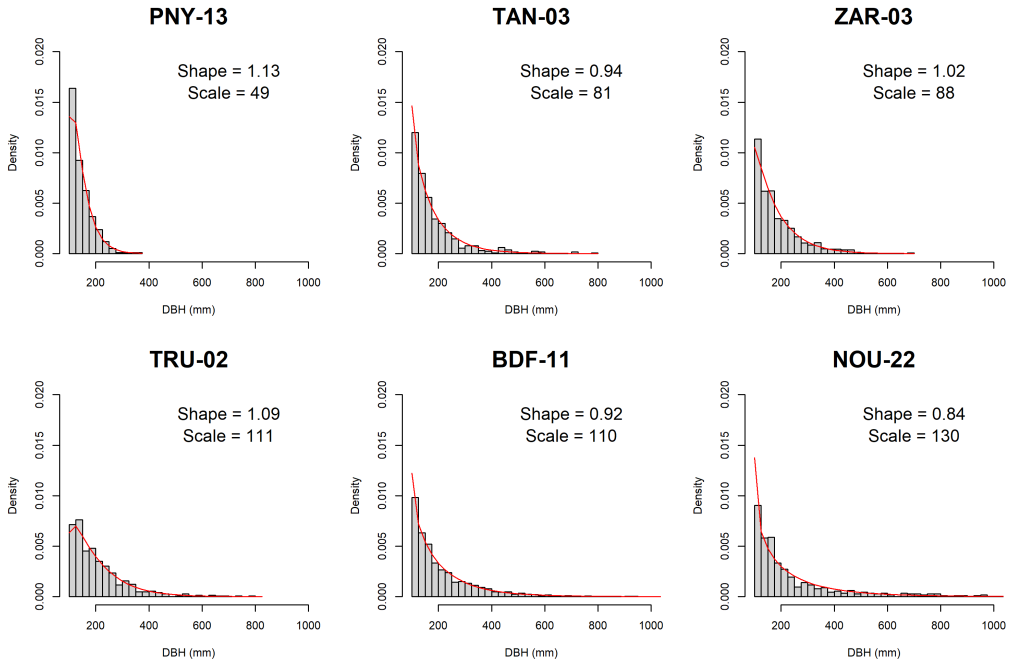

Figure 2.3: Examples of variation in estimated stem size distribution parameters in relation to observed variation in stem size distributions.

Uncertainty of the size distribution parameters was assessed by evaluating standard errors of the parameters. These were extracted for each plot following maximum likelihood fitting of the Weibull distribution to the SSDs, using the fitdistrplus package in R. Standard error values were standardised to a percentage of each parameter, for comparison across the dataset.

Additionally, a range of descriptive structural parameters were calculated for each plot as follows: mean, median and maximum DBH values; the 25% and 75% quantiles; number of stems >10cm DBH per hectare; and basal area per hectare. Total basal area (BA) is calculated as $BA = \sum_1^n \pi(DBH/2)^2$ and standardised by plot area.

2.3.3 Calculating demographic rates

Mean stem mortality rates were calculated as the exponential mortality coefficient μ,

$$\mu = \frac{ln(n_0) - ln(n_0 - n_d)}{t} * 100$$

where n_0 is the number of stems at the start of the census interval, n_d is the number of stems that die in the census interval, and t is the census interval length. Mean growth rate was calculated as the mean DBH change per stem per year. For each plot, both mean stem mortality and mean growth rate were calculated for each census interval, and an average was taken across census intervals, weighted by census interval length. A census interval correction was applied with the formula $\mu * t^0.08$ where μ is the rate estimate, and t is the census interval length (Lewis et al., 2004b).

2.3.4 Soil and climate data

Additional environmental data layers describing mean annual precipitation (MAP) and mean annual temperature (MAT) were downloaded from the WorldClim database at a 1km^2 resolution (Fick and Hijmans, 2017). An estimate of each parameter for each site was extracted from the layers, based on the geographic co-ordinates for each site. There is a wide range of temperature and precipitation represented by these plots (Figure 2.1). Broadly, lower MAP values are seen in the dry plots and the plots of the Brazilian Shield, while lower MAT values are seen in the montane forest plots.

Site-specific soil data is available for 43 of the sites from the database collected by Quesada et al. (2010). Only sites from the East-Central Amazon, the Western

Amazon, and the Brazilian Shield are represented in this dataset. Soil fertility parameters extracted from the database were: cation exchange capacity, soil water pH, nitrogen content, organic phosphorus content, and the carbon:nitrogen ratio. In addition, a number of structural indices were extracted: a soil structure index, a soil depth index, a soil topography index, and a summary index, calculated as the sum of the three indices. Methods for calculating these indices are detailed in Quesada et al. (2010).

2.3.5 Analyses

A principal component analysis (PCA) was conducted first to explore variation in structural parameters across the full range of plots. Parameters included in the PCA were: scale parameter; shape parameter; number of stems per hectare; median, mean, and maximum stem DBH; basal area; the 25% quantile (Q1); and the 75% quantile (Q3). Parameters calculated from the power-law distribution fits were excluded, due to the poor fit of the power-law distribution to the SSDs.

To assess variation in structure between forest types, for each of the four stem size distribution (SSD) parameters, the mean for each forest type was calculated, with plots weighted according to the square root of plot area multiplied by census interval length. Significant differences between forest types were identified using a one-way ANOVA, with a Tukey's test.

To test for relationships between forest structure, demographic rates and environmental variables, I used a combination of weighted least squares regression models and generalised least squares regression models. In building each model, I first used a weighted least squares approach, and then used a Moran's I test to assess spatial autocorrelation of the residuals. Where this identified signifi-

cant spatial autocorrelation, I used a generalised least squares model with a term specifying a spatial autocorrelation structure. The best spatial autocorrelation structure was selected on a case-by-case basis using AIC scores. Where spatial autocorrelation was not found to be significant, weighted least squares regression models were used. Within each model, plots were weighted by the square root of plot area multiplied by census interval length (Lewis et al., 2009; Brienen et al., 2015). This weighting helps to account for the influence of stochasticity on plot dynamics, which has the greatest effect on small plots and plots with shorter total monitoring periods. All models were run using the scale parameter and the shape parameter individually as response variables.

I first tested the effect of demographic rates on forest structure across the whole dataset. I then tested how these relationships varied with environmental variables. I tested for a significant interaction between demographic rates and forest type. To then explore these interactions more mechanistically, I tested for significant interactions between demographic rates and two key climate variables, mean annual temperature (MAT) and mean annual precipitation (MAP). I identified the best combination of explanatory variables using AIC scores. Finally, for the subset of data for which I had soil data, I tested for significant interactions between demographic rates and soil parameters, and identified the best combination of explanatory variables using AIC scores. As the subset of soil data was only available for a limited range of sites, and represented a very narrow range of climate parameters, I chose to analyse the effects of climate and soils separately.

I estimated the slope and significance for individual relationships within the models using the emmeans package in R (Lenth, 2021), and estimated a pseudo-R squared value for each model using the rsquared function in the piecewiseSEM

packages (Lefcheck et al., 2020). Multicollinearity between predictor variables was checked in all models using the VIF function within the MASS package (Ripley, 2021), and was shown to be negligible.

Finally, in order to visualise variation between forest types, I generated approximations of an average 10ha SSD for each forest type, using mean values for the shape parameter, scale parameter and number of stems per hectare to carry out repeated sampling (n = 100) of fitted Weibull distributions.

2.4 Results

In total, data from 242 plots were included in the analysis, including 37 plots from the Guiana Shield, 43 from the East-Central Amazon, 89 from the Western Amazon, 29 from the Brazilian Shield, 13 dry forest plots, and 31 montane forest plots. Among lowland moist forests there is spatial variation in biomass, basal area (BA), mean stand DBH, and stem mortality and growth rates (Table 2.1). This occurs along a broadly east-to-west gradient, with biomass and BA decreasing, and demographic rates increasing from east to west. Demographic rates in dry and montane forest fall broadly in the middle to upper part of the range of rates observed in lowland moist forest, though, by comparison, basal area in dry and montane forest is relatively low, particularly in dry forest (Table 2.1).

2.4.1 Variation in stand structure across tropical South American forests

Of the two distributions, the Weibull distribution proved the better fit, showing a significant fit across 90% of plots ($p \leq 0.05$), compared with a significant fit across just 4% of plots ($p \leq 0.05$, Kolmogorov-Smirnoff test) for the power-law

Table 2.1: Mean values for stem demographic rates and basal area across forest types. Means are calculated from plot level values from the full dataset used in analysis, and weighted by the square root of plot area multiplied by census interval length, as specified in the methods.

Forest biogeographic type	Stem mortality rate (% year $^{-1}$)	Stem growth rate (mm year^{-1})	Stem recruitment rate (% year^{-1})	Basal area (m^2 ha^{-1})
Guiana Shield	1.45	1.74	1.38	26.17
East-Central Amazon	1.44	1.57	1.45	27.38
Western Amazon	2.58	2.33	2.49	23.18
Brazilian Shield	3.17	2.09	2.26	22.35
Dry	2.28	1.83	2.23	18.85
Montane	2.69	1.94	2.41	23.72

fit. This result demonstrates the utility of the Weibull distribution for accurately describing size distributions of old-growth forest plots down to 0.8 ha in size, and in capturing variation in forest structure at continent-wide scales. Examples of the Weibull and powerlaw distribution fits to the observed plot census data are presented in the appendix (Figures A2.1 and A2.2). Because of the poor fit of the power-law parameters, they are not used in further analyses.

Standard errors of the Weibull distribution parameters were found to be small. The mean standard error across all plots for the scale parameter was 4.98, equivalent to a percentage error of 4.68% (range: 1.00 - 7.50%). The mean standard error across all plots for the shape parameter was 0.03, equivalent to a percentage error of 3.16% (range: 0.67 - 4.97%). Relative to the effect size in model outputs, this error is negligible, and so is not expected to have a significant impact on model results.

I find significant variation in SSD parameter values across the full dataset (Table 2.2). Plot-level values of the weibull distribution parameters vary between 49.4 - 182.0 for the scale parameter, and 0.71 - 1.21 for the shape parameter. I find no significant correlation between the shape and scale parameters.

The first two axes of the PCA analysis captured 75.2% of variation in the struc-

Table 2.2: Mean values for the Weibull distribution parameters across forest types, weighted by the square root of plot area multiplied by census interval length. Bootstrapped 95% confidence intervals shown in brackets.

Forest type	Scale	Shape
Guiana Shield	127.6 (121.9, 133.1)	0.91 (0.89, 0.93)
East-Central Amazon	113.1 (108.7, 117.3)	0.92 (0.90, 0.93)
Western Amazon	106.0 (104.2, 109.7)	0.92 (0.91, 0.94)
Brazilian Shield	93.2 (89.6, 97.0)	0.92 (0.90, 0.95)
Dry	112.1 (94.7, 129.3)	0.93 (0.89, 0.96)
Montane	97.8 (91.4, 104.2)	1.02 (0.99 1.06)

tural data (Figure 2.4; 55.7% and 19.5% respectively). PC1 is defined most strongly by the scale parameter and the 75% quantile, with the mean and median stem DBH also being important variables. This suggests that the primary axis of variation is shaped by stand evenness, with more even stands showing a higher proportion of large stems relative to small stems. PC2 is most strongly determined by the shape parameter, indicating that the second axis reflects variation in the tail of the distribution and maximum stem DBH. In comparison to the SSD parameters, other structural parameters, such as basal area, number of stems per hectare, and maximum stem size, are of secondary importance in defining PC1 and PC2, suggesting that application of SSDs in describing forest structure may offer a more parsimonious approach to summarizing forest structure than using large numbers of descriptive parameters.

Results from the PCA analysis suggest continuous variation in forest structure across Neotropical forests, suggesting high variation within, as well as among forest types. In particular, the results reveal that across the lowland moist forests the primary axis of variation in stand structure among forest categories is in stand

evenness: forests show low regional variation along PC2, indicating similarities in maximum stem size across these regions, but show much higher variation along PC1. There is lower variation between forest types along PC2, with the exception of montane forest, which shows a relatively distinct cluster defined by a lower maximum stem size than the other forest types (Figure 2.4).

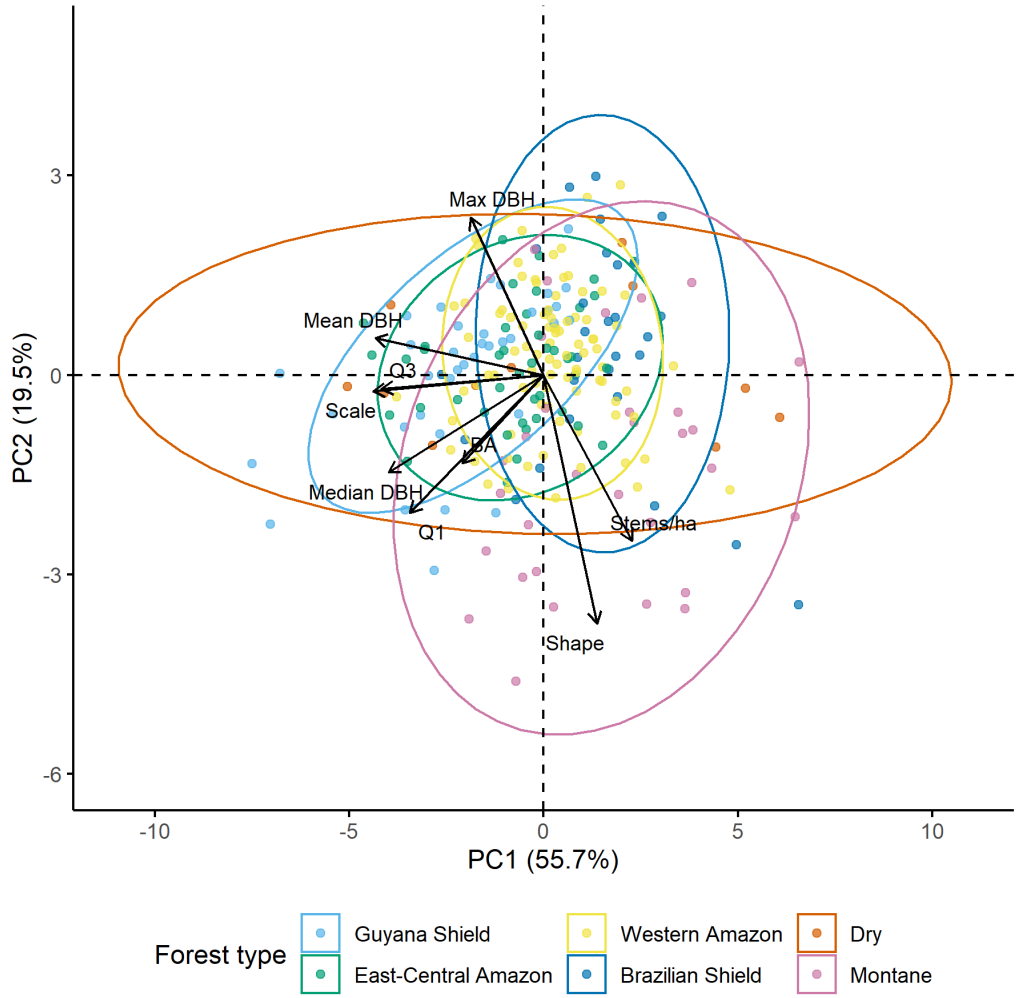

Figure 2.4: Primary axes of structural variation across the full plot dataset. Arrows show loadings of different structural variables on the first two PCA axes. Points show locations of individual plots along these axes, coloured by forest type. Ellipses show 95% confidence for each forest type.

Variation between forest types along the PCA axes is supported by the results of the ANOVA and TukeyHSD analysis, which reveal a number of significant differences in SSD parameters between forest types (Table A2.2). The scale parameter shows the highest number of significant differences among forest types ($p \leq 0.05$, TukeyHSD), with clear variation in these parameters between forest types. Scale parameter values are highest in the Guiana Shield, East-Central Amazon, and lowest in montane forest and the Brazilian Shield, suggesting that stand evenness is higher in the Guiana Shield and East-Central Amazon, and lower in montane forest and the Brazilian Shield.

Variation between forest types in the shape parameter shows fewer significant differences, though I still find significant differences between montane forest and all other forest types ($p \leq 0.05$, TukeyHSD), reflecting the differences seen along the second PCA axis, and suggesting a lower maximum DBH in montane forest compared to other forest types.

2.4.2 Variation of stem size distributions with demographic rates

As with structural parameters, I find significant variation in demographic rates across forest types. Demographic rates are lowest in the northern and eastern lowland forests of the Guiana Shield and East-Central Amazon, and increase towards the south-west of the basin (Table 2.1).

Across all plots, I find a significant negative association between stand structure and stem mortality ($p \leq 0.0001$, $R^2 = 0.08$), suggesting that plots with lower stem mortality rates have SSDs with higher evenness. I find no significant relationship between stem mortality rates and the shape parameter. I find no significant effect of stem growth on any of the SSD parameters at this scale.

2.4.3 Effect of forest type on demographic control of stem size distributions

Relationships between SSD parameters and demographic rates vary strongly across forest types. When modelling the scale parameter, I find a significant interaction between stem mortality rate and forest type ($p \leq 0.0001$, $R^2 = 0.47$), and stem growth rate and forest type ($p \leq 0.0001$, $R^2 = 0.43$). When modelling the shape parameter, I find a significant interaction between stem growth rate and forest type ($p \leq 0.003$, $R^2 = 0.20$).

Individual forest types have significant relationships between structural parameters and demographic rates but these relationships differ in their strength and directionality. In the Guiana Shield, East-Central Amazon and Western Amazon, stand structure is more even where mortality rates are lower, shown by the strong negative correlations between stem mortality and the scale parameter (GS $p \leq 0.0001$, slope = -17.2; EC $p \leq 0.01$, slope = -9.7; W $p \leq 0.05$, slope = -3.9; Figure 2.5 and A2.5). I also find a significant negative correlation between the scale parameter and stem growth rate within the Guiana Shield ($p \leq 0.0001$, slope = -18.5).

In contrast, within dry and montane forests and the Brazilian Shield, the scale parameter correlates positively with stem growth rates (BS $p \leq 0.05$, slope = 11.1; Dry $p \leq 0.01$, slope = 31.6; Montane $p \leq 0.001$, slope = 15.3; Figure 2.5 and A2.5), showing that stand structure is more even where stem growth rates are higher. I find a significant positive correlation between the scale parameter and stem mortality rate within dry forest ($p \leq 0.0001$, slope = 16.9). In montane forest, there is a significant negative correlation between the shape parameter and stem growth rate ($p \leq 0.001$, slope = -0.08), indicating that higher stem growth

rates are associated with a higher maximum stem size.

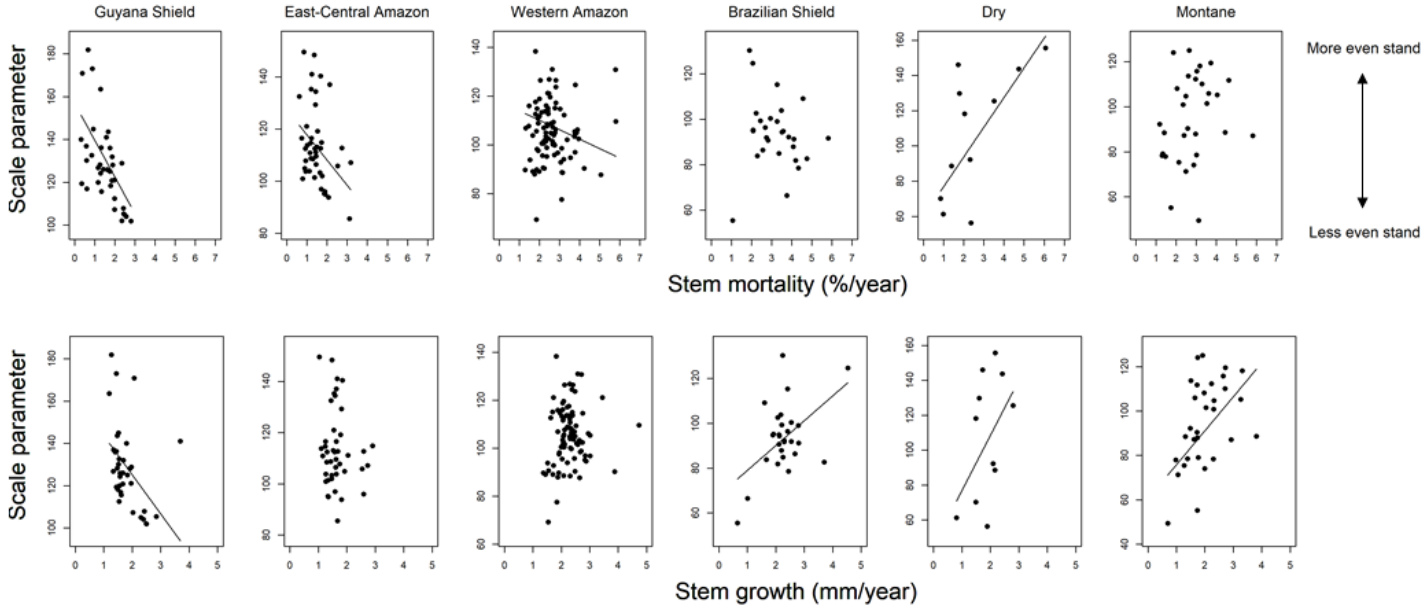

Figure 2.5: Relationships between the scale parameter and stem demographic rates broken down by forest type, visualising interaction effects between stem demographic rates and forest type. Lines are plotted to show significant relationships ($p \leq 0.05$) by forest type.

2.4.4 Effect of soils and climate on demographic control of stem size distributions

I find that a number of climate and soil parameters are important in mediating relationships between stem demographic rates and stand structure.

For the scale parameter, I find a significant interaction effect between stem mortality rate and MAP ($p \leq 0.0001$) and stem growth rate and MAT ($p \leq 0.01$), and a marginally significant interaction effect between stem mortality rate and MAT ($p = 0.057$; total model $R^2 = 0.23$). Stem mortality rates show a very weak positive correlation with the scale parameter in forests with low MAP, but a strong negative correlation in forests with high MAP. Stem mortality rates show a negative correlation with the scale parameter across all temperatures, but the relationship is stronger in forests with low MAT. In contrast, stem growth rates show a very weak positive correlation with the scale parameter in forests with high MAT, but a strong positive correlation in forests with low MAT.

For the shape parameter, I find a significant interaction effect between stem growth rate and MAT ($p \leq 0.0001$; total model $R^2 = 0.19$). Stem growth rates correlate negatively with the shape parameter in forests with low MAT, but show a slight positive correlation in forests with high MAT.

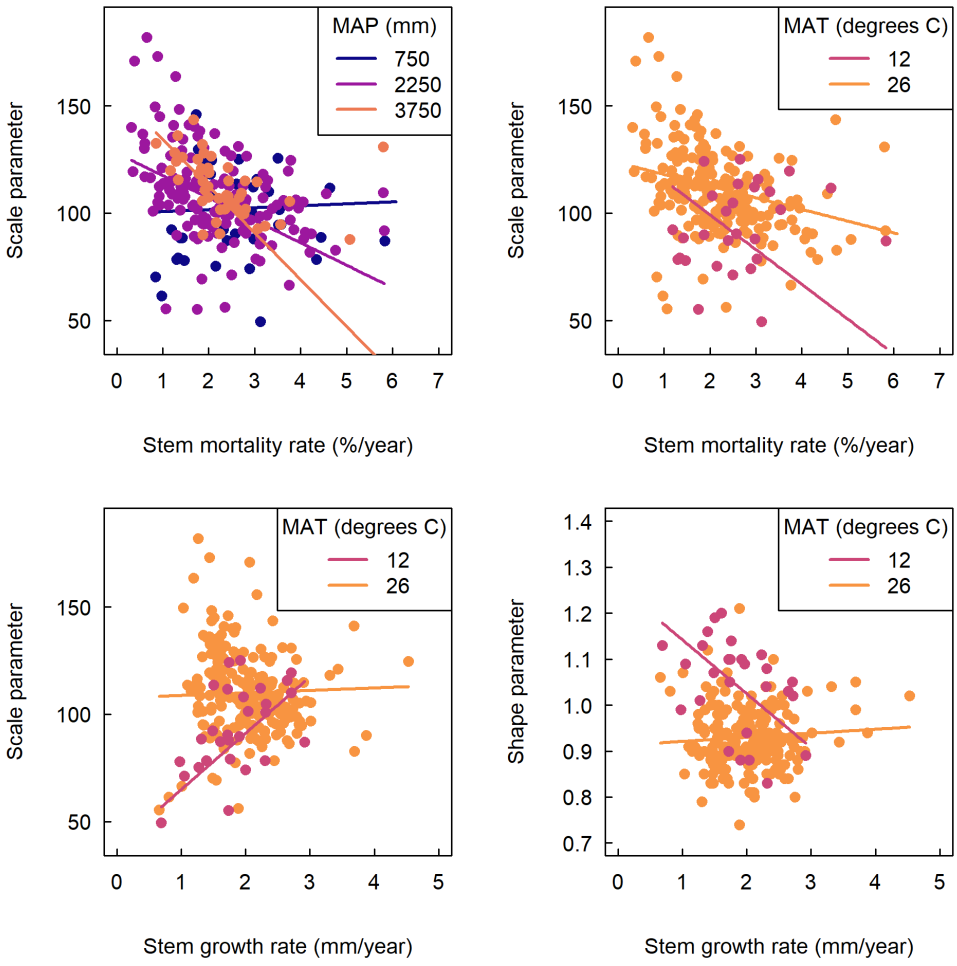

Figure 2.6: Relationships between the scale parameter and stem mortality rate, visualising significant interaction effects between stem mortality rate and (a) MAP and (b) MAT. To visualise interactions, data points are grouped into bins, and lines of best fit models are plotted for the mid-point values of each bin, detailed in the legend.

For the scale parameter, I find a significant interaction effect between stem mortality rate and the soil structure summary index ($p \leq 0.05$; total model $R^2 = 0.35$). Stem mortality rates correlate positively with the scale parameter in forests with poorer, less stable soil structure, and correlate negatively in forests with more stable soil structure.

I find no significant interaction effects between stem demographic rates and any of the soil fertility parameters for the scale parameter. For the shape parameter, I find no significant interaction effects between stem demographic rates and any of the soil parameters.

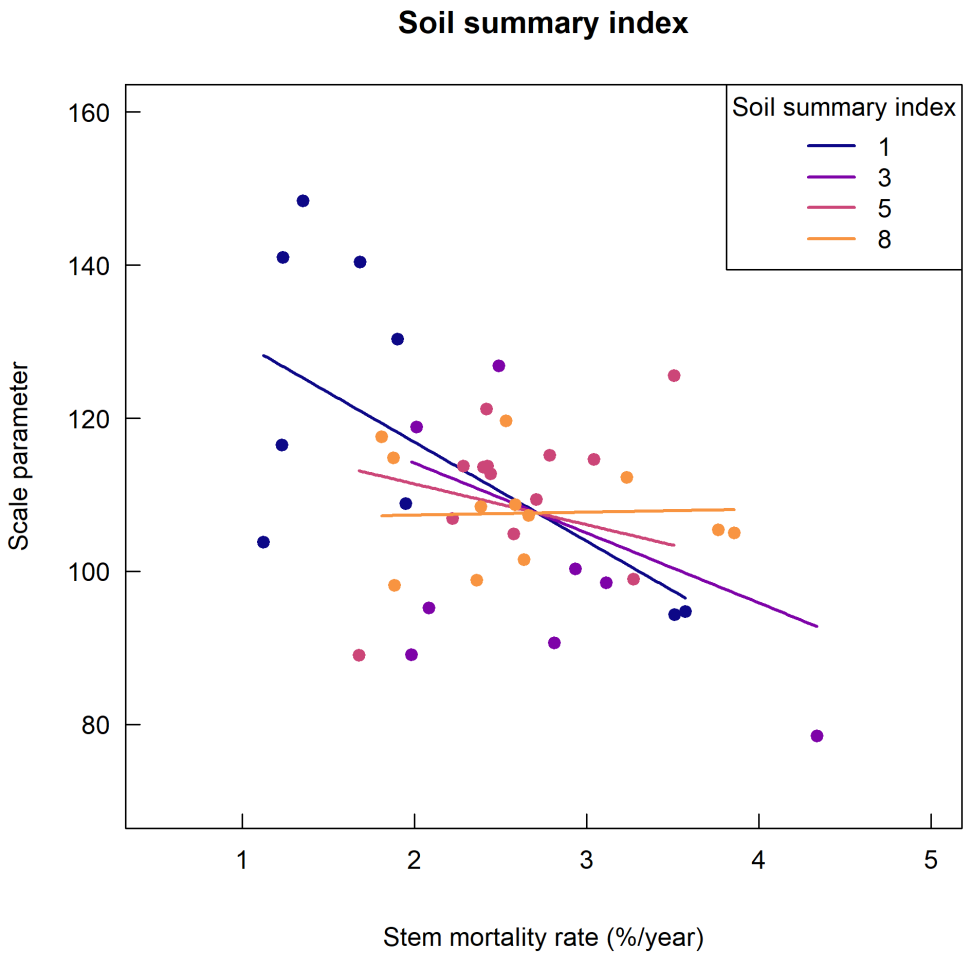

Figure 2.7: Relationships between the scale parameter and stem mortality rate, visualising significant interaction effects between stem mortality rate and (left) soil summary index; (right) soil structure index. Lower index values indicate a higher soil stability and/or a higher quality soil structure. To visualise interactions, data points are grouped into bins, and lines of best fit models are plotted for the mid-point values of each bin, detailed in the legend.

2.5 Discussion

My results show that there is significant variation in SSDs among forest types, and that this variation relates in different ways to variation in stem demographic rates. Across Neotropical forests, I find variation in SSDs both between and within forest types is high, suggesting that forest structure is shaped by continuous variation in demographic rates, climate, and soils (see also de Castilho et al., 2006; Quesada et al., 2012), rather than clustering into distinct structural types. Furthermore, across the full dataset the shape of size distributions appears relatively constrained (Figure 2.8), with low variation in the shape parameter, suggesting some universal constraints on the structure of old-growth forests across environmental gradients. However, my results do show a broadly east-to-west gradient of increasing stand evenness across lowland moist Amazonian forests, with highest evenness in the northern and eastern regions, declining to the south and west. This is consistent with previously documented gradients in basal area and mean stand DBH (Baker et al., 2004a; Baraloto et al., 2011; Quesada et al., 2012), and suggests that increases in AGB along this gradient are partly shaped by increases in the proportion of large stems.

Previous research has shown that stand structure is strongly contingent on the proportion of the largest stems (Bastin et al., 2015; Lutz et al., 2018; Araujo et al., 2020; Alves et al., 2010), findings which help to explain the variation in SSDs across different forest types. Light availability in the understorey is limited by frequencies of the largest, canopy-reaching, stems, such that frequencies of the smaller, understorey, stems are structured by competition for light (Farrior et al., 2016; Araujo et al., 2020). Therefore higher relative frequencies and larger average size of canopy trees act to constrain numbers of smaller stems (see e.g. Araujo

et al., 2020, comparisons with BCI size distributions; also Segura et al., 2002, in dry forests; Baker et al., 2016): the higher relative frequency of large canopy stems in the Guiana Shield and East Central Amazon appears to limit frequencies at the smallest stem sizes, as well as reducing overall stem numbers. Across the lowland moist forests my results indicate a broadly south-west to north-east gradient of increasing dominance of large canopy trees, which shapes the frequencies of smaller stems through competition for light.

Stand structure in montane and dry forest is more distinctive, as expected from previous studies of these forest types. Montane forest has a lower maximum DBH value, a very strong skew towards the smallest stem sizes - reflected in the on-average significantly lower shape value - and a high density of small stems. This result supports previous studies which find montane forests are characterised by lower AGB, basal area, and canopy height than lowland moist forest (Homeier et al., 2010; Spracklen and Righelato, 2014). Size distributions in dry forest are highly variable, particularly in terms of stand evenness. Overall, dry forests have lower stem numbers and lower maximum DBH than moist forests, suggesting a more open canopy. This is consistent with previous studies suggesting that dry forests show lower basal area, lower biomass, and a smaller stature than lowland moist forest (Murphy and Lugo, 1986; Malhi et al., 2006; Pennington et al., 2009).

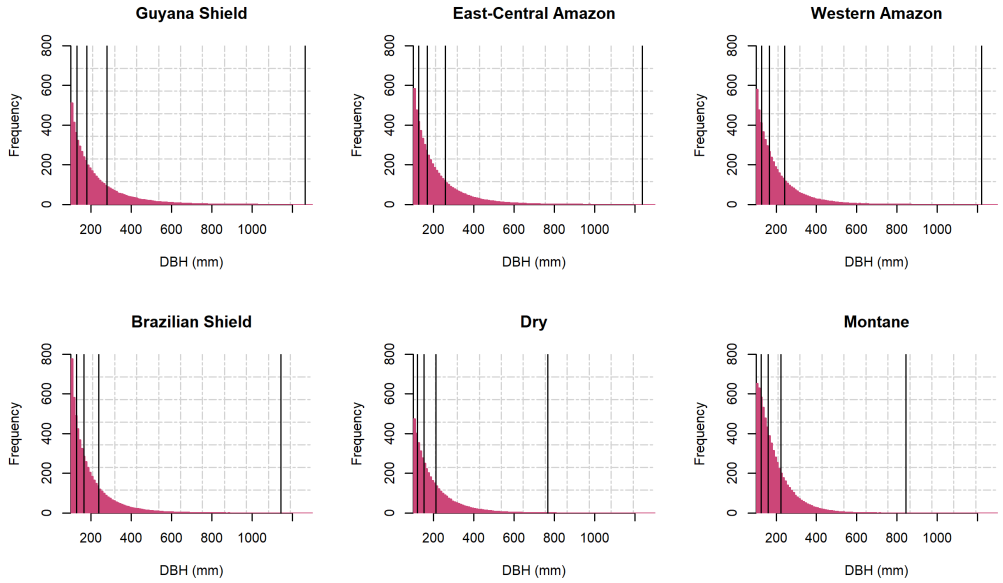

Figure 2.8: Histograms to visualise typical SSDs for 10ha stands of each forest type. Stem frequencies are calculated based on mean values for the scale parameter, shape parameter, and number of stems for each forest type, resampled (n = 100) from the corresponding Weibull distribution. Vertical lines show mean values for the 25% quantile, median DBH, the 75% quantile, and maximum DBH respectively.

While light availability appears to be structuring SSDs in lowland moist forests, my results suggest that different mechanisms may be occurring in dry and montane forests. The shapes of SSDs are similar across all forest types, however dry and montane forest stands are more open compared to the lowland moist forests: both forests, but particularly montane forest, show a low maximum stem size, suggesting a low frequency of canopy-dominating large stems, and dry forest supports a much lower stem density than other forests. This points to a more open canopy in both of these forest types, suggesting that, while these forests are perhaps less light-limited than lowland moist forest (Brienen et al., 2010; Lebrija-Trejos et al., 2011), stems are limited in their ability to attain large sizes. In dry forests, water availability is likely to place limits on maximum stem size (Segura et al., 2002;

Becknell et al., 2012), while in montane forests frequent physical disturbances such as landslides may reduce the frequencies of large stems (Dislich and Huth, 2012; Freund et al., 2021), with implications that these forests may not be at structural equilibrium.

The finding that higher stem mortality rates are associated with a less even stand structure and relatively fewer large stems, suggests that high rates of mortality limit survivorship of stems to the largest sizes, and thereby maintain a distribution skewed towards small stems. This corroborates previous findings that AGB stocks are structured by mortality rates, particularly stem mortality rates, and that AGB stocks are highest where mortality rates are low (Johnson et al., 2016; Rödig et al., 2017).

Forests in the Guiana Shield and East Central Amazon typify this pattern and show declines in stand evenness in response to increases in mortality and growth rates, such that the forests with the highest proportions of large trees occur where demographic rates are lowest. This indicates the importance of stem mortality in shaping the size structure of these forests (Johnson et al., 2016); where stem mortality rates are low, survivorship of stems to the largest sizes is higher, and so stands are able to support a high proportion of large stems (e.g. Nascimento et al., 2005). It is likely that the sensitivity of these forests to variation in mortality rates is a result of both the relatively low background mortality rates, and the relatively high proportion of large stems. Forests with this combination of characteristics may be disproportionately vulnerable to small increases in mortality, as losing a small number of the largest stems would disproportionately open up the canopy, stimulating growth of smaller stems, and further skewing the distribution (Laurance et al., 2006; de Paula et al., 2011). This points to the unique

importance of large canopy trees in structuring the forest (Farrior et al., 2016; Bastin et al., 2015), and I suggest that the demographic rates of the largest trees may be most important in determining forest structure in 'typical' lowland moist forest (Muller-Landau et al., 2006a; Malhi et al., 2015).

In contrast, stand structure in dry forests, montane forests, and the forests of the Brazilian Shield shows a very different relationship with demographic rates, with higher stand evenness associated with higher growth rates. These relationships suggest that these forests are structured by quite different mechanisms. Dry forests, montane forests, and forests on the south-eastern edge of the Amazon are more dynamic than the lowland forests of the Guiana Shield and central Amazon, and exhibit a high frequency of gap-creating disturbance events (Dislich and Huth, 2012; Marimon et al., 2014; Dalagnol et al., 2021; Freund et al., 2021). Here, it seems that variation in stand structure in these forests may be more strongly determined by variation in growth rates among sites, which controls the speed at which recovery from disturbance occurs (Dislich and Huth, 2012; Freund et al., 2021); the relative proportion of large stems in these forests is therefore positively associated with variation in growth rates.

These patterns are corroborated by my results illustrating that relationships between forest structure and demographic rates are mediated by a number of environmental variables. In warmer, wetter forests, typical of lowland Amazonia, higher stand evenness is associated with lower mortality and growth rates. In constrast, in forests with low MAP, stem mortality rates have a much smaller effect on stand evenness. In cooler forests - represented in this dataset by montane forests - stem mortality still has a negative effect on stand evenness, however growth appears to be a stronger control, with higher stand evenness and higher

maximum stand DBH strongly associated with higher growth rates. These forests are closer to environmental limits to growth than lowland moist forests - limited by water availability (Lebrija-Trejos et al., 2011) or temperature (Homeier and Leuschner, 2021) - resulting in growth limitation within stands, which may reduce the effect of stem mortality, but exacerbate the effect of growth on stand structure.

I also find evidence of interactions between soil physical structure and demographic rates in shaping forest stand structure. In forests on more stable soils, higher stand evenness is associated with lower mortality rates, while in forests on less stable soils, this association disappears or is reversed. Structurally poor soils are primarily concentrated in the Western Amazon, with soils of higher structural quality situated in the East-Central Amazon (Quesada et al., 2010, 2012), so this finding is consistent with the variation observed across forest types. Poorer soil structures are hypothesised leave forest stands more vulnerable to instability and structural damage, driving higher rates of stand turnover (Quesada et al., 2010): it is therefore likely that stand structure in forests on less stable soils would be shaped more strongly by stand growth rates, and the ability to recover more rapidly from perturbations to stand structure. The available soil data was limited to lowland Amazonian forests, and did not represent the full range of forest types considered in this paper; however it is expected that this relationship would be maintained or even strengthened by the inclusion of soil data from a wider range of sites. Montane forests in particular are located on unstable soils, with frequent disturbances and landslips creating a stand structure characterised by a higher frequency of canopy gaps (Asner et al., 2014) and fewer large, tall stems than moist, lowland forests (Murphy and Lugo, 1986; Becknell et al., 2012). As a result, a strong relationship between stand structure, growth rates and soil insta-

bility in these forests would be expected, with high growth rates being associated with greater stand evenness for the forests on highly unstable soils.

These results indicate that we might expect significantly different responses and resilience to environmental change across Neotropical forests. Most research to date has focused on understanding mortality as the primary driver of forest change (e.g. Johnson et al., 2016; Gora and Esquivel-Muelbert, 2021). Based on these results, it is likely that forests in the north-eastern Amazon Basin will be particularly sensitive to increases in mortality rates, with increases in mortality rates in these regions expected to result in a change in stand structure characterised by a loss of large stems (Esquivel-Muelbert et al., 2020) and, as a result, a loss of biomass potentially disproportionate to the observed increase in mortality. Low growth rates in these forests are also likely to result in slower recovery from disturbance than in more dynamic forests (Chave et al., 2020). The forests of the Guiana Shield and East-Central Amazon hold some of the largest biomass stocks in the Neotropics (Rödig et al., 2017), and so reductions in biomass in these forests will have significant implications for carbon storage in Amazonia.

However, my results also highlight the importance of understanding growth responses. Growth responses are relatively understudied; indeed the results show that when trends are considered at a regional scale, the strength of growth controls on forest stands are masked, and so appear secondary to mortality controls. However, for certain forest types, understanding growth controls will be essential for accurately parameterising forest responses to change. Dry forests, montane forests, and the forests of southern Amazonia appear to be more resilient to increases in mortality rates, but may be sensitive to declines in growth rates, such as due to increasing temperatures (Feeley et al., 2007; Battipaglia et al., 2015;

Sullivan et al., 2020). Equally, these forests would be expected to respond quickly to any increases in growth rate, as might be expected from carbon fertilisation effects (Cox et al., 2013; Hofhansl et al., 2016). These forests are significant, but often undervalued, components of the tropical carbon sink (Duque et al., 2021; Becknell et al., 2012): understanding their diverse responses to global change will be essential for the future of the South American carbon sink.

Chapter 3: Using forest census data to simulate forest structure

3.1 Abstract

Individual-based modelling approaches are very useful in modelling forest dynamics, with strong potential to provide insights into controls on forest structure and function, and to generate accurate predictions of forest responses to global change. Monitoring data from permanent sample plots (PSPs) represent an important dataset on forest dynamics which is long-term and global in nature, but under-utilised in broad-scale modelling approaches.

Previous work has used annual growth data from tree rings to accurately simulate individual tree growth trajectories within a single species. Here, I extend this approach to use multi-species data from the PSP network of the Quebec provincial forest inventory program. I use growth rate data from repeated plot census measurements to build individual tree growth trajectories.

I test these trajectories in combination with four different mortality functions - fit using the census data - to simulate stand structure of mature forest stands. I compare and validate the simulation outputs from different mortality functions using observed tree ring growth trajectories.

I find that this approach is able to accurately simulate a number of key stand structural parameters. In particular, I show that these simulations successfully capture variation in structural parameters among forest types and across different bioclimatic domains, suggesting that this approach will be of use in understanding global variation in forest responses to change.

My results also highlight the importance of mortality in shaping stand structure. The accuracy of the simulation outputs varies among mortality functions, suggesting high sensitivity of stand structure to variation in mortality rates.

The methods I develop in this chapter will be broadly applicable to typical PSP datasets with ≥ 3 censuses, and so I anticipate that this method will have a wide range of applications in exploring the links between demographic rates, stand structure and biomass stocks across forests globally, and by extension in understanding and predicting forest responses to global change.

3.2 Introduction

Forests hold a large proportion of terrestrial biomass and as such are a key component of global carbon stocks and flows (Pan et al., 2011; Anderson-Teixeira et al., 2016). Understanding forest responses to environmental change is a key research priority; in particular, improving our knowledge of the effects of environmental drivers on forest stand structure and dynamics is essential to constrain future projections of forest trajectories.

Forest stand structure, or the frequency distribution of stems across different size classes, is a key determinant of aboveground biomass (AGB), and, by extension, an important component in predicting biomass responses to global change (Baraloto et al., 2011). Stand structure is ultimately shaped by demographic rates: recruitment, growth, and mortality (Coomes and Allen, 2007; Caspersen et al., 2011). Demographic rates are determined by a complex range of factors, both intrinsic (species identity and life history traits) and extrinsic (climate, soils, and environmental disturbances); however at a fundamental level the magnitude, both absolute and relative, of these demographic rates is likely to shape stand structure

in predictable ways. As a result, there is high value in developing a mechanistic understanding of the influence of demographic rates on stand structure in order to improve our understanding of the impacts of global environmental change on forest biomass. In particular, a mechanistic approach is likely to highlight potential non-linearities between changes in demographic rates and changes in forest structure and biomass, which are challenging to detect in correlative approaches (Fauset et al., 2019).

Individual-based modelling approaches are well-suited to explore these relationships; they model stems individually, and so are able to link information on demographic rates, species traits and responses to disturbance with whole-forest outcomes (Pacala et al., 1996; Fischer et al., 2016; Rödig et al., 2017). Models are typically built around core assumptions of forest dynamics which are used to drive the model function, including gap formation (Pacala et al., 1996; Fischer et al., 2016), forest succession (Maréchaux and Chave, 2017), and competition for light (Chave, 1999). More complex approaches may integrate information on plant physiology and include representation of photosynthetic production and resource allocation (e.g. Fauset et al., 2019).

Because of the range of ecosystem processes included in most modelling approaches, specific data inputs are often required to calibrate and parameterise models, including data on plant functional traits (Rüger et al., 2020), crown position (Farrior et al., 2016), resource use (Pacala et al., 1996; Chave, 1999), or photosynthetic rate (Fauset et al., 2019). Data for model calibration can be sourced from forest inventories (Farrior et al., 2016; Rüger et al., 2020), functional trait databases (Maréchaux and Chave, 2017) and remote sensing (Fischer et al., 2019). Although the use of this data can result in accurate simulations of stand structure

for individual sites, it is often intensive to gather and may not be readily available beyond the site studied. As a result, scaling up these models to simulate forest dynamics across wider regions may rely on extrapolation of data from a limited number of sites or broad ecological assumptions to generate summary parameters (e.g. Rödig et al., 2017). Furthermore, models which are driven by processes such as tree physiology or resource use dynamics, are less well-suited to testing how simple demographic processes affect long-term forest structure and biomass.

Instead, simpler approaches will enable mechanistic analysis of the effect of demographic rates on forest structure, and allow models to be applied to a wider range of sites without relying on generalised assumptions. One approach is through use of simple stochastic growth simulations, which randomly sample growth increment data to generate simulated trajectories of individual stem growth (Lieberman and Lieberman, 1985; Lieberman et al., 1985). Initial development of these simulations used growth rate estimates derived from forest inventory data (Lieberman and Lieberman, 1985; Lieberman et al., 1985); the approach has been subsequently adapted to use growth increments measured from tree rings as input data (Brienen et al., 2006). In addition, autocorrelated growth was incorporated by sampling based on the previous years growth rate and DBH of the stem; this produced a realistic spread of trajectories when validated against the tree ring data (Brienen et al., 2006).

These models are simple, require minimal data input, and use observed growth data, meaning that they offer a foundation for building a widely-applicable individual-based model to explore links between demographic rates and forest structure. Because of the small range of input parameters required, a model could be parameterised using forest inventory data generated from long-term forest

permanent sample plots. Worldwide, strategic networks of PSPs have collected decades of data on forest structure, function, and composition, and represent a huge diversity of data across local, national, and international scales, with monitoring efforts continuing to develop and expand rapidly (ForestPlots.net et al., 2021). Studies range in size from intensive monitoring of individual plots, through national inventory networks (Bechtold and Patterson, 2005; Gray et al., 2012), up to significant international collaborations, such as the ForestPlots and ForestGEO initiatives (ForestPlots.net et al., 2021; Lopez-Gonzalez et al., 2011; Anderson-Teixeira et al., 2015). The consistency in monitoring methodologies among and within networks mean that there is comprehensive data available on stem DBH, growth, and mortality across large spatial scales, and so a simulation approach using inventory data would be transferable across plot networks.

The accuracy of using growth increment data to simulate individual tree trajectories has not yet been validated using independent datasets, and, while the approach has been applied to a number of species individually, the it has not been tested with data from multi-species forest stands. Validation of a simulation using forest inventory input data could be achieved using tree ring data, using a similar method as that of Brienen et al. (2006), but ensuring independence between the datasets. Tree ring measurements provide annual estimates of individual tree growth over long time periods, with growth sequences potentially extending over several centuries (Babst et al., 2014). Because tree ring data can provide estimates of stem and stand age, lifetime growth dynamics, and historic stand growth rates (Baker, 2003; Brienen and Zuidema, 2006), tree ring data be used to validate growth trajectories and stand age distributions simulated from inventory data, and ultimately determine whether short-term growth measurements can be used simulate long-term growth trends.

This approach requires spatially overlapping datasets of forest inventory data and tree ring data. To be able to fully validate a simulation, tree ring data needs to be representative of the forest stand, and so available for the majority of species present, and randomly sampled across species and size classes. This is uncommon, as tree ring data is often sampled opportunistically or non-randomly. Additionally, many sites are dominated by species that don't set down tree rings, and so any available data is unrepresentative of the species composition of the site. The PSP network of the Quebec provincial forest inventory program (Ministère des Forêts, 2016; Ministère des Ressources naturelles et des Forêts (MRNF), 2022) contains forest census data and randomly sampled tree ring data surveyed from across the same set of plots, providing a unique dataset of forest structure and dynamics across a broad bioclimatic gradient with which to build and validate an individual-based simulation.

Here, I integrate forest inventory data and tree ring data from the PSP network of the Quebec provincial forest inventory program to extend the methods developed by Brienen et al. (2006), and build and validate a full individual-based simulation of forest stand structure. This scales up the approach from simulation of single-species growth trajectories, to simulate growth trajectories within diverse multi-species stands, allowing ultimately for stand-level stem size distribution estimates to be generated. In developing the approach, I test application of growth trajectories in combination with four different mortality functions, parameterised using the census data, to explore the influence of mortality on stand structure. Using a combination of forest inventory and tree ring data, I validate the simulation across axes of space and time, including validation of stand structure, lifetime stand growth rates, and stand age across four diverse ecological regions. I show that stand structural parameters, and variation in stand structure across a

significant environmental gradient, can be accurately simulated using basic forest inventory data on stem DBH, annual stem growth rates, species wood densities, and stand-level estimates of mortality rates.

3.3 Methods

3.3.1 Quebec provincial forest inventory program

I used data from the "BAS1" basic permanent sample plot network of the Quebec provincial forest inventory program (Ministère des Forêts, 2016; Ministère des Ressources naturelles et des Forêts (MRNF), 2022), across bioclimatic domains 3 - 6, defined based on climate and vegetation composition (Figure 3.1). There are two temperate domains, which are situated between 45°N and 48°N: domain 3, which is deciduous forest dominated in composition by maple and yellow birch, and domain 4, which is mixed forest, dominated by balsam fir and yellow birch. Domain 3 has a mean annual temperature (MAT) of 3°C, and domain 4 has MAT of 2°C. Domains 5 and 6 are both closed-canopy boreal forest domains, situated between 48°N and 52°N. Domain 5 is dominated by balsam fir and white birch, with MAT of 0.8°C and domain 6 is dominated by spruce with MAT of -1°C. A network of ~12000 permanent sampling plots was established in the early 1970s at varying sampling intensities across these domains:

- One plot per 26km^2 in the bioclimatic domain 3
- One plot per 103km ^{2} in the bioclimatic domains 4 and 5
- One plot per 259km^2 in bioclimatic domain 6

All plots are circular, with a radius of 11m (Duchesne et al., 2019). Plots have been repeatedly resampled since the 1970s, with data from up to 6 censuses available

across all bioclimatic domains. At each census, all trees with diameter at breast height (DBH) >91mm in the plot are measured and their species identity, DBH, and status (e.g. recruit, alive, or dead) recorded.

Plots were excluded from use in this analysis if they showed:

- Evidence of disturbance that had removed >75% of the canopy (e.g. as a result of fire, clear cutting, severe insect outbreaks etc.)

- Evidence of disturbance that had affected >25% of the canopy (e.g. as a result of partial clearance or stand thinning interventions, partial burning, partial dieback etc.)

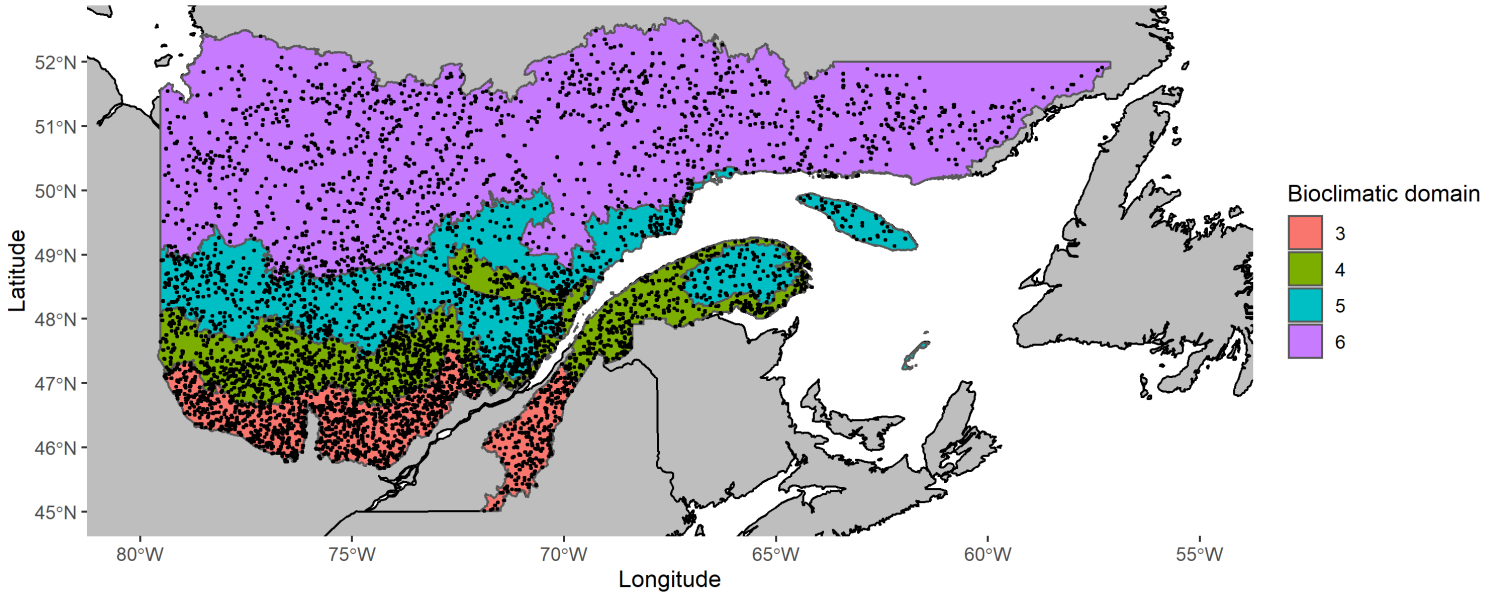

Figure 3.1: Map to show locations of all the forest inventory plots used in the analysis, within bioclimatic domains 3-6.

3.3.2 Data processing

For growth trajectory simulations, only stems recorded as "alive" or "recruits" were selected from the plot dataset. For mortality rate calculations, dead stems were additionally included. Individual stem measurements were removed if measurement inconsistencies were recorded in the database (e.g. as a result of errors in species identification, DBH inconsistencies, or duplication of records).

Annual growth rates for each census interval were calculated by dividing census interval growth by census interval length. Annual growth rate measurements of $<$ -2mm were removed, and annual growth rate measurements between -2mm and 0mm were set to 0mm for the purpose of the growth trajectory simulations. Previous growth rates were calculated for each census interval where applicable: for the simulations and growth-dependent mortality calculations, measurements without previous growth rates were excluded. Within each dataset, recruits were pre-identified by a code, and a subset of annual growth data for new recruits was compiled.

All stems for species with an unknown wood density were removed.

3.3.3 Model specification

3.3.3.1 Growth trajectories I use an approach similar to that applied by Brienen et al. (2006; 2012) to build growth trajectories for individual stems. In this approach, trajectories are built incrementally by repeated sampling of growth rates from a set of observed growth rate data.

The starting diameter at breast height (DBH) for each simulated tree was obtained by randomly sampling a stem from the subset of recruits. The initial growth

increments were then generated by adding the measured annual growth rates of the sampled recruit to the starting DBH. I used an initial growth window of 10 years, corresponding approximately to the average census interval length in the dataset.

Further growth increments were then generated by sampling annual growth rates from the full dataset. Growth increments tend to increase with stem diameter, such that small stems grow more slowly than large stems, and within-stem growth increases as stem diameter increases (Brienen et al., 2006). Growth increments are also dependent on previous stem growth rates; stems with higher previous growth rates will tend to have higher growth at the next growth step than stems with lower previous growth rates (Kohyama et al., 2005; Brienen et al., 2006). Accounting for this autocorrelation of growth is essential in generating a realistic spread of growth rates, and to prevent all growth trajectories from converging on a similar mean growth rate. This can be done by sampling stems based on the stem's current diameter and previous year's growth increment, in order to generate autocorrelation within the simulation (Brienen et al., 2006).

Work by Brienen et al. (2006) only considered growth trajectories of individual species, whereas here I aim to adapt this work to generate growth trajectories for complete forests, including multiple species. Therefore, I also consider the effect of creating a sampling frame based on the wood density of the initial stem, to approximate species identity. Wood density also correlates negatively with growth rate, and so is expected to further increase the autocorrelation of trajectory growth.

I tested five different approaches to build individual growth trajectories, such that the next growth increment was sampled from stems with parameters falling

within:

1. The full stem dataset; or a subset of the dataset based on:
2. A diameter window, set as the current DBH of the simulated stem +/- 1%;
3. A growth rate window, set as the mean annual growth rate of the simulated stem over the preceding 10 years +/- 0.25; or
4. A wood density window, set as the exact wood density of the initial sampled stem
5. The combined effect of the above approaches, sampling according to growth rate, wood density, and diameter (Figure 3.2)

Once an annual growth increment was sampled, annual growth steps were added to the trajectory according to the length of the census interval from which the sampled growth increment was calculated. This was repeated until a total of 300 growth steps had been generated, giving each trajectory a length of 300 years. A unique diameter window and growth rate window were calculated for each sample, based on the DBH at the most recent growth step and the mean annual growth rate over the previous 10 years (Figure 3.2).

I tested the simulation approaches by simulating growth trajectories and comparing the spread of individual trajectories to observed tree ring trajectories. This was done for each bioclimatic domain, with domain-specific growth-dependent mortality equations applied to the trajectories, as detailed below, to ensure comparability with the observed tree ring trajectories. To compare trajectory spreads, I assessed the ability of each approach to accurately simulate the spread of ages across stems of set sizes, and the spread of sizes across stems of set ages, by comparing histograms of size and age distributions between simulated trajectories

and observed tree ring trajectories. I used Kolmogorov-Smirnov tests to test for significant differences in the distributions of simulated and observed age and size distributions. I tested size distributions at 16 ages, and age distributions at 16 DBH values across all 4 bioclimatic domains, to give a total of 128 tests. Where the distributions were significantly different from each other, I used the D statistic as a measure of difference to determine which approach generated the simulations with the greatest similarity to the observed data.

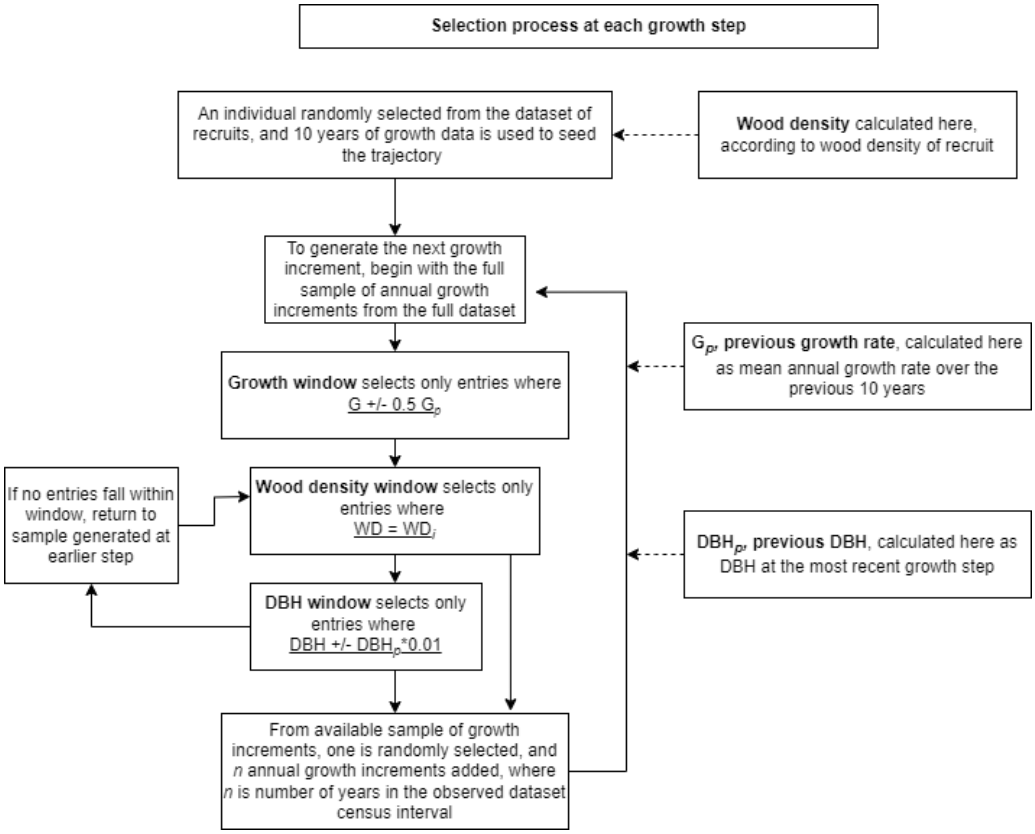

Figure 3.2: Schematic to show method for building trajectories

3.3.3.2 Mortality models To simulate full forest dynamics, at each annual growth step from the starting DBH a model of the mortality probability distri-

bution was applied to calculate a unique annual probability of mortality for each stem. Each trajectory, at each growth step, would have a chance of being killed according to this probability. Trajectories were allowed to continue growing until stems were killed by the mortality function.

For each bioclimatic domain, I estimated the stand-level mortality from the census data across all census intervals and plots. Data for each stem at each census interval was included as a separate entry, and the stem was identified as either alive or dead at the end of the census interval. Mortality was then estimated using a sample of 2000 stems from the full dataset of stem mortality.

Mortality was modelled in four different ways:

1. **A constant stem mortality rate**, calculated as the exponential mortality coefficient μ,

$$\mu = \frac{ln(n_0) - ln(n_0 - n_d)}{t} * 100$$

   where n_0 is the number of stems at the start of the census interval, n_d is the number of stems that die in the census interval, and t is the mean census interval length (Lewis et al. 2004).

2. **A size-dependent stem mortality function**, using the equation

$$M(x) = a \exp^{b(x)} x^c$$

   where $M(x)$ is the instantaneous mortality rate ($year^{-1}$), and a, b and c are plot-specific parameters (Kohyama et al. 2015) (Figure A3.1).

3. **A growth-dependent stem mortality function**, using the equation

$$M(x) = a \exp^{-b(x)} + c$$

where $M(x)$ is the instantaneous mortality rate ($year^{-1}$), and a, b and c are plot-specific parameters (Camac et al. 2018) (Figure A3.2).

4. **A combination of a growth-dependent mortality function and a size-dependent mortality function**, where, at each annual growth step, the higher mortality rate of equations 2. and 3. was selected.

Mortality rate estimates are influenced by the census interval length, as within each census interval there are some trees which recruit and die without being measured in either census. As a result, as census interval lengths increase, the mortality calculation will increasingly underestimate the true mortality rate (Lewis et al., 2004b). This effect can be corrected for by using a correction of

$$\mu * t^0.08$$

where μ is the rate estimate, and t is the census interval length (Lewis et al., 2004b). I apply this correction to all mortality rate calculations used in this chapter, using the mean census interval length for each bioclimatic domain or species dataset.

Mortality is applied at each annual growth step in each trajectory, and the trajectory either ends (the stem is killed) or continues to the next growth step (the stem survives) according to the probability of mortality. Where the constant mortality rate is used, the probability of mortality does not vary within the simulation.

However, where mortality is modelled as growth- or size-dependent, a unique probability of mortality is calculated for each annual growth step in each trajectory, based either on the previous years growth rate (growth-dependent mortality), or the current DBH of the stem (size-dependent mortality).

Sets of 5000 trajectories, with each trajectory representing the growth of an individual stem from 91mm to death, were generated for each bioclimatic domain and each mortality function.

3.3.3.3 Stand structure simulations To simulate stand structure from the simulated growth trajectories, I randomly sampled each year a cohort of 100 growth trajectories from the full set of trajectories, and "recruited" them into the stand (Figure A3.3). This was repeated each year for 300 years, to ensure that all of the stems initially recruited in year 1 had died and the stand was "mature" (i.e. had reached an equilibrium). The DBH of all stems alive at year 300 were sampled to provide a simulated stand structure and stem size distribution. I tested the sensitivity of the simulation to recruitment and time to maturity by running the simulation with a range of sample sizes of recruits and different lengths of time to maturity, and compared parameter estimates across the ranges. I found that parameter estimates are robust to variation in recruitment sample size and time to maturity (Figure A3.1).

3.3.4 Quebec tree ring data

To validate the simulation approach (see next section) I used tree-ring measurement data compiled by the Quebec provincial forest inventory program. Between 1996 and 2012, tree cores were sampled from permanent sample plots. In each

plot, 5 trees >91mm DBH were selected randomly and sampled at a height of 1m above ground level.

Cores were processed following standard procedure (dried, glued to a wooden tray, and sanded), so that ring boundaries could be detected under magnification and measured using the WinDendro image analysis system to an accuracy of 0.001mm. Tree growth trajectories were then compiled from annual growth steps. Quality control on core data was conducted to remove incomplete cores and to remove cores where significant differences between measured field DBH and DBH calculated from tree rings were recorded. Following the quality control method used by Caldwell (2018), for each species a linear model was fit to the relationship between DBH as measured at sampling and DBH as calculated from tree growth rings. If the DBH as calculated from the tree growth rings fell outside +/- 25% of the expected value for the measured DBH of that individual, the individual was discarded.

For the tree ring data to be suitable for validating the simulations, it is important that it is representative of the forest stand, and aligns with the parameters observed in the forest inventory data. Not all species are represented in the tree ring dataset. Conifer species are fully represented, along with several deciduous species, however a number of deciduous species are missing. This is particularly significant in the most southerly bioclimatic domains, where there are a greater proportion of deciduous species. In contrast, in bioclimatic domains 5 and 6 - the most northerly domains - the vast majority of species are represented in the tree ring sample.

Despite the discrepancies in species composition between the datasets, the size structure of the tree ring sample is broadly representative of the size structure

observed from the plot data (Fig. 3.3, Table 3.1). The largest deviations are seen, as expected, in bioclimatic domains 3 and 4, while the tree ring sample from bioclimatic domain 6 is highly representative of the plot census stand structure in this domain. The tree ring sample does fail to capture the maximum DBH recorded in the stand, which is expected as very large stems are rare in natural forests and the tree ring sample is significantly smaller than the plot census sample.

Table 3.1: Comparisons of stand structure summary statistics between plot census data and the tree ring sample, calculated for each bioclimatic domain. All values are in mm.

		Q1 DBH	Mean DBH	Median DBH	Q3 DBH	Maximum DBH
Bioclimatic domain 3	Plot data	112	178	145	209	880
	Tree ring data	112	170	148	204	567
Bioclimatic domain 4	Plot data	110	161	137	185	1089
	Tree ring data	114	166	149	201	583
Bioclimatic domain 5	Plot data	107	146	129	166	740
	Tree ring data	109	149	135	174	496
Bioclimatic domain 6	Plot data	106	138	127	158	583
	Tree ring data	107	138	127	158	505

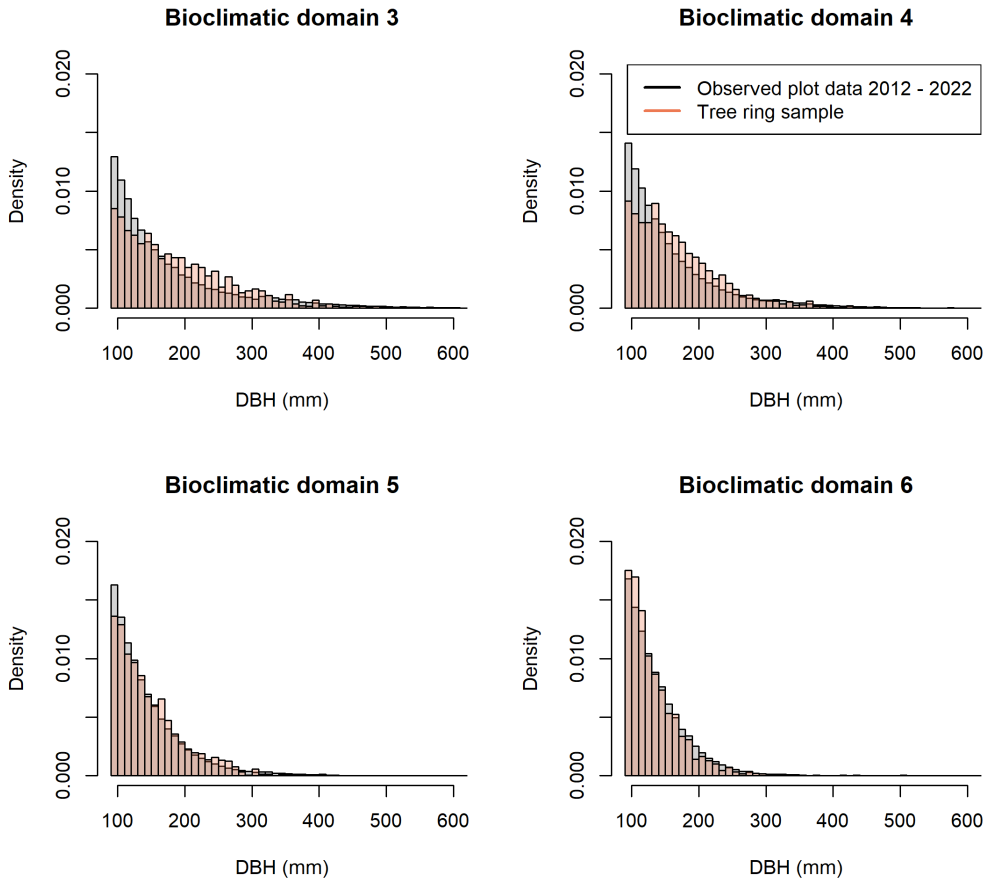

Figure 3.3: Stem size distributions for plot census stand structure vs. stem size distributions in the tree ring sample

3.3.5 Stand structure validation

The outputs of the simulation were validated against observed plot census data and tree ring data, to assess the ability of the simulation to accurately model stem growth dynamics and stand structure across multiple parameters. I assessed parameters describing the immediate stand structure, as well as parameters relating to stand dynamics, such as mean growth rate and stand age, to assess the

accuracy of the simulation.

Stand structures generated from the simulated trajectories for each bioclimatic domain were compared against observed plot census data and tree ring data to validate the simulation approach. I simulated two different sets of stands for these comparisons: 1) for comparisons of simulated and observed size structures, I simulated stands using all data from all species and plots for each bioclimatic domain; 2) for comparisons of stand age structures and growth rates obtained from tree ring data, I simulated stands including only data from the species represented within the tree ring dataset.

For comparison 1), within each bioclimatic domain I compared the outputs of all four mortality functions against the stand structures observed in the plot data, including the most recent census of each plot recorded between 2009 and 2018. If no censuses were available for the plot within these dates, the plot was excluded. I compared mean, median, the 75% quantile, and maximum DBH, and the shape and scale parameter of the distribution based on a Weibull distribution fit.

For comparison 2), I used only the growth-dependent mortality function to simulate stand structure, as this function performed best at simulating stand structure when assessed against observed plot data using the above parameters (comparison 1). I compared mean and median DBH and the shape and scale parameter of the distributions based on a Weibull fit between the simulated distributions and the tree ring sample. I compared mean stand age of the simulated stand with that of the tree ring sample, where mean stand age was calculated as the mean of all individual ages since 91mm. I also compared the distribution of annual growth rates, calculating the mean of all the annual growth rates of the stems throughout their lives for the simulated stand and the tree ring sample.

3.4 Results

3.4.1 Simulating trajectories

I find that carrying out simulations without diameter-dependent growth, growth autocorrelation, or wood density-dependent growth generated a poor simulation of the range of trajectories observed in the tree ring data across bioclimatic domains. The simulated trajectories tend to converge on a similar mean growth rate, and so fail to cover the spread of growth rates seen in natural forests. This approach is poor at simulating accurate age and DBH distributions across the full range of trajectories considered, and 70% of the age and DBH distributions tested were found to be significantly different from the observed distributions.

I find that the best method for simulating an accurate spread of trajectories, as well as accurate distributions of ages and sizes, is to include growth autocorrelation, diameter-dependent growth, and wood density-dependent growth. Inclusion of all of these factors generates trajectories with a spread similar to that observed in the tree ring data, as well as generating age and size distributions that realistically simulate observed age and size distributions across the full range of ages and sizes considered (Figures 3.4 - 3.7; Table A3.1 - A3.2). I found no significant differences between observed and simulated age and DBH distributions in 88% of tests.

Use of growth autocorrelation alone is nearly as effective at simulating the spread of trajectories, and I found no significant differences between observed and simulated age and DBH distributions in 87% of tests. However, I find that, where distributions are significantly different, inclusion of growth autocorrelation, diameter-dependent growth, and wood density-dependent growth, generates

simulated distributions which are more similar based on the D statistic to the observed distributions than use of growth autocorrelation alone. This was observed in 10% of total tests, and occurs in particular in accurately simulating the age distributions of the largest stems. As a result, going forward I use a simulation approach which includes growth autocorrelation, diameter-dependent growth, and wood density-dependent growth.

I find that, on its own, the effect of including diameter-dependent growth using DBH windows is relatively small, and I found no significant differences between observed and simulated age and DBH distributions in only 34% of tests. The effect of including wood density-dependent growth on its own is larger, and I found no significant differences between observed and simulated age and DBH distributions in 41% of tests. Both the use of diameter-dependent growth and wood density-dependent growth alone are able to generate accurate DBH distributions up to around 15 years of age, and accurate age distributions up to around 160mm DBH, but decline in accuracy beyond this.

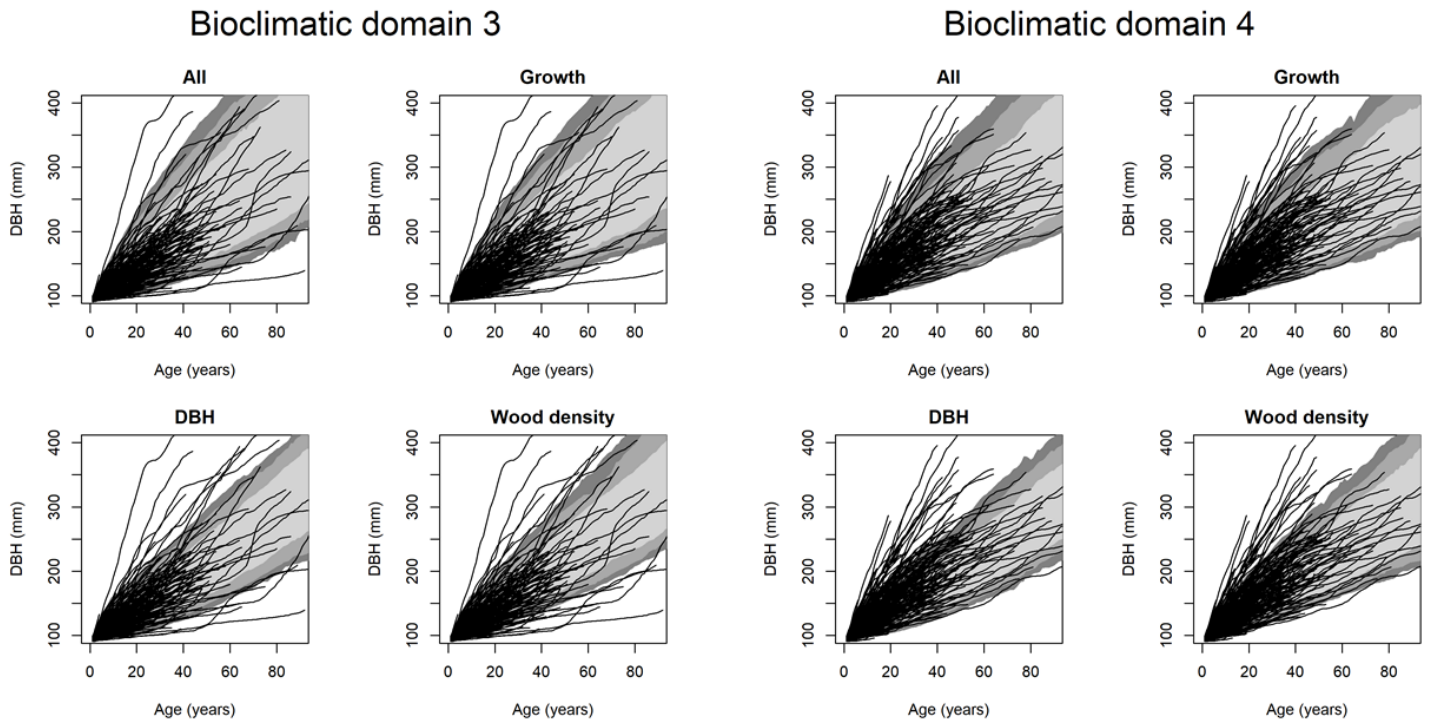

Figure 3.4: Trajectory outputs under different sampling frames for (left to right) bioclimatic domains 3 and 4. From light to dark, shaded grey areas show the 75%, 90% and 95% quantiles of simulated trajectories, while black lines show a sample of 300 observed tree ring trajectories.

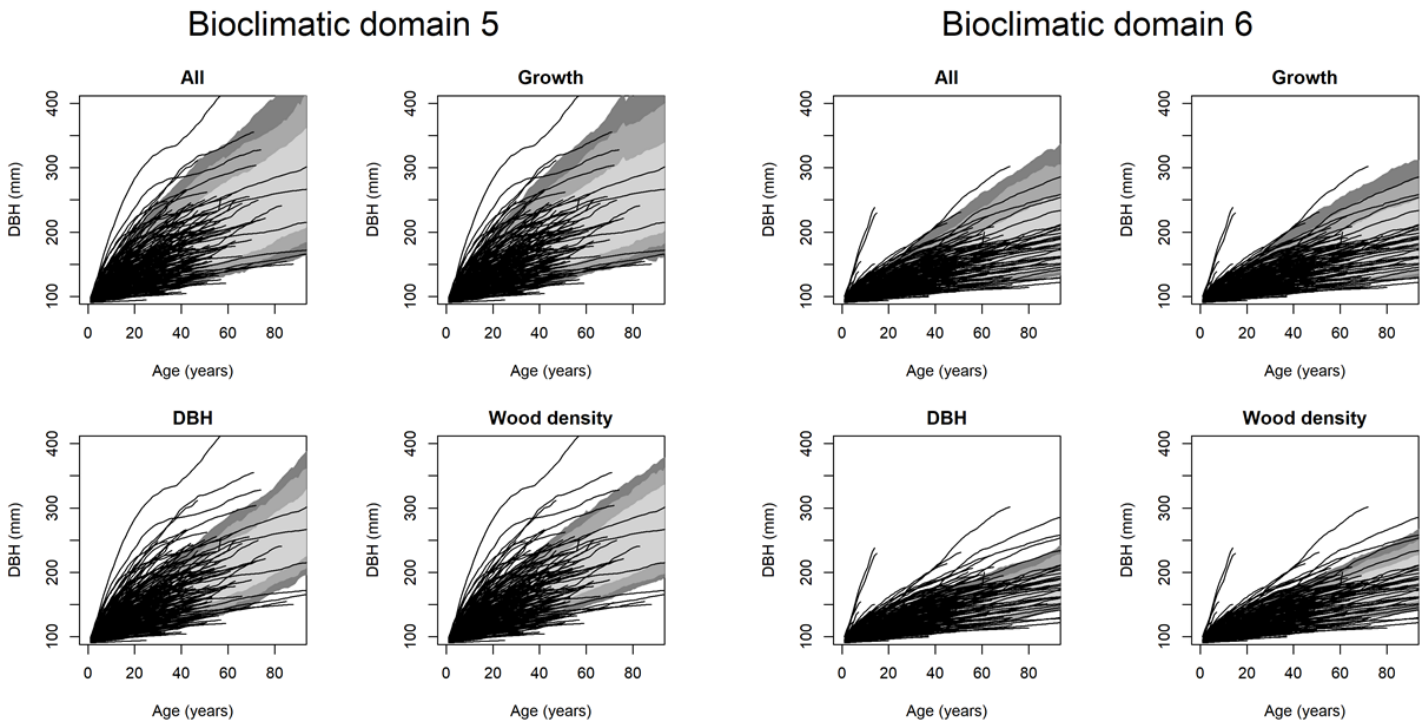

Figure 3.5: Trajectory outputs under different sampling frames for (left to right) bioclimatic domains 5 and 6. From light to dark, shaded grey areas show the 75%, 90% and 95% quantiles of simulated trajectories, while black lines show a sample of 300 observed tree ring trajectories

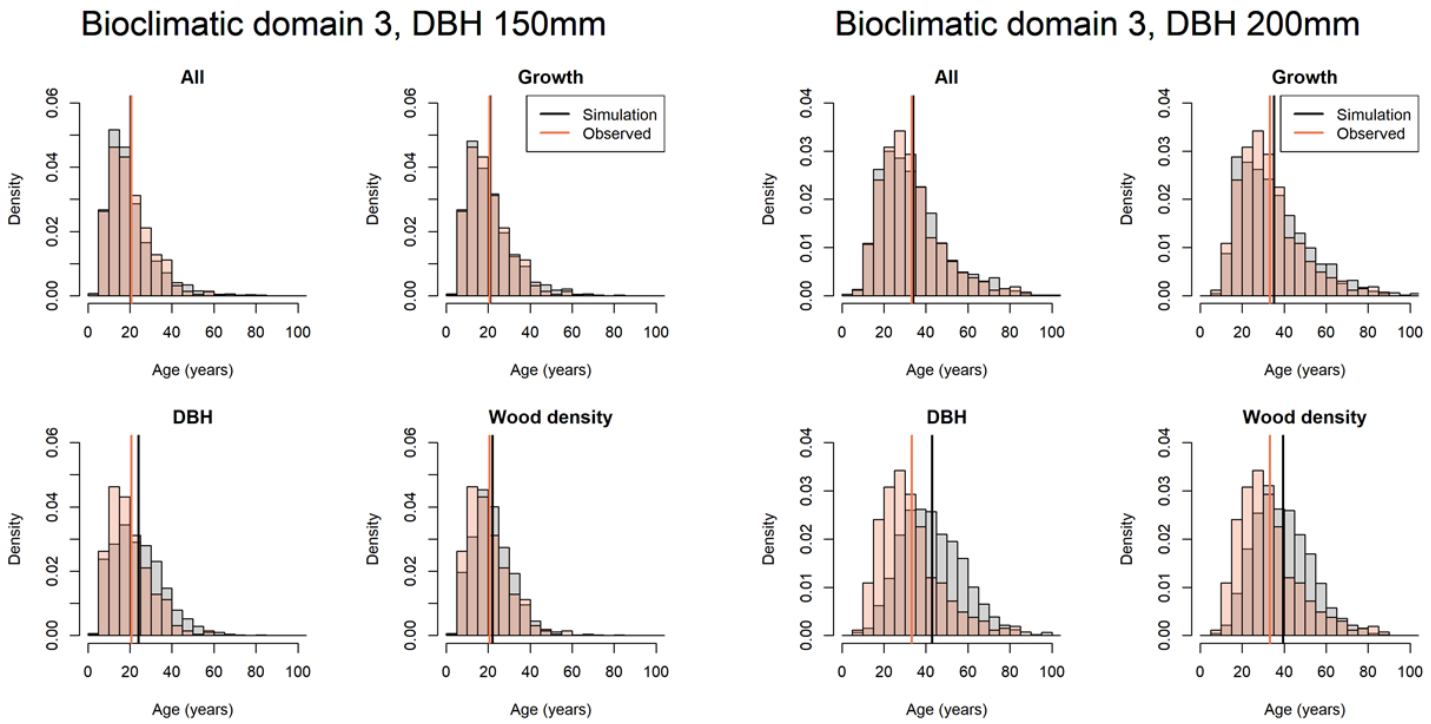

Figure 3.6: Histograms to compare the spread of simulated and observed stem ages across stems with DBH of 150mm and 200mm respectively, under different sampling frames. Vertical lines show the mean stem age for each distribution.

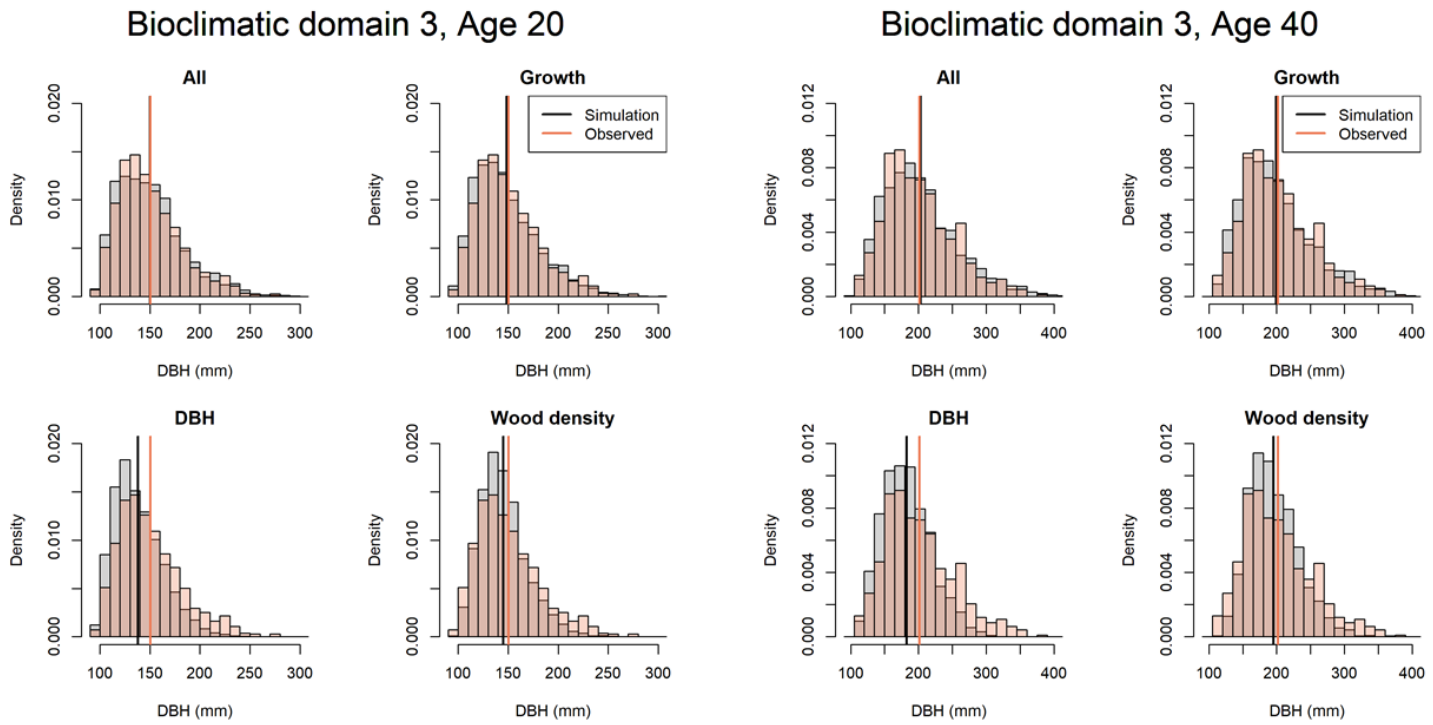

Figure 3.7: Histograms to compare the spread of simulated and observed stem sizes across stems with ages of 20 and 40 years respectively, under different sampling frames. Vertical lines show the mean stem size for each distribution.

3.4.2 Stand simulations

Stand structure, stem growth rates, and stem mortality rates vary between bioclimatic domains in Quebec (Table 3.2). Mean and median stand DBH and the scale parameter are highest in bioclimatic domain 3, and decrease towards bioclimatic domain 6. The scale parameter describes the evenness of the stand, where a higher scale parameter value is associated with a greater relative frequency of large stems. Mean stem growth rates are also highest in bioclimatic domain 3, and lowest in bioclimatic domain 6. Age also varies across bioclimatic domains, with the lowest mean stand age recorded in bioclimatic domain 5, and the highest mean stand age recorded in bioclimatic domain 6. Estimates of stem mortality rates are highest in bioclimatic domain 3, and decrease towards bioclimatic domain 6, mirroring the trends observed in stem growth rates. The variation in mortality rates across bioclimatic domains is consistent regardless of which mortality model is applied.

Table 3.2: Stand structure summary statistics for each bioclimatic domain based on observed plot data, observed tree ring samples, and modelled mortality rates from plot census data

	Bioclimatic domain 3	Bioclimatic domain 4	Bioclimatic domain 5	Bioclimatic domain 6
Mean stem size (mm)	183.00	165.0	148.00	139.00
Median stem size (mm)	149.00	140.0	132.00	127.00
Shape parameter	0.95	1.0	1.06	1.14
Scale parameter	91.00	75.0	60.00	51.00
Age	33.00	31.0	26.00	42.00
Growth rate (mm/yr)	2.90	2.5	2.20	1.00
Constant mortality rate (%)	4.70	4.0	4.00	3.00
Mortality rate at annual growth 0mm/yr (%)	16.60	16.9	15.20	8.60
Mortality rate at annual growth 1mm/yr (%)	4.00	4.8	5.40	2.10
Mortality rate at annual growth 10mm/yr (%)	2.60	2.6	2.60	1.80

Fitting of mortality functions to the census data indicates that mortality is strongly growth-dependent across all bioclimatic domains, with very high probability of mortality (8.6 - 16.9% annual mortality) observed for annual stem growth rates of 0mm yr^{-}1 (Figure A3.2). Probability of mortality declines rapidly as annual stem growth rates increase, and levels off at annual stem growth rates of approximately 1mm yr^{-}1. I find much less variation in mortality rates across stem sizes, suggesting a smaller effect of size-dependency on mortality rates. Patterns of size-dependent mortality are also less consistent across bioclimatic domains, though broadly I see a trend of highest probability of mortality at mid to large stem sizes (Figure A3.1).

3.4.2.1 Comparison 1 - Comparisons with plot data All simulated stand structure outputs show variation across bioclimatic domains, broadly consistent with the variation in observed stand structure. I find that the accuracy of the simulations is strongly dependent on the mortality function used, and that use of the growth-dependent mortality function best simulates observed stand structure. Across all four bioclimatic domains, simulations using the growth-dependent mortality function estimate 22 out of 24 stand structure parameters to within 10% of observed parameters, and all parameters to within 20% (Table 3.3). Of the parameters tested, the growth-dependent mortality function is most accurate in simulating mean, median, and Q3 DBH across all bioclimatic domains. The growth-dependent mortality function performs least well in bioclimatic domain 5, where it overestimates the scale parameter and basal area by over 10% (Table 3.3), suggesting that it underestimates mortality rates at the largest stem sizes.

In contrast, I find that outputs from simulations using the other mortality functions are much less accurate in comparisons with observed structural parameters,

with simulations using these mortality calculations generating some significant errors in parameter estimation (Table 3.3). Application of these functions consistently results in underestimates of parameter values. In particular, all three mortality functions significantly underestimate the maximum DBH, the scale parameter, and the basal area, with estimation errors of over 20% (Table 3.3). This suggests that the functions are overestimating the mortality of the largest stems and as a result failing to accurately simulate large stem frequencies.

Table 3.3: Percentage differences between simulated stand structure parameters from observed tree ring data and simulated stand structure parameters from simulated trajectories. Cells are coloured to indicate the percentage difference between each simulated parameter and the observed parameter, where green cells show simulations within 10% of the observed parameter, yellow cells between 10 and 20% of the observed parameter, and orange cells over 20% difference from the observed parameter.

	Mean DBH	Median DBH	Q3 DBH	Maximum DBH	Shape parameter	Scale parameter	Basal area
Bioclimatic domain 3							
Growth dependent mortality	-2	1	1	-10	3	-4	2
Size dependent mortality	-10	-7	-11	-19	0	-21	-22
Growth and size dependent mortality	-11	-8	-11	-17	0	-23	-24
Constant mortality	-13	-10	-15	-25	2	-28	-30
Bioclimatic domain 4							
Growth dependent mortality	6	4	6	-5	-3	9	9
Size dependent mortality	-7	-6	-8	-36	-2	-20	-18
Growth and size dependent mortality	-7	-6	-7	-36	-2	-18	-16
Constant mortality	-8	-7	-9	-50	-3	-21	-18
Bioclimatic domain 5							
Growth dependent mortality	6	3	8	-16	-7	14	19
Size dependent mortality	-5	-4	-5	-37	-3	-15	-11
Growth and size dependent mortality	-4	-3	-5	-43	-3	-14	-10
Constant mortality	-6	-7	-8	-29	-7	-21	-13
Bioclimatic domain 6							
Growth dependent mortality	4	-2	2	-2	-17	1	8
Size dependent mortality	-9	-9	-12	-46	-8	-31	-20
Growth and size dependent mortality	-8	-9	-11	-31	-11	-29	-17
Constant mortality	-9	-11	-12	-40	-15	-34	-20

With application of the growth-dependent mortality function, stand structure simulations are accurate when compared to observed plot data (Figure 3.7). The simulations capture the size distributions observed within individual bioclimatic domains well across multiple size distribution parameters, indicating that the observed and simulated distributions are very similar (Table 3.3). Furthermore, the simulations capture the differences in size distributions among the bioclimatic domains, and accurately model the decline in the frequency of large stems from bioclimatic domains 3 to 6.

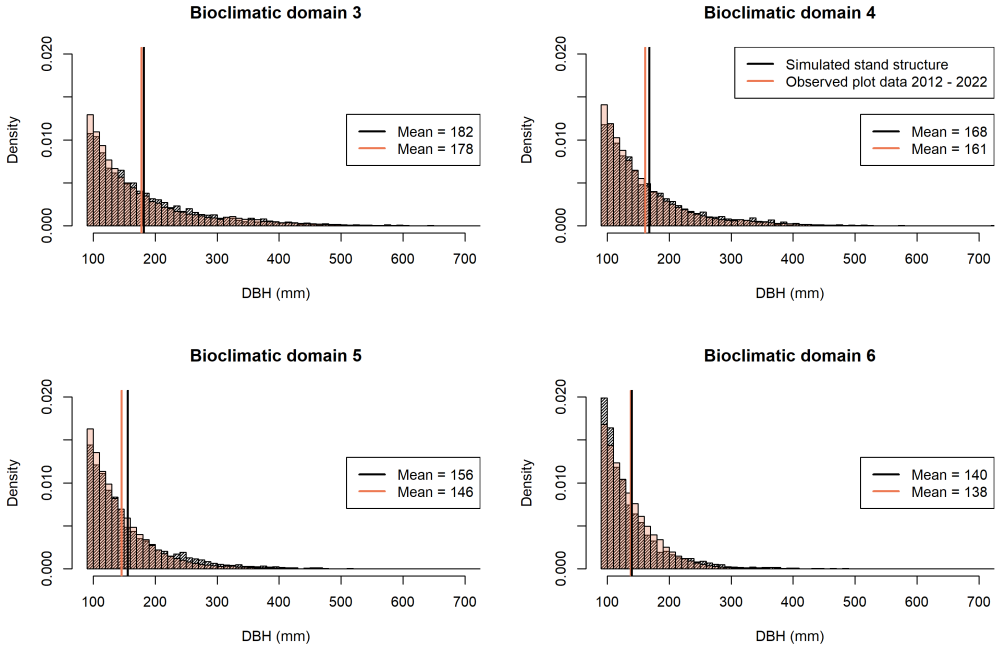

Figure 3.8: Comparisons of example stem size distributions between stands generated from simulated stem growth trajectories using the growth-dependent mortality function (black hatched) and observed stand structure from plot census data.

3.4.2.2 Comparison 2 - Comparisons with tree ring data Results of the simulations are similarly accurate when compared against the tree ring data. Mortality functions and stand structure parameters generated from the subset of

species sampled in the tree ring data are very similar to those generated from the full dataset, as expected. With the exception of the shape parameter, all stand structural parameters are estimated to within 10% of the tree ring data (Table 3.4).

Table 3.4: Comparisons of stand structure summary statistics between simulated data and the tree ring sample, calculated for each bioclimatic domain.

		Mean DBH	Median DBH	Shape parameter	Scale parameter	Mean annual growth rate	Mean stand age
Bioclimatic zone 3	Simulated data	166	140	0.96	73	2.72	27
	Tree ring data	170	148	1.01	79	2.77	29
Bioclimatic zone 4	Simulated data	168	141	0.94	74	2.52	30
	Tree ring data	166	149	1.06	77	2.61	29
Bioclimatic zone 5	Simulated data	157	134	0.94	64	2.12	31
	Tree ring data	149	135	1.07	60	2.14	27
Bioclimatic zone 6	Simulated data	139	120	0.91	46	1.12	43
	Tree ring data	138	127	1.10	49	1.10	43

Simulating estimates of stand-level mean annual growth rates and mean stand age offer an additional dimension with which to evaluate the accuracy of the simulations. Simulated estimates of mean stand annual growth rate, based on the lifetime annual growth rates of all surviving trees in the stand, are found to be within +/- 3% of the mean annual growth rate calculated from the tree ring sample. The distributions of annual growth rates are also very similar in shape between the simulated data and tree ring data (Figure 3.8), though I note that the distribution of simulated growth rates tends to underestimate the frequency of low growth rates, and slightly overestimate the frequency of growth rates in the middle of the range.

Simulated estimates of stand age are accurate to within 10% of the tree ring data for bioclimatic domains 3, 4, and 6, and to within 20% for domain 5, and also

show similar overall distributions to each other (Figure 3.9).

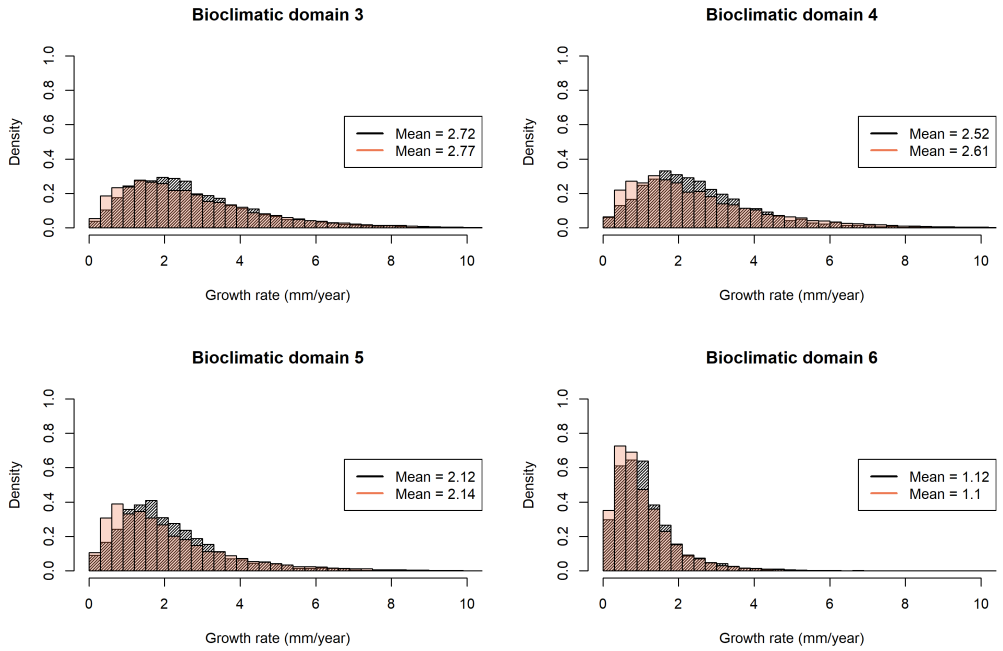

Figure 3.9: Comparisons of example growth rate distributions between stands generated from simulated stem growth trajectories using the growth-dependent mortality function (black hatched) and observed stand structure from plot census data.

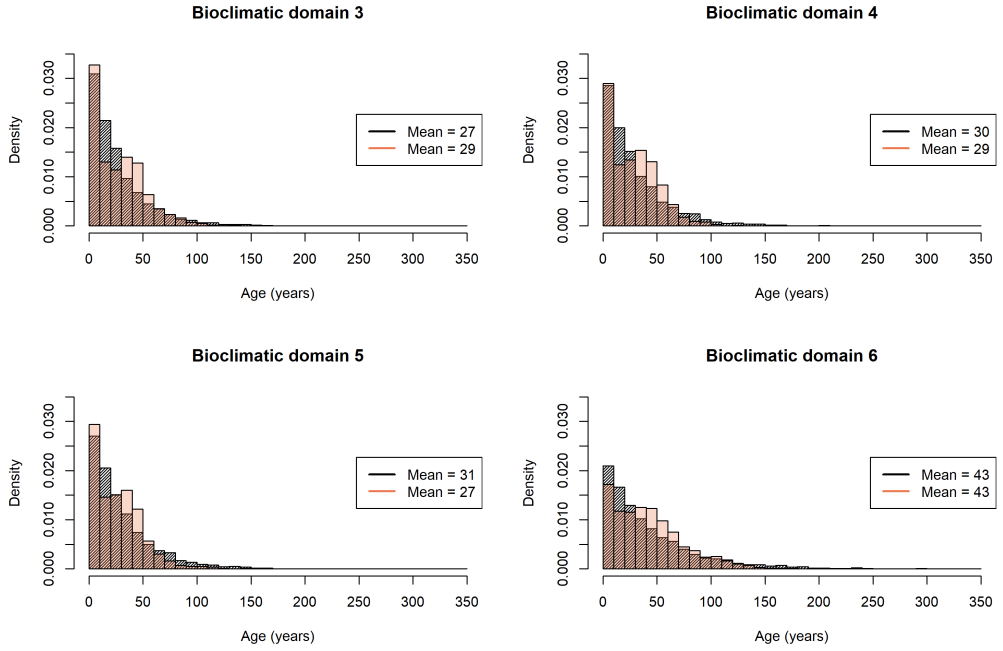

Figure 3.10: Comparisons of example age distributions between stands generated from simulated stem growth trajectories using the growth-dependent mortality function (black hatched) and observed stand structure from plot census data.

3.5 Discussion

The results presented here show that stem growth trajectories can be modelled using repeated sampling of annual growth rates derived from plot inventory data. This is the first time that this approach to simulating growth trajectories has been validated using independent datasets to build and validate the trajectories (but see Brienen et al. (2006) for validation with a non-independent dataset). I find that inclusion of growth autocorrelation in the approach greatly improves the spread of trajectories, while inclusion of diameter-dependent growth and wood density-dependent growth have a smaller effect. As wood density correlates negatively with growth rate (Chave et al., 2005), inclusion of growth autocorrelation may

already account for much of the wood density-dependent variation in growth, reducing the effect of including wood density. These results suggest that, where wood density data is unavailable, growth autocorrelation alone may be sufficient to simulate trajectories to a reasonable accuracy, though this approach is less accurate at larger stem sizes. As well as their application in larger stand-level modelling approaches, simulated growth trajectories will be a valuable tool in estimating stand and species age distributions. This approach will be particularly useful in the tropics, where ring formation is rare, and estimation of species ages and longevities is challenging (Vieira et al., 2005; Brienen et al., 2016).

At a stand level, the simulation approach accurately models a number of key stand structure parameters, alongside stand growth rate and stand age. The approach is strongly data-driven, but uses only data which are typically recorded in, or derived from, PSP census datasets, namely stem DBH, annual stem growth rates, wood densities, and stand-level estimates of mortality rates. Many individual-based models are built on core assumptions about individual responses to gap formation, light availability, and resource use, and the role of plant functional traits in mediating these responses (e.g. see FORMIND, Fischer et al., 2016; TROLL, Maréchaux and Chave, 2017). However, my approach models stand structure without the need for these assumptions. Even using only basic field data for parameterisation, the approach is sensitive to the variation among bioclimatic domains observed in the dataset, accurately capturing variation in structural parameters across diverse forest types.

The simplicity of this simulation highlights the importance of demographic rates in determining stand structure: across the four bioclimatic domains assessed here, variation in stand structure can be described almost entirely through simple data

on growth and mortality. Importantly, very limited information on species identity is required for accurate simulation; outside of demographic rate information, only data on wood density is necessary. The success of this approach is probably a result of (1) the close association between wood density and growth rates, such that sampling frames based around wood density drive stronger autocorrelation of growth rates, and increase the spread of trajectories; and (2) the importance of demographic rates as a species functional trait in themselves. Demographic rates like growth and mortality are one of the most important plant functional traits, which clearly differentiate species along a spectrum of fast to slow traits (Reich, 2014; Rüger et al., 2020). As a result, information on species traits and composition is inherent in the sample of demographic rates measured in PSP datasets, regardless of whether species identity is explicitly recorded. By employing autocorrelation of growth as a central component of building realistic growth trajectories, this approach captures the variation in growth dynamics seen in natural forests, without requiring detailed analysis of plant functional traits. Rüger et al. (2020), showed that grouping species into 5 plant functional clusters across two axes of variation (a growth-survival trade-off and a stature-recruitment trade-off) was sufficient to accurately model stand structure in a tropical forest; this result suggests that, at least for certain forests, even simpler approaches may be sufficient.

The results also point to the importance of mortality in determining stand structure, and the key role that accurate parameterisation of mortality rates plays in simulation development. I find that simulation outputs vary strongly according to the mortality function used, particularly when considering parameters beyond mean and median stem size, such as stand age, scale parameter, growth rate, and basal area. Stand evenness, basal area, and biomass are disproportionately influ-

enced by the relative frequency of large stems (Lindenmayer and Laurance, 2017; Poorter et al., 2017) and so the ability of a simulation to accurately model the abundance of the largest size classes is of particular importance when outputs are extrapolated to basal area and biomass estimates. The results clearly illustrate that mis-estimates of large stem numbers are not necessarily reflected by mean and median DBH values. In the simulation results presented here, the models using size-dependent mortality and constant mortality consistently underestimate basal area, the 75% quantile, and the scale parameter, pointing to a general underestimate in large stem numbers not indicated by the mean and median DBH estimates, and highlighting the importance of assessing model performance across a diversity of parameters.

Stand-level generalisations of mortality rate are likely to be sufficient to model stand structure, but this approach should be used with care: it is important to correctly identify the mechanisms of mortality. Forests in Quebec showed very strong growth-dependency in fitted mortality functions, but much weaker size dependency (Figures A3.1 and A3.2). The strikingly high mortality rates of individuals with low growth rates (up to ~20% annual mortality for stems which showed no growth in the previous year) indicate that this is the dominant mechanism shaping mortality in these forests. A strong influence of growth-dependent mortality in shaping forest stand dynamics, structure, and composition has been observed in other temperate and high-latitude forests (Kobe et al., 1995; Kobe, 1996; Cailleret et al., 2016). However, a growth-dependent mortality function may not be applicable across all modelling scenarios, as the relative influence of different modes of mortality is known to vary strongly with forest type and age, with important implications for stand development and forest structure (Larson et al., 2015; Cailleret et al., 2020). Previous research has identified pre-mortality

declines in growth as much greater in gymnosperms than angiosperms (Cailleret et al., 2016), so other mortality functions may be more applicable to broadleaf forests. For example, strong size-dependency of mortality has previously been identified in tropical forests, where it is expected to be important in structuring carbon cycling and biomass (Gora and Esquivel-Muelbert, 2021). As a result, determination of an appropriate mortality function on an individual basis is likely to be important in wider application of this approach.

The divergence in outputs generated from different mortality functions is likely to become even more pronounced if this approach is used to project forest structure under different future change scenarios. Previous studies have found that different approximations of mortality which may generate reasonable simulations of forest stands under current conditions can produce highly divergent predictions under scenarios of future change (Bircher et al., 2015; Bugmann et al., 2019); the observed sensitivity in these simulations could therefore propagate into significant differences when projected forward. This would likely be exacerbated when considering the influence of size- or growth-dependent mortality functions, as variation in mortality rate change across different size or growth rate classes is likely to have strong impacts on stand structure.

While this model is simple, it offers an exciting foundation for more detailed parameterisation and modelling of stand dynamics, with the potential to be easily applied to forest inventory sites worldwide. This could enable both detailed studies of stand dynamics and stand age estimates at individual sites, alongside comparisons of stand dynamics, demographic controls on stand structure, and sensitivities to variation in demographic rates across regional and global gradients. Further, the model could be applied to project forest structural responses

under different scenarios of demographic change. Demographic trends can now be derived from many plot networks (e.g. Brienen et al., 2015); coupling this approach with regional projections should produce more accurate predictions than an approach based on simple extrapolation of trends.

In considering future applications, I identify two key areas for further development; firstly, the inclusion of site-specific recruitment data would allow for spatially explicit modelling of forest stands, and could be calibrated based on forest inventory data. Secondly, while a stand-level mortality function performs sufficiently well to model stand structure, there is also the potential to develop more detailed parameterisation of mortality rates to allow for more detailed analysis of mortality controls on forest stands. For example, different size- or growth-dependent mortality functions could be parameterised across different wood density classes, or across different plant functional groups. Differentiating mortality functions within forests stands has been shown to improve model predictions (Johnson et al., 2018), and could be particularly important in applying the approach to tropical forests, where high species and life history diversity may mask any strong size- or growth-dependencies in mortality at the stand level.

Chapter 4: Intrinsic variation in the resilience of South American forests to increases in mortality rate

4.1 Abstract

Increasing tree mortality rates across Amazonian forests, driven by environmental change, are expected to drive declines in forest biomass stocks, through declines in basal area and shifts in stem size distributions. However, the likely trajectory, magnitude, and variability of these declines across forests is poorly understood. In particular, studies typically assume that responses will be uniform across forests, follow linear trends based on past trajectories, or use spatial variation in environmental factors and stand-level biomass stocks to estimate the sensitivity of forests to change. These approaches do not account for the wide variation in baseline demographic rates, stand structure, and biomass among Amazonian forests, nor the strongly skewed stem size distributions of old-growth forests, where the majority of biomass is found in a small number of large stems.

Here, I use an individual-based modelling approach, parameterised with forest inventory data from South American RAINFOR plot network, to simulate forest stand structure for 19 forest sites across the Amazon, representing a wide range of forest structures and demographic properties. I show that the approach accurately simulates stand structural properties and captures key structural differences among tropical forests. I then apply the simulation approach across the forests to test (1) the sensitivity of stand basal area and mean stand DBH to variation in mortality rates at steady state; (2) forest structural responses to a 50 year increase in mortality rates to a new stable state; (3) forest structural responses to a 50 year period of repeated cycles of high mortality rates, followed by recovery.

The results show that forest structural parameters show an approximately exponential decline with increasing mortality rates, and that current baseline mortality rates are therefore an important factor shaping forest sensitivity to mortality rate change. The forests of the north-eastern Amazon, which have low background mortality rates, show greater sensitivity to increases in mortality rate than the more dynamic forests of the south-western Amazon. For a given percentage increase in mortality rate, the low mortality forests of the Guiana Shield and East-Central Amazon show greater absolute declines in basal area and take longer to recover stand stand structural parameters than the higher mortality forests in the Brazilian Shield and Western Amazon. This suggests strong spatial variation in intrinsic responses to mortality rate change, with low mortality, high biomass forests showing high vulnerability and low resilience to increases in mortality rate. Both observational and modelling studies need to account for this variability in forest response to accurately assess the impacts of increasing mortality on forest function and carbon stocks.

4.2 Introduction

Recent decades have seen a marked increase in mortality rates across Amazonian forests, leading to a decline in the carbon sink of intact forests. (Brienen et al., 2015). Linear extrapolation of this trend suggests that intact Amazonian forests will become a net carbon source by 2035 (Hubau et al., 2020). However, these regional-scale trends may mask very different local responses to mortality regime change. Amazonian forests show high heterogeneity in functional characteristics, including demographic rates (Johnson et al., 2016), stand structure (Quesada et al., 2012) and species composition (Esquivel-Muelbert et al., 2019); as well as

encompassing large gradients in climate and soils (Quesada et al., 2012). As a result, responses to environmental change will be mediated by a wide range of parameters, resulting in potentially diverse outcomes across the basin. In addition, mortality impacts are expected to vary significantly across Amazonian forests, with mortality rates increasing non-uniformly across the basin (Esquivel-Muelbert, in prep). Similarly, the impacts of historic drought events have varied spatially and temporally across Amazonia (Aragão et al., 2007; Feldpausch et al., 2016; Jiménez-Muñoz et al., 2016). This spatial heterogeneity in mortality impacts means that it is important to calibrate forest responses over local scales in order to accurately predict patterns of forest change.

Understanding these responses requires an understanding of how the resilience of Amazonian forests varies across the basin. There are two key components to resilience: resistance, or the ability of the system to resist change and maintain function; and recovery, or the ability of a system to return to its original state following disturbance (Oliver et al., 2015). Observational studies of Amazonian forest responses to environmental change or disturbance indicate high variation in resilience. For example, studies have estimated that recovery times following disturbance range from a few decades (Rutishauser et al., 2015) to several centuries (Cole et al., 2014). Even under comparable disturbance scenarios responses vary greatly: for example, secondary forest biomass recovery following land clearance was shown to vary up to 11-fold across Amazonian forests (Poorter et al., 2016). This variation in resilience is driven by a variety of intrinsic and extrinsic factors. Extrinsic factors include the type and magnitude of disturbance, and the environmental context, including soil structure, soil nutrients and water availability. Factors such as water stress or poor soil structure may increase forest vulnerability to disturbance (Xu et al., 2018); on the other hand, higher water availability

and increased soil fertility may elevate rates of forest recovery from disturbance (Poorter et al., 2016).

Equally important are characteristics intrinsic to forest functioning, such as demographic rates and species composition, which are important in determining stable state variation in forest dynamics and structure, and so will also mediate forest responses to change. For example, variation in mortality rates is known to be a key parameter shaping stand structure and biomass across Amazonia (Johnson et al., 2016); while these relationships are mediated by environmental factors, the strength of the associations suggests that intrinsic variation in forest dynamics and function is important for determining forest structure at steady state. This is corroborated by studies of stand dynamics, which show that stem size distributions in natural forests are structured by the balance of growth and mortality (Muller-Landau et al., 2006b), with the gap-creating mortality rates of large trees being particularly important in determining forest structure at steady state (Farrior et al., 2016). These findings suggest that under scenarios of environmental change, forests with high demographic rates may respond rapidly and show lower resistance to environmental change, as changes propagate more rapidly through the stand structure, but may also recover more quickly from disturbance due to high growth rates.

The range of intrinsic and extrinsic factors which may generate spatial variation in how forests respond to increasing mortality rates make comprehensive predictions of future forest trajectories challenging. Firstly, forest responses are strongly contingent on the type and magnitude of disturbance (e.g. Rutishauser et al., 2015; de Avila et al., 2018, Kalamandeen et al. (2020)), meaning that comparisons across different disturbance types may not match future responses under differ-

ent scenarios. Furthermore, even where disturbance events are widespread, they rarely impact forests in a spatially consistent way, meaning disentangling the influence of the disturbance magnitude from intrinsic variation in forest sensitivities is challenging, even where monitoring is extensive (e.g. Phillips et al., 2010). Finally, the influence of intrinsic variation in forest function is poorly understood; as a simplification uniform responses are often assumed across forests, but this overlooks potentially significant divergence in response dynamics.

Most studies of forest responses to mortality impacts are based on monitoring approaches; while this offers detailed site-level data, observational studies have limited temporal scope. Even the longest studies typically only span 25-30 years, while the impacts of disturbance may last for centuries. This is particularly true for recovery to old-growth status; while initial recovery may be rapid, studies suggest that recovery rates are saturating (Poorter et al., 2016), as full recovery is likely to be limited by the growth rates and re-establishment of the largest stems (Silva et al., 2018). Recovery of stand structure at the largest stem sizes may lag recovery of the rest of the forest by many years and, even where biomass appears to have recovered, significant perturbations may persist in the frequencies of the largest trees (West et al., 2014; Vidal et al., 2016). As a result, observational studies which extrapolate rates of recovery from short-term studies may tend to under-estimate recovery times, and fail to accurately capture the dynamics present at later stages of recovery.

Integrating field data gathered from forest monitoring into individual-based modelling approaches offers a way for predictive methods to move away from a simple correlative approach towards better prediction of non-linear forest responses to change (Fischer et al., 2016; Fauset et al., 2019). These models simulate stems

individually, and so are well-placed for exploring linkages between demographic rates, stand structure, and disturbance events (Fischer et al., 2016; Rödig et al., 2017). Furthermore, it is straightforward to calibrate them to different forests using data from forest inventories (Rödig et al., 2017), meaning they can be employed to explore variation in forests across large environmental and functional gradients. Modelling approaches complement forest monitoring studies; while monitoring is effective in characterising past changes in forest structure and function, modelling allows us to look forward and better predict forest change over longer timescales than could be readily achieved by extrapolating from monitoring alone.

Here, I therefore use an individual-based modelling approach to simulate forest stand structure. By taking a simulation approach with standardised disturbance events, it is possible to remove the influence of extrinsic disturbance dynamics, and explore the importance of intrinsic dynamics in shaping forest responses to mortality rate change. I simulate stand structure of 19 Amazonian plot clusters across the ForestPlots network (Lopez-Gonzalez et al., 2011, 2012), representing a wide range of forest structures and demographic properties. I show that the approach, previously tested on temperate and boreal forests, can accurately simulate stand structural properties and capture key structural differences for tropical forests. I then apply three different scenarios of mortality rate change to test the sensitivity, response, and recovery of stand structure to changes in mortality rate, and analyse variation in forest responses with respect to baseline mortality rates.

4.3 Methods

4.3.1 Plot selection

All data was obtained from the ForestPlots database (Lopez-Gonzalez et al., 2009, 2011; ForestPlots.net et al., 2021), and all analyses were conducted in R version 3.5.1 (R Core Team, 2020).

I selected 19 clusters of plots from the South American RAINFOR database, managed within the ForestPlots database (Figure 4.1). From the full South American ForestPlots database, I selected all plots meeting the following criteria: plots following the standard ForestPlots measurement protocol (all stems $\geq$ 10cm DBH recorded and measured at 1.3m); plots over 0.25ha in size with >3 censuses; plots classified as old-growth forest, with no recent disturbance from burning, grazing, or logging; plots classified as mixed or mono-dominant forest. From this selection, plots were grouped into clusters based on a distance matrix of 50km, such that all plots within a cluster fell within 50km of each other. 19 clusters were selected based on the total number of stems sampled, and the total number of recruits sampled. Clusters were also chosen to create a spatially representative sample, with plots representing all four biogeographic regions of lowland Amazonian forests (Feldpausch et al., 2011), and a broad range of structural and demographic parameters (Table 4.1).

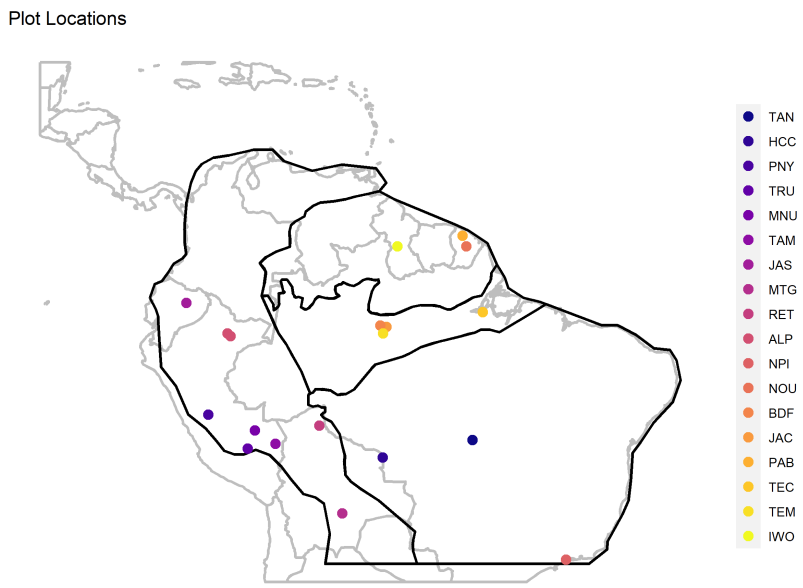

Figure 4.1: Map of plot cluster locations

Table 4.1: Summary statistics for the 19 plot clusters included in the analysis

Plot cluster code	Number of plots in cluster	Total combined plot area (ha)	Total monitoring period (years)	Mean census interval length (years)	Total number of stem measurements	Mean stand DBH (mm)	Mean stand basal area (m^2 ha^{-1})	Mean stem number (stems ha^{-1})	Mean stand mortality rate (% $year^{-1}$)
TAN	10	8.0	20	2.3	9558	185.0	17.2	503	3.6
HCC	4	4.0	20	2.7	5779	193.0	23.7	589	3.5
PNY	15	14.2	15	2.9	9659	195.0	22.2	558	3.2
TRU	8	8.3	14	3.3	12206	194.0	26.8	760	3.1
CUZ	3	3.0	28	3.3	6266	198.0	21.2	482	2.9
MNU	7	13.8	28	4.6	16178	206.0	22.0	463	2.5
TAM	7	6.5	38	2.9	18888	205.0	23.9	540	2.4
JAS	4	4.0	32	3.7	7588	200.0	26.6	648	2.7
MTG	8	2.0	8	2.6	1259	212.0	27.0	566	2.0
RET	4	4.0	24	2.4	12169	203.0	21.6	472	2.0
ALP	9	14.7	29	2.6	22262	205.0	27.6	650	2.3
NPI	6	6.0	14	3.0	17927	200.0	34.0	798	1.8
NOU	22	22.0	21	5.2	12275	216.0	23.8	454	1.7
BDF	13	28.0	29	5.5	45780	206.0	26.9	595	1.5
JAC	2	10.0	15	1.9	26181	209.0	25.4	570	1.6
PAB	2	31.3	35	1.9	181665	224.0	31.1	549	1.5
TEC	9	9.0	25	2.0	23259	236.0	30.0	467	1.2
TEM	11	11.0	25	1.0	48462	209.0	28.0	621	1.1
IWO	10	10.0	24	4.1	7624	241.7	29.7	461	0.6

4.3.2 Simulation approach

I used the simulation approach set out in Chapter 3. This approach first simulates growth trajectories of individual trees, by repeated sampling of growth rates from a set of observed growth rate data to incrementally build a lifetime growth trajectory. At each sampling step, a unique sampling frame is generated, to create growth rate autocorrelation as the trajectories are built. At each growth step, the next growth increment was sampled from a subset of the dataset, defined by:

1. A diameter window, set as the current DBH of the simulated stem +/- 5%;
2. A growth rate window, set as the mean annual growth rate of the simulated stem over the preceding 10 years +/- 0.5mm/year; and
3. A wood density window, set as the wood density of the initial sampled stem +/- 0.1

Once an annual growth rate was sampled from the sampling frame, annual growth steps were added to the trajectory according to the length of the census interval from which the sampled growth rate was calculated.

At each annual growth step, a mortality function was applied to calculate a unique annual probability of mortality for the stem. Trajectories were continued until the stem was killed by the mortality function. I modelled stand-level mortality separately for each cluster, using stem mortality data from across all census intervals and plots. Data for each stem at each census interval was included as a separate entry, and the stem was identified as either alive or dead at the end of the census interval. Mortality was then estimated using a sample of 2000 stems from the full dataset of stem mortality. For all clusters, I tested the use of (1) a size-dependent function and (2) a growth-dependent function. For the size-dependent mortality

function, I used the equation

$$M(x) = a \exp^{b(x)} x^c$$

where x represents the DBH of the stem, $M(x)$ is the instantaneous mortality rate ($year^{-1}$), and a, b and c are plot-specific parameters (Kohyama et al., 2015). For the growth-dependent mortality function, I used the equation

$$M(x) = a \exp^{-b(x)} + c$$

where $M(x)$ is the instantaneous mortality rate ($year^{-1}$), and a, b and c are plot-specific parameters (Camac et al. 2018). The growth-dependent mortality function to the plot data failed to converge when fit to the plot data for 8 out of the 19 plot clusters, and so only the size-dependent function was used for the full simulation approach.

Simulated stand structures were generated from the growth trajectory outputs. Each year, 100 growth trajectories were randomly sampled from the full set of trajectories and "recruited" into the stand. Trajectories were recruited for 600 years, to ensure that all of the stems initially recruited in year 1 had died, i.e., the stand was "mature". The DBH of all stems alive at year 600 were sampled to give a simulated stand structure and stem size distribution.

4.3.3 Validation of simulations

For the simulation of each plot cluster at steady state I calculated mean and median DBH, and the scale parameter of the distribution based on a Weibull fit (Muller-Landau et al., 2006b). The scale parameter describes the evenness of the

stand, where a higher scale parameter value is associated with a greater relative frequency of large stems. I also calculated an estimate of basal area per hectare. As recruitment is constant each year in all simulations, the simulations are not spatially explicit. To estimate basal area, I calculated the mean number of stems per hectare for each plot cluster, based on the observed plot data. From this, I estimated the number of hectares simulated in each simulation output, based on the number of stems simulated at year 600. I calculated total basal area at year 600, and divided it by the estimate of number of hectares simulated, to gain an estimate of basal area per hectare.

4.3.4 Testing plot sensitivity to variation in mortality rate

Simulation 1: Variation in forest stand structure across different mortality rates at steady state To test the effect of different steady-state mortality rates on structural parameters I first determined a mean stand-level mortality rate. Individual probability of mortality based on DBH was calculated for all stems in each plot cluster using the cluster-specific size-dependent mortality function, and the mean of these probabilities calculated. This value was taken as the baseline mortality rate for each plot cluster. From this baseline, I ran the simulations for each plot cluster, each time increasing or decreasing mortality by set increments. For each simulation, the mortality probability of each stem was calculated according to the size dependent mortality function, and then modified with the incremental mortality change, to increase or decrease probability of mortality. The full set of increments used were: +5, +4.5, +4, +3.5, +3, +2.5, +2, +1.5, +1, +0.75, +0.5, +0.25, +0.1, -0.1, -0.25, -0.5, -0.75, -1, -1.5, -2, -3, -4, -5, where the units are annual probability of mortality (%). For each simulation, I

calculated mean DBH and mean basal area.

4.3.5 Simulating structural responses to variation in mortality regimes

Simulation 2: A 50 year increase in mortality rates To assess variation in the response of forest structure to a long-term increase in mortality rates, I simulated a 50-year increase in mortality rates. The full simulation was run for a period of 1000 years; the first 600 years were to allow the stand to 'mature', as in the steady-state simulations. Once the stand was mature, mortality rates were maintained at the baseline rate for a further 50 years, to give a baseline period of stand structure. Following this, each year for 50 years, mortality rates were increased by 1% of the previous years mortality rate. After the 50 year period, mortality rates were maintained at the new, higher mortality rate, allowing a new steady state stand structure to be reached. The simulations were run for a further 300 years to allow the full response of the stand to occur and assess the time to equilibrium.

In addition to simulating a percentage-based mortality rate increase, I also simulated a mortality rate increase based on absolute rates. Each year for 50 years, the mortality rate was increased by an absolute value of 0.025, giving a total absolute increase of 1.25. Results for these simulations are presented in the appendix.

Simulation 3: Recovery from a period of elevated mortality rates As with the previous simulation, stands were allowed to 'mature' for 600 years, followed by a baseline period of 50 years. Over the following 50 year period, every five years for a period of two years, mortality rates were increased by 75% on the baseline mortality rate. This gave a total of 10 periods of elevated mortality

rates. After the 50 year period, mortality rates returned to the original baseline mortality rate, allowing the stand to recover. Again, the simulations were run for a further 300 years to allow the stands time to recover.

In addition to simulating a percentage-based mortality rate increase, I also simulated a mortality rate increase based on absolute rates. Over the 50 year period of varying mortality rates, every five years for a period of two years, mortality rates were increased by an absolute value of 1.25. Results for these simulations are presented in the appendix.

4.3.6 Parameterising forest responses to variation in mortality regimes

To parameterise the variation in simulated forest responses to variation in mortality rates, I first fit splines to all response curves, to reduce interannual noise in the simulation and capture the primary response trends. Splines were fit with 20 knots in order to account for the complexity of the response curves, and were observed to fit well to the response data. Using the splines, I identified a number of key parameters that describe the response of mean stand DBH and mean basal area per hectare to variation in mortality rates.

1. For simulation 1, the 50 year increase in mortality rates I calculated:

   a. Length of the response period: calculated as the time period (years) between the onset of mortality rate increases at 50 years and the stabilisation of the structural parameter, estimated to be the first inflection point of the fitted spline

   b. Percentage change in mean DBH and basal area per hectare: calculated as the percentage difference between the mean parameter value in years 1-50 and the mean parameter value in years 351-400

c. Absolute change in mean DBH and basal area per hectare: calculated as the absolute difference between the mean parameter value in years 1-50 and the mean parameter value in years 351-400

2. For simulation 2, recovery from a period of elevated mortality rates

   a. Length of the recovery period: calculated as the time period (years) between the minimum value of the fitted spline and the first year of recovery, defined as the first year that the fitted spline falls within the range of values recorded in the baseline period

   b. Length of the perturbation period: calculated as the time period (years) in which the spline falls outside the range of values recorded in the baseline period

4.4 Results

4.4.1 Accuracy of simulation approach

Simulations using a size-dependent mortality function predict current stand structure parameters well (Figure 4.2). Predicted parameter values correlate strongly with mean observed parameter values (mean DBH: p-value < 0.0001, $R^2 = 0.94$; median DBH: p-value < 0.0001, $R^2 = 0.69$; scale parameter: p-value < 0.0001, $R^2 = 0.90$; basal area: p-value < 0.0001, $R^2 = 0.79$). In contrast to my findings in Chapter 3, the growth-dependent mortality function fails to fit to data from 8 out of the 19 plot clusters, highlighting the importance of identifying a suitable plot-specific mortality function when applying this simulation approach to new datasets.

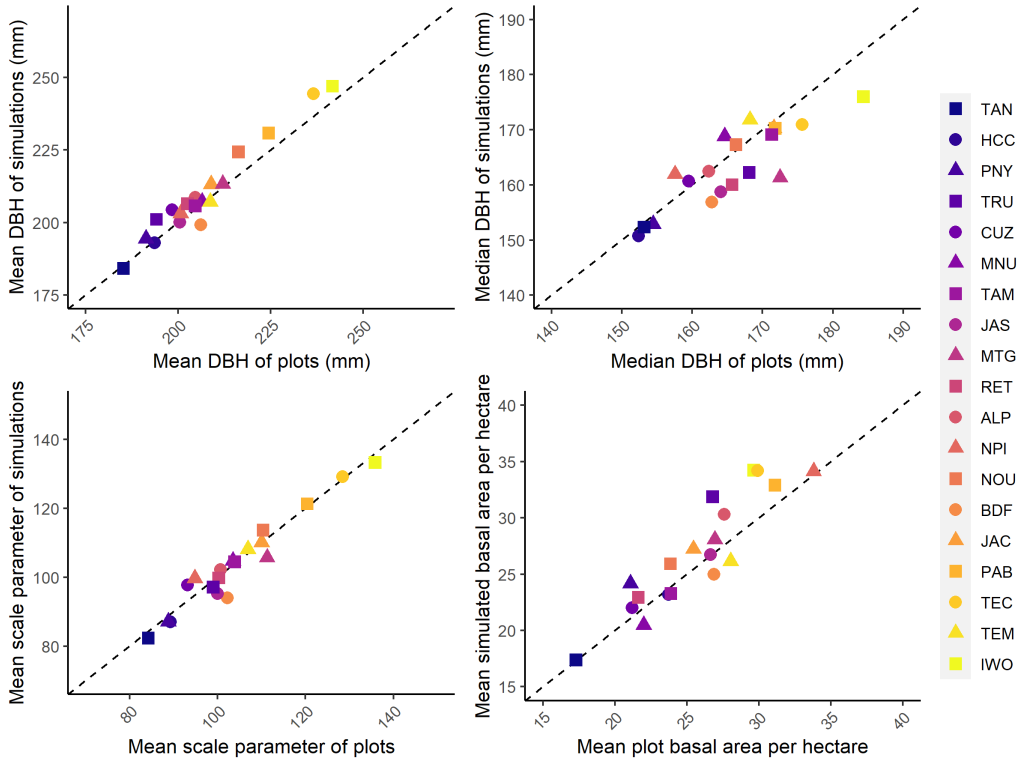

Figure 4.2: Simulated stand structure parameters plotted against mean observed stand structure parameters, where dotted line shows x = y. Structural parameters (clockwise) are: mean, median, basal area, scale parameter.

4.4.2 Testing plot sensitivity to variation in mortality rates

Mean stand DBH and mean basal area per hectare both show an approximately exponential decline in response to increasing mortality rates (see SI for relationships plotted on log-log axes), with the most rapid declines occurring as mortality rates increase from the lowest values (Figure 4.3 and 4.4). The rate and magnitude of declines are much more extreme for basal area estimates than for estimates of mean stand DBH, suggesting much stronger sensitivity of basal area than stand DBH to variation in mortality rates. The simulated relationships between mean annual mortality rate and stand structural parameters are much steeper than the

observed spatial relationship across plot clusters, suggesting that spatial patterns of variation between mortality and stand structure are strongly distinct from the instantaneous within-cluster variation. Paired comparisons between sites, where stand structure of selected clusters is simulated at the observed mortality rates of paired clusters, and structural parameters are compared, show that stand structural parameters show much greater declines than would be predicted by spatial comparisons across the mortality gradient (Table A4.1).

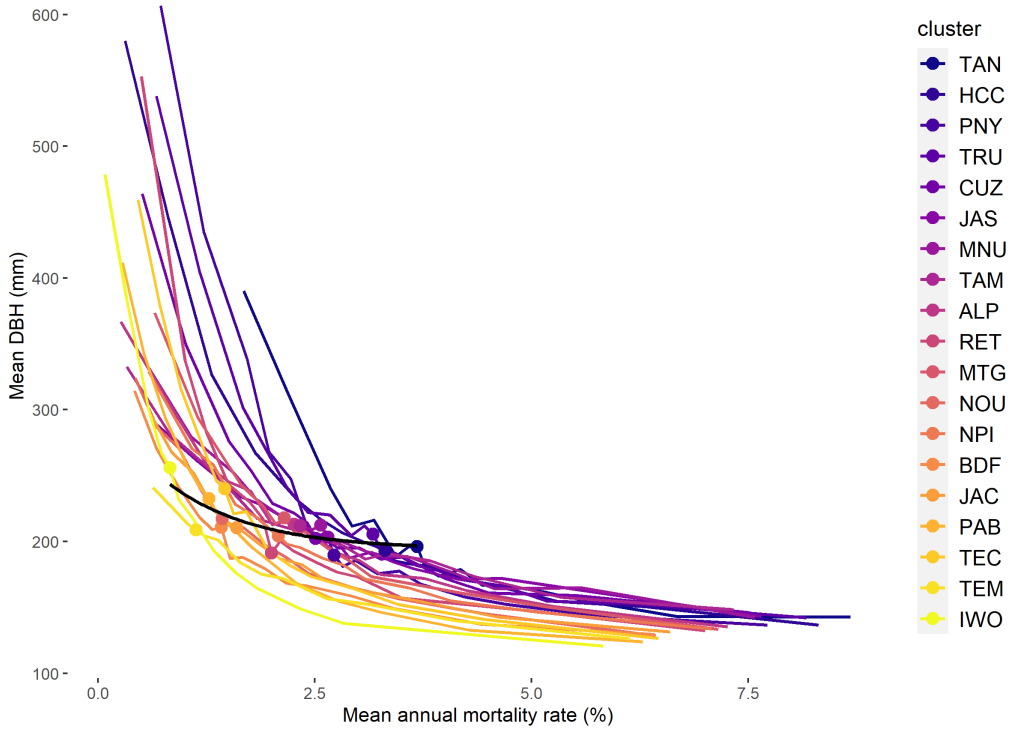

Figure 4.3: Mean DBH responses of stands to variation in mortality rates. Lines show mean DBH of simulated stands across a range of mean annual mortality rates. Points show approximations of the current status of plot clusters, based on the simulation outputs. The black line shows the line of best fit across current variation in mean stand DBH, i.e. the spatial variation in mean stand DBH.

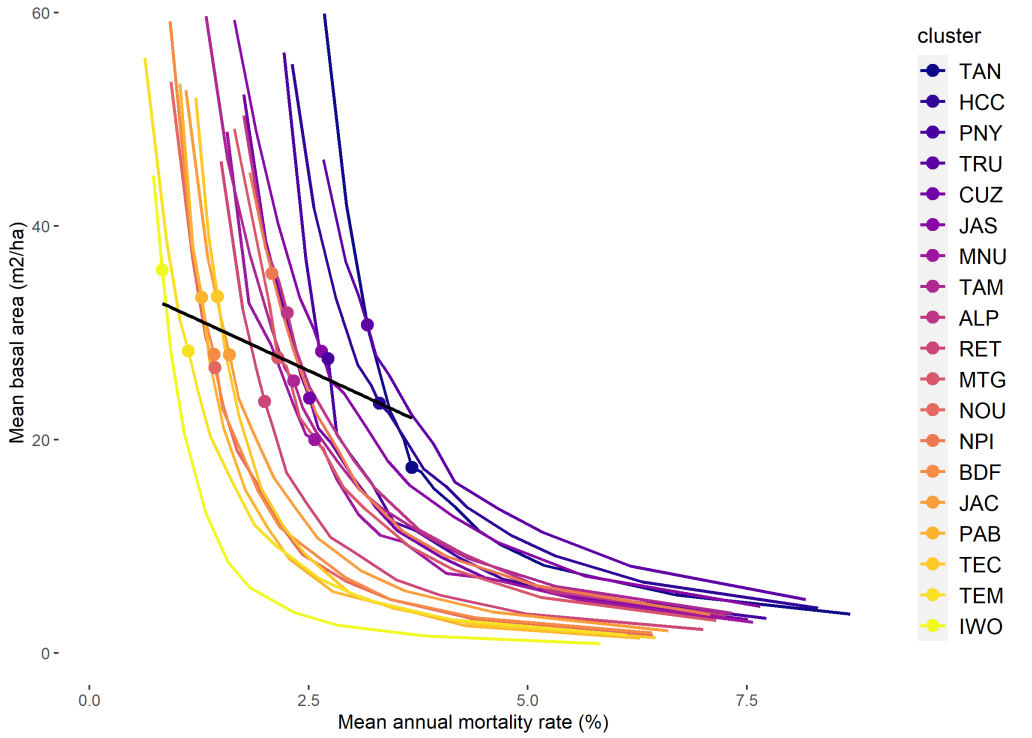

Figure 4.4: Basal area responses of stands to variation in mortality rates. Lines show basal area per hectare of simulated stands across a range of mean annual mortality rates. Points show approximations of the current status of plot clusters, based on the simulation outputs. The black line shows the line of best fit across current variation in basal area, i.e. the spatial variation in basal area.

4.4.3 Responses to a 50 year increase in mortality rates

All plots show a similar shaped response to a 50 year increase in mortality rates, with stand structure parameter values beginning to decline within the 50 year period of mortality rate increase, and continuing to decline for up to 350 years after the onset of mortality rate increase. The majority, though not all, of plots reach a new structural equilibrium at the new elevated mortality rate (Figure 4.5, 4.6 and A4.1). All plots show significant declines in stand structural parameter values during this period, with mean stand DBH values showing a mean decline

of 18.5% (SD = 2.1), mean BA declining by an average of 63.0% (SD = 3.6), and mean stem numbers per hectare declining by an average of 39% (SD = 2.8).

I find positive relationships between the baseline mortality rate and the decline in mean stand DBH, both in percentage ($p < 0.05$, $R^2 = 0.21$), and absolute ($p < 0.01$, $R^2 = 0.45$) terms, with the plots with the lowest baseline mortality rates showing the greatest declines in mean stand DBH. I find a positive relationship between the baseline mortality rate and the absolute decline in mean BA per hectare ($p < 0.01$, $R^2 = 0.29$), but no significant relationship between baseline mortality and the percentage decline in mean BA per hectare, indicating lower resilience to absolute basal area decline in the lower mortality plots (Figure A4.3 and A4.4).

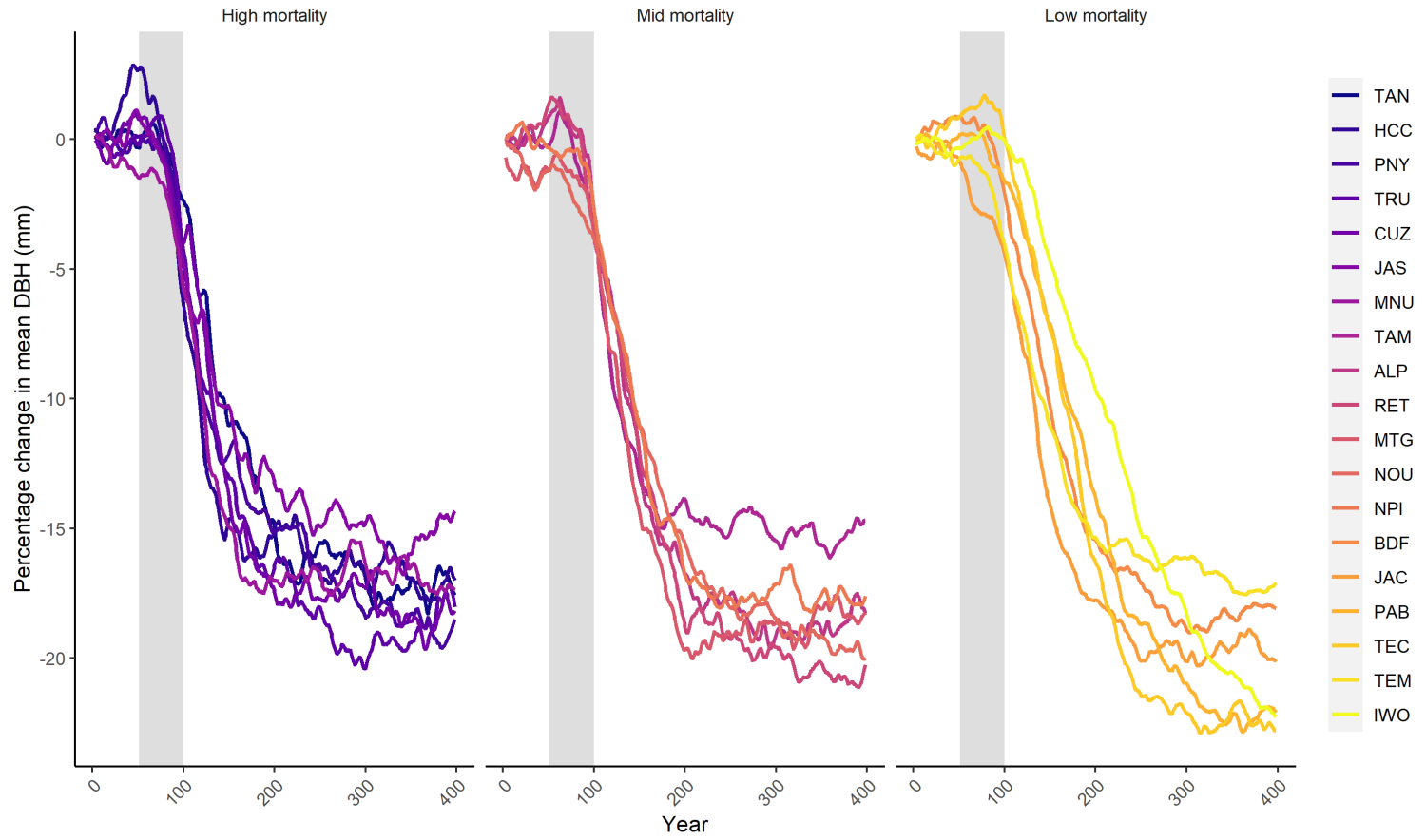

Figure 4.5: Percentage change in mean stand DBH in response to a 1% annual increase in mortality rate over a 50 year period (period of mortality rate increase shaded grey).

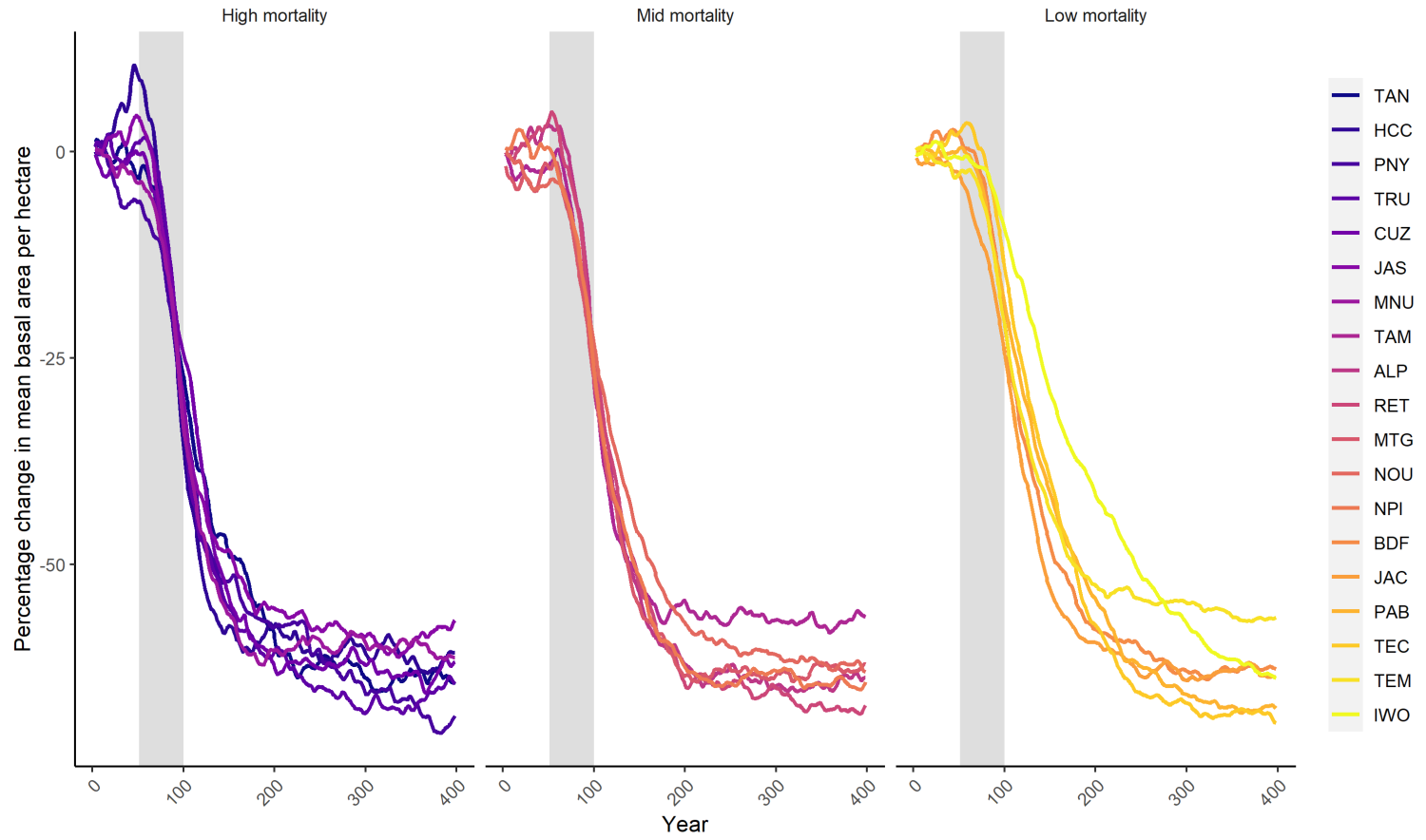

Figure 4.6: Percentage change in mean basal area per hectare in response to a 1% annual increase in mortality rate over a 50 year period (period of mortality rate increase shaded grey).

I find a strong negative relationship between the baseline mortality rate and the length of the response period taken reach a new stable state for mean stand DBH ($p < 0.001$, $R^2 = 0.53$) and mean BA per hectare (p-value < 0.001; $R^2 = 0.47$). Response times to estimated new stable states from the onset of mortality impacts range from 118 to >350 years (where clusters do not reach a new stable state within the time-frame of the simulations), with plots with lower initial mortality rates showing a much longer response period than plots with higher initial mortality rates.

4.4.4 Recovery from a period of elevated mortality rates

Again, there are similar patterns of response to the 50 year period of elevated mortality rates across all plot clusters. Stand structure parameter values begin to decline quickly in response to elevated mortality rates, and reach a minimum value before beginning to recover following the return of mortality rates to baseline levels (Figure 4.7, 4.8 and A4.2). The recovery curves are broadly saturating, with the fastest rates of recovery occurring immediately after mortality impacts cease. Recovery rates decline with time since mortality impacts.

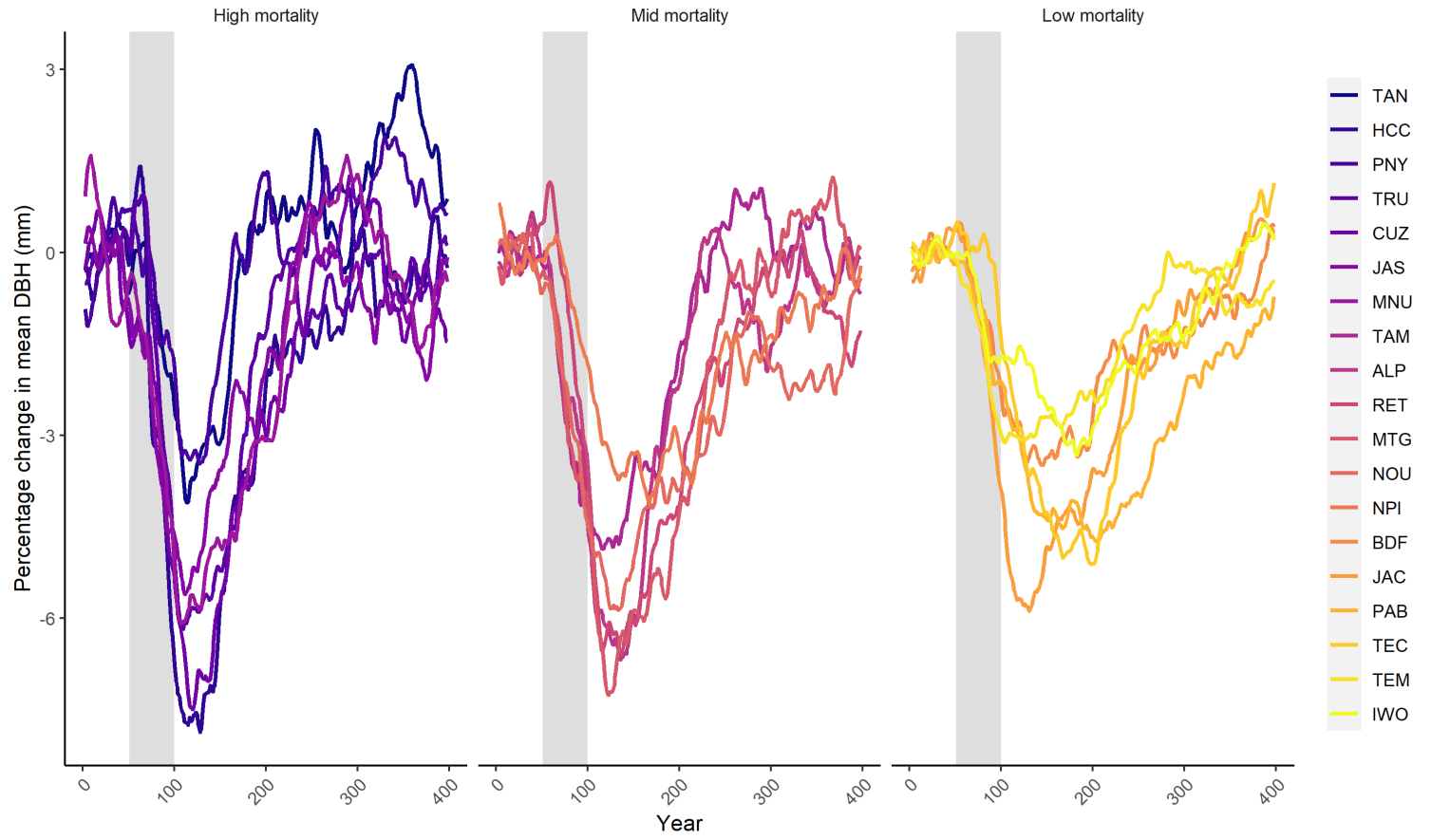

Figure 4.7: Percentage change in mean stand DBH in response to a 50 year period of elevated mortality impacts. During this period, mortality rates were increased by 75% for two years every five years, over a period of 50 years (period of mortality rate increase shaded grey). Following this, mortality rates returned to baseline levels

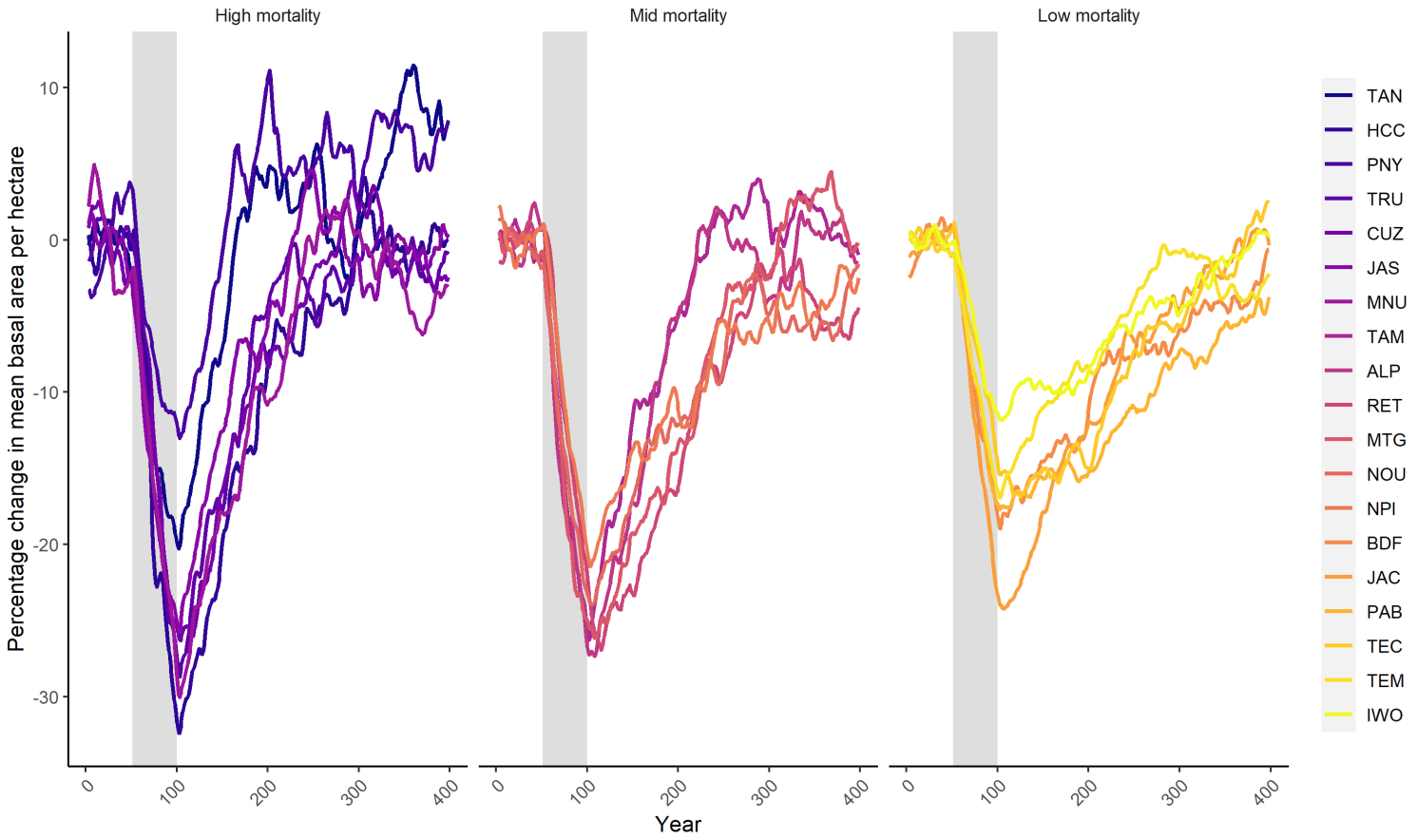

Figure 4.8: Percentage change in mean basal area per hectare in response to a 50 year period of elevated mortality impacts (period of mortality rate increase shaded grey). During this period, mortality rates were increased by 75% for two years every five years, over a period of 50 years. Following this, mortality rates returned to baseline levels

As with the previous simulations, I find a negative relationship between the baseline mortality rate and the length of the response period for mean stand DBH ($p < 0.01$, $R^2 = 0.34$). There is no significant relationship between the baseline mortality rate and the length of the response period for mean BA per hectare. For both mean stand DBH and mean BA per hectare, I find a strong negative relationship between the baseline mortality rate and the length of the recovery period (DBH: p-value < 0.01, $R^2 = 0.39$; BA: p-value < 0.001, $R^2 = 0.57$; Figure 4.9 and A4.3). I also find a strong negative relationship between baseline mortality rate and the length of the perturbation period for both mean stand DBH (p-value < 0.0001, $R^2 = 0.55$) and mean BA per hectare (p-value < 0.001, $R^2 = 0.57$; Figure 4.9 and A4.5).

The length of the recovery and perturbation periods vary according to which stand structural parameter is measured: I find that the recovery and perturbation periods are significantly longer for mean BA than for mean stand DBH (recovery: p-value < 0.0001; perturbation: p-value < 0.0001), with mean BA taking on average 37 years longer to recover than mean stand DBH.

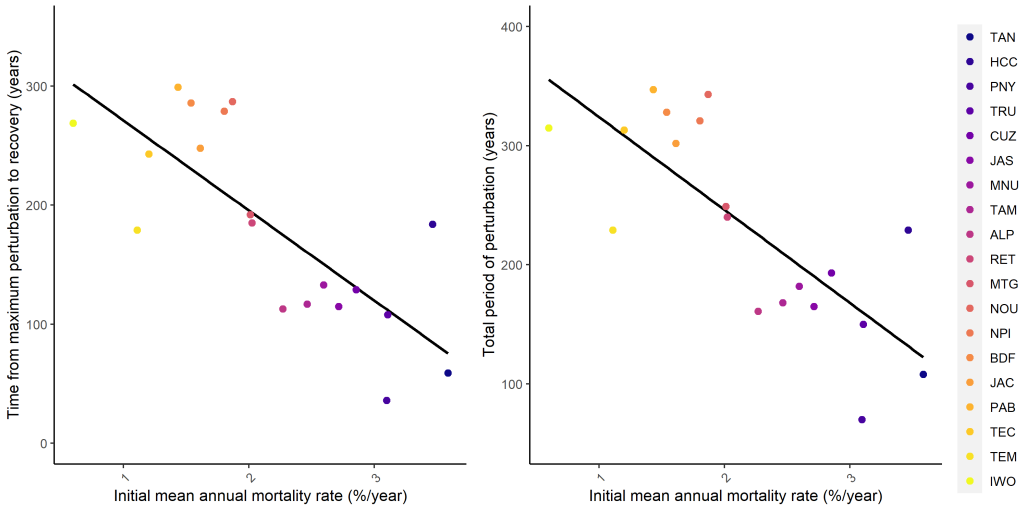

Figure 4.9: Relationships between perturbations in mean basal area and baseline mortality rate in response to 50 years of elevated mortality impacts. Left: length of total period from maximum perturbation to recovery of mean basal area, plotted against baseline mortality rate; Right: length of total perturbation period for mean basal area, plotted against baseline mortality rate.

4.5 Discussion

The simulations indicate significant variation in the intrinsic responses of Amazonian forests to increases in mortality rate. Variation in response time, recovery time, and the magnitude of perturbation are all found to be associated with variation in the baseline mortality rate, suggesting that demographic rates are an important parameter mediating forest responses to change.

Although all plot clusters show an approximately exponential decline in mean stand DBH and mean BA as mortality rates increase, the point on each curve at which the cluster is currently located according to its observed baseline mortality rate varies greatly. Plots with lower observed mortality rates fall on a much steeper part of their curve than plots with lower observed mortality rates, suggesting that for a given (absolute) increase in mortality rate, the effect on stand structure

will be much more significant for lower mortality plots. This is consistent with previous observations that relationships between stand structure parameters and stem mortality rates are steepest, and strongest, in regions of Amazonia with lower mortality rates (Johnson et al., 2016). This is particularly significant, as these are the forests which contain the highest levels of biomass (Feldpausch et al., 2012; Quesada et al., 2012), and so rapid changes in stand structure in these forests may have significant implications for the carbon source-sink dynamics of these forests. In contrast, for plots with high baseline mortality rates, increases in mortality rate appear to have comparatively small effects on stand structure. At the highest mortality rates simulated, the results suggest that the differences in stand structure between the clusters are primarily influenced by variation in growth rate between the clusters. This corresponds with findings from Chapter 1 of this thesis, which show a greater influence of growth rate in stand structure in higher mortality regions. Similarly, Johnson et al. (2016) show a much shallower relationship between AGB and stem mortality rates for plots in higher mortality regions of Amazonia.

Across the Amazon Basin, mortality and stand structure co-vary spatially, with south-western forests generally having higher mortality rates and lower basal areas, and north-eastern forests having lower mortality rates and higher basal areas (Johnson et al., 2016) (Figure 4.2). I find that, across the range of mortality rates tested, the variation in instantaneous stand structure does not correspond with the spatial patterns (Figure 4.3 and 4.4), but instead shows a much steeper negative relationship between stand structural parameters and mortality rates. These results highlight the limitations of space-for-time substitutions: extrapolation of spatial associations between mortality rates and stand structure would significantly underestimate structural change, particularly in the lowest mortality

forests. This is probably because of the co-variation in growth and mortality across Amazonian forests. The low mortality forests of the north-eastern Amazon have much lower growth rates than the higher mortality forests in the south-western Amazon, and so are much more strongly impacted by increases in mortality than spatial extrapolation would predict. Although growth and mortality are closely linked, and so increases in growth rate are often concurrent with increases in mortality rate (Brienen et al., 2020), variation in species composition and associated functional traits is likely to constrain the growth response of these forests, at least in the short term. Therefore, although increases in mortality rates may drive long-term shifts in community composition resulting in adaptive changes in forest function, in the short-term my results indicate dramatic changes beyond what would be expected from observed spatial variation.

In addition to the intrinsic variation observed in the magnitude of mortality impacts, I find consistent variation among plot clusters in the length of the response and recovery periods. The time period from the onset of mortality rate increases to establishment of a new stable stand structure is longer in plots with lower baseline mortality rates, as is the time period taken for recovery from the maximum structural perturbation back to the original stand structure. Overall, this results in significantly longer overall perturbation periods in stands with lower baseline mortality rates. I suggest that this variation is due to the intrinsic dynamics of these plots: turnover rates in plots with higher baseline demographic rates are much higher (Phillips et al., 2004; Quesada et al., 2012), and so mortality impacts pass through the plot rapidly, translating into rapid structural change. However, when mortality rates return to baseline levels, the high growth rates in these plots drive rapid recovery of stand structure; as a result these forests may actually have relatively high resilience to mortality rate change.

I find that there are large differences in the responses of different stand structural parameters to mortality rate changes. For a given mortality rate increase, mean BA values show a much steeper rate of decline than mean stand DBH in the first analysis, and a much larger percentage decline in the second analysis. This suggests a very high sensitivity of mean BA to changes in mortality rates compared with mean stand DBH. There are two explanations for this: firstly, while mean stand DBH is relatively unaffected by declines in stem number (provided the overall size distribution does not change), mean BA declines rapidly as stems are lost. Secondly, large stems are disproportionately important in determining mean BA (and, by extension, biomass) (Lutz et al., 2018), but have a smaller effect on mean stand DBH; here, the shift in size distributions towards a stand structure defined by higher frequencies of small stems results in a rapid decline in mean stand BA. Similarly, I find that the BA recovery takes much longer than recovery of mean DBH and mean stem number. This is in part a result of the bigger percentage declines in BA, but is also related to the slow recovery of large stems, which are so important in shaping overall stand BA. This relationship is exacerbated spatially, as the lowest mortality forests in the Guiana Shield and East-Central Amazon also support the highest frequency of large stems (Feldpausch et al., 2011); the loss of these stems results in a larger relative decline in BA, but also takes longer to recover from, as a result of the inherently low growth rates of these forests.

My findings suggest that forest responses to mortality impacts could be heavily influenced by within-stand variation in mortality. Many mortality drivers show strong size-dependency in their impacts (Gora and Esquivel-Muelbert, 2021): for example, previous observational studies of drought impacts observed much higher mortality increases in the largest size classes (Nepstad et al., 2007; da Costa et al., 2010). The strength of size-dependent impacts may also vary spatially: currently

across Amazonia, there is observed spatial variation in mortality risk factors, with larger trees experiencing greater relative hazard in the East-Central Amazon, while smaller trees experience greater relative risk in the Western Amazon (Esquivel-Muelbert et al., 2020). Previous studies have found that the rate of forest recovery from disturbance is positively associated with the percentage of basal area retained (de Avila et al., 2018), suggesting that relatively higher mortality in the largest size classes could further exacerbate the trends and recovery times captured here. Further consideration of the influence of growth-dependent mortality may also be worthwhile. The influence of growth rates on mortality probabilities varies among tropical species, with the strongest effect of growth-dependent mortality being observed in light-demanding species at small stem sizes (Camac et al., 2018). This may explain why a growth-dependent mortality function failed to fit to stand-level data, and indicates that a more detailed approach which parameterises mortality functions by according to life-history traits or functional group may be valuable in offering further insights into the role of growth-dependent mortality in shaping forest stand structure. Exploring the potential influence of size- and growth-dependent mortality on forest responses and recovery should be a priority for research. The approach used here offers a suitable and novel way to explore this further, as mortality functions could easily be parameterised to explore the effects of size- and growth- dependent variation in mortality, and could be further extended, for example to explore the outcomes of observed variation in mortality impacts across functional groups (Aleixo et al., 2019).

There are a huge range of factors that may mediate forest responses to change. In this simulation I chose to focus on intrinsic responses to mortality rate change, assuming no growth response or shift in species composition. In reality, an increase in mortality rates, and, in particular, the loss of large canopy trees, would

be expected to drive some level of growth rate and/or recruitment rate increase as the canopy opens up and light availability increases (Numata et al., 2006; Muscolo et al., 2014). We might also expect to see a compositional response, whether towards 'pioneer' functional groups with faster life histories (Laurance et al., 2018), or towards species groups better adapted to the specific mortality drivers (Esquivel-Muelbert et al., 2019). As a result, the parameters of the response trajectories presented here are not anticipated to be accurate future predictions, and it is likely that observed structural responses to mortality rate increase will be less severe than these trajectories. However, the spatial patterns of intrinsic variation in responses identified here may actually be further exacerbated by growth responses: in lower mortality forests, most species have high wood densities, slow life histories, and low growth rates (Baker et al., 2004b; Quesada et al., 2012; Johnson et al., 2016), meaning that they may exhibit weaker initial growth responses than more dynamic forests (Rüger et al., 2012).

These results have important implications for long-term monitoring of tropical forests. My findings indicate that structural responses to increases in mortality rates are most likely to be detected first in forests with higher baseline demographic rates, which could initially imply lower resilience of these forests to mortality increases. However, these simulations suggest that responses are likely to be equally, if not more, severe in forests with lower baseline demographic rates, as, despite showing fewer immediate structural changes, perturbations to these plots may persist over much longer periods, resulting in overall greater structural change. Long-term extrapolation from observed short-term forest responses may simultaneously over-estimate the vulnerability of the more dynamic forests of the south-western Amazon, and under-estimate the vulnerability of the less dynamic forests of the north-eastern Amazon, highlighting the importance of maintaining

forest monitoring approaches over long time-scales.

My findings here show a significant influence of intrinsic forest dynamics on forest resilience to environmental change. Predictive approaches based only on identifying areas of high mortality rate change may fail to identify the regions with the highest vulnerability to functional change and ecosystem collapse, as forest vulnerability to mortality rate change is seen to vary independently of the magnitude of the mortality increases. In these simulations, although absolute mortality increases are highest in the forests of the Brazilian Shield and Western Amazon, impacts on forest function and biomass are greatest in the Guiana Shield and East-Central Amazonian forests, because of their intrinsic vulnerability. Forests in the Guiana Shield and East-Central Amazon are some of the highest biomass forests in Amazonia (Johnson et al., 2016), and so large shifts in forest stand structure and declines in basal area in these forests will have significant implications for the pan-Amazonian carbon sink. Better integration of spatially explicit variation in forest dynamics into future modelling studies will be important in accurately capturing spatial and temporal variation in forest responses to change, and in improving forecasting of future carbon sink dynamics.

Chapter 5: Synthesis and Conclusions

This thesis investigated the relationship between demographic rates and forest stand structure, with a focus on understanding controls on forest structure across the full range of Amazonian forests.

Chapter 2 of my thesis used forest inventory data from the RAINFOR plot network to describe variation in forest structure across the Amazon, and relate this to variation in demographic rates. Chapter 3 used a forest inventory and tree ring dataset from Quebec to build a simulation method that could accurately simulate current stand structure across a large bioclimatic gradient. Finally, Chapter 4 employed this method to test how resilience of Amazonian forests to changes in mortality rate is influenced by variation in baseline demographic rates.

Overall, the results presented in this thesis clarify the relationships between stem demographic rates and forest structure, as well as exploring what this means for forest responses to increases in mortality rates. Here, I first summarise the key findings of my thesis, before discussing their broader implications.

5.1 Research synthesis and key findings

5.1.1 Variation in stand structure is well-described by Weibull function size distribution parameters

In Chapter 2, I show that the primary axis of variation in stand structure across Amazonian forests is related to the evenness of the stem size distribution, or the relative proportion of small and large stems. Stand evenness is well-described by the scale parameter of the Weibull distribution, which appears as a better descriptor of structural variation than simple metrics such as mean, median, or maximum

DBH. I suggest that the scale parameter is a valuable metric for describing stand structure, in particular because its sensitivity to the relative frequency of large stems means that it relates closely to variation in forest biomass. The value of describing stand structure through Weibull distribution parameters is further illustrated in Chapter 3, where the scale parameter shows great utility in validating the accuracy of simulations of stand structure, because it shows greater sensitivity than other metrics to small differences in the frequencies of large stems.

5.1.2 Variation in stand structure is closely related to variation in mortality rates

Each chapter of my thesis clearly demonstrates a strong relationship between stand structure and demographic rates. In Chapter 2, I find a negative relationship between stem mortality rates and stand evenness across all Amazonian forests, but show that this relationship varies with climate, soil structure and by forest type. In addition, the simulations I develop in Chapter 3 illustrate that variation in stand structure across a major bioclimatic gradient can be simulated using only information on demographic rates and wood density, further illustrating the close links between demographic rates and forest structure. These results also highlight the importance of mortality rates in shaping stand structure, as stand structure is sensitive to size- and growth-dependent variation in mortality. Finally, in Chapter 4, my analyses further clarify the relationship between mortality rates and stand structure, with basal area declining exponentially with increasing mortality rates.

5.1.3 The influence of demographic rates on stand structure is mediated by environmental variation

Across the Amazon Basin, I find that the relationship between demographic rates and stand structure varies with climate, soils, and forest type. In the moist, lowland forests of the Guiana Shield and East-Central Amazon, which have high precipitation and deep stable soils, higher demographic rates are associated with a less even stand structure. However, in drier and cooler forests, and forests with less stable shallower soils, such as in the Brazilian Shield, higher demographic rates are associated with a more even stand structure.

5.1.4 Stand structure can be accurately modelled across diverse forest types using forest inventory data on demographic rates, stem DBH, and wood density

In Chapter 3, I develop an individual-based simulation to model stand structure of mature forests, using demographic rate, stem DBH, and wood density data from the Quebec provincial forest inventory program. Using tree ring data to validate the simulation outputs, I show that this approach accurately simulates a range of stand structural parameters across a large bioclimatic gradient. Importantly, this approach avoids the need for parameterisation of complex ecophysiological processes or disturbance dynamics, making the model simple to apply to new datasets. In Chapter 4, I apply this approach to Amazonian forests, and show that it is also able to accurately simulate stand structure in species-rich tropical forests. This suggests that the simulation approach should be widely applicable to mature forests across boreal, temperate and tropical regions, and highlights the universal importance of demographic rates in shaping stem size distributions

in forests globally.

5.1.5 Intrinsic variation in demographic rates mediates forest responses to increases in mortality rate

In Chapter 4, I show that current baseline mortality rates shape forest sensitivity to increases in mortality rates. In response to a given percentage increase in mortality rate, forests with lower baseline mortality rates exhibit greater declines in basal area and have longer recovery times than forests with higher baseline mortality rates. This suggests that the intrinsic dynamics of forests are important in determining forest resilience to environmental change. These findings are consistent with the results I present in Chapter 2, which show that there are strong negative correlations between stem mortality rate and stand evenness in the regions of Amazonia with the lowest mortality rates, indicating strong sensitivity to variation in mortality rate in these regions.

5.2 Research implications

5.2.1 Future applications of the simulation approach

The simulation approach developed in Chapter 3 shows great potential to be applied more widely in future research. The method uses data which is readily available in the majority of forest inventory datasets, meaning that the simulation can be applied to other forest inventory networks across a range of forest types and bioclimatic domains. Examples of networks which could make use of the approach include the broader ForestPlots network, including sites in tropical Africa and Asia (ForestPlots.net et al., 2021), or across other national forest inventory networks

(Bechtold and Patterson, 2005; Gray et al., 2012). In particular, it would be valuable to apply this approach to plots from the ForestGEO network (Anderson-Teixeira et al., 2015). ForestGEO plots are typically much larger than the plots in RAINFOR and the Quebec provincial forest inventory network (up to 50ha in size), are located across both tropical and temperate regions, and census all stems $\geq$ 1cm DBH (Anderson-Teixeira et al., 2015). This dataset would therefore offer an opportunity to test the application of the simulation across a more complete stem size distribution, with the potential to clarify variation in size distribution controls across different stem sizes and functional types.

Currently, estimates of basal area can be derived from the simulation outputs, however it would be ideal to develop the simulation further to produce spatially-explicit biomass estimates. Two additional model components would be necessary for this: firstly, inclusion of site-specific recruitment, and secondly, incorporation of allometric equations for biomass estimation. In its current iteration, the model assumes a constant recruitment rate, whereby a fixed number of new stems (typically 100 individuals) are recruited into the stand annually to generate a stem size density distribution. Per-hectare estimates of stand-level parameters can be derived from this distribution, but the outputs are not spatially-explicit per se. As recruitment data are available from forest inventory datasets, it would be possible to calculate a site-specific recruitment rate (e.g Lewis et al., 2004b) to replace the constant rate. This would enable the simulation to directly produce spatially-explicit estimates of forest basal area, which could be used as the basis for biomass estimation. The simulation approach already assigns a wood density value to each simulated stem, and so the biomass of each stem could be estimated by combining this with application of site-specific height/diameter allometries (Chave et al., 2005; Feldpausch et al., 2011), to generate estimates of stand-level biomass.

Chapter 4 illustrates how the approach can be successfully applied to test the sensitivity of forest structure - and by extension, forest biomass - to variation in mortality rates, with the results of this analysis clearly showing the role of intrinsic demographic rates in shaping forest responses to change. There is great potential to further extend this type of analysis to test the sensitivity of forest responses to a range of scenarios. For example, increases in growth rates and productivity have been observed across forest ecosystems, as a result of carbon fertilisation (Terrer et al., 2019); by varying growth rates within this simulation, it would be possible to test the outcomes of enhanced growth on forest structure and biomass. Concurrent increases in growth and mortality rates have been observed across tropical regions, though mortality is appearing to lag growth (Brienen et al., 2015; Hubau et al., 2020). Analyses of growth rate increases could therefore be combined with simulated increases in mortality, such as those applied in Chapter 4, to assess the combined impact of increases in growth and mortality rates, and the effect of different time lags between growth increases and mortality increases on carbon sink dynamics. Outputs could be compared with observed changes in stem size distributions to explain current trajectories, and scenarios then extended into the future. This type of analysis would be much better able to capture non-linear responses of stand structure and biomass than simple correlative approaches, and so could offer valuable insights into the future of the carbon sink.

Because the simulation is an individual-based approach, there is also potential to use this method to test for the impacts of size-dependent variation in growth and mortality. Mortality drivers vary in their relative impact across size distributions (Gora and Esquivel-Muelbert, 2021); for example, drought has been found to have a disproportionate impact on larger trees (Phillips et al., 2010; Bennett et al., 2015). By varying the mortality function used in the simulation approach,

or by applying variable demographic rate increases according to size, it will be possible to explore how size-dependency of demographic rate change influences stand structure and biomass stocks. A similar approach could be taken with regards to functional traits, in order to explore the relationship between species composition and forest resilience. Trees with low wood densities have been found to be more vulnerable to drought impacts than trees with higher wood densities (Phillips et al., 2010); similarly variation in hydraulic traits is related to variation in growth and mortality and may mediate biomass responses to environmental change (Tavares et al., 2023). Where functional trait information is available, traits could be associated with specific mortality responses within the simulation, in order to explore the implications of variation in species composition for forest responses to changes in mortality rates. Overall, incorporating greater detail of individual stem responses to mortality drivers could result in more accurate predictions of forest responses to specific mortality drivers or environmental impacts.

The simulations presented in this thesis assume no growth response to mortality impacts. In reality, increased mortality, particularly of canopy trees, is likely to reduce competition for light and generate a competitive release, resulting in increases in growth and recruitment (Yamamoto, 2000). Increases in growth and recruitment may be particularly marked in small understorey and early-successional trees, as these benefit the most from creation of canopy gaps (Yamamoto, 2000; Laurance et al., 2006), which could lead to shifts in size distributions. Growth responses are likely to be constrained by community composition; stems with lower wood densities tend to have faster growth (Chave et al., 2005). As a result, stands dominated by low wood density species may show on average faster diameter growth responses than stands dominated by higher wood density species, leading to spatially heterogeneous responses. The growth responses of forests

will therefore be important in shaping their resilience to increases in mortality rates, so incorporating this into the simulation would be very valuable in more accurately quantifying future trajectories of the carbon sink in these forests. Accurately parameterising growth responses is challenging, and will require detailed observational data collected across a range of sites and stem characteristics. Calibrating the simulation based on accurate real-world data would be ideal, and could be done using forest inventory data to determine how growth rates respond following canopy mortality (e.g. Baker et al., 2016). However, in the absence of empirical data, the simulation could still be used to test how theoretical growth and recruitment responses influence forest responses and resilience.

Developing the simulation approach further in regards to forest growth responses would greatly increase the applicability of the approach in guiding forest management. For example, accurate parameterisation of mortality, growth, and recruitment would enable high quality predictions of forest recovery following disturbance events. This has applications in guiding forest conservation in secondary and recovering forests - for example by providing realistic timeframes for conservation planning - but could also be used in the development of management plans for sustainable logging. Because the approach models stems individually, it would be possible to assess the impacts of removal of individual stems on biomass and stand structure, facilitating development of selective logging strategies. Further, the approach enables detailed assessment of stand structure across the full range of stem sizes. As even reduced-impact logging has significant impacts on the frequencies of the largest trees (West et al., 2014; Vidal et al., 2016), being able to compare recovery metrics across stem size classes would be valuable in identifying sustainble levels of harvest of the largest stems.

5.2.2 Perspectives on integrating data across diverse forest types and biomes

Previous research investigating spatial patterns in forest function, structure, and composition across Amazonia has typically focussed on lowland moist forests (e.g. Quesada et al., 2012; Johnson et al., 2016; Esquivel-Muelbert et al., 2019). In Chapter 2, in order to fully assess the relationship between demographic rates and forest structure in Amazonian forests, I extended my analysis beyond lowland Amazonian forests to include data from dry and montane forests. This proved extremely valuable, as incorporating data from a wider range of biomes enabled my analysis to capture the way that forest type, climate, and soil structure interact with demographic rates to shape stand structure. Including data from dry and montane forests not only highlighted the unique nature of structural controls in these forest types, but also helped to clarify the dynamics of lowland forests, by providing contrasting datasets against which their dynamics could be compared. Previous studies have highlighted mortality rates as the key control on forest biomass (e.g. Johnson et al., 2016; van der Sande et al., 2017). However, by broadening the range of biomes considered, my results showed that, in some forest types, forest structure is more sensitive to variation in growth rate than in mortality rate. This provides a more nuanced understanding of how the influence of growth and mortality rates on forest structure may vary across environmental gradients.

Similarly, in Chapter 3, I used data from across a large environmental gradient in Quebec, extending over four distinct bioclimatic domains. Across this latitudinal gradient, there is significant variation in forest structure and dynamics, which enabled me to carry out a robust validation of the simulation approach across

distinct forest types. Often models are built, calibrated, and validated using data which is limited in extent; for example many tropical models are developed using forest inventory data from a single, intensively sampled, site (Köhler and Huth, 1998; Chave, 1999; Farrior et al., 2016). While this can be useful in accurately parameterising a model for a specific context, it can make it challenging to validate application of the model beyond the original site. By developing my simulation using data from forests with distinct characteristics across a range of bioclimatic domains, I was able to confirm the robustness of the simulation approach across different forest ecosystems. Furthermore, this approach highlighted the close relationship between forest demographic dynamics and stand structure in sites across the gradient, supporting the application of the simulation approach to forest systems beyond Quebec.

While the focus of my thesis was on the forests of tropical South America, the analytical approaches I used extended beyond the tropics to make use of data from temperate and boreal forests in Quebec. By integrating data from the Quebec provincial forest inventory program into my analyses I was able to overcome the lack of tree ring data available in the RAINFOR dataset, and additionally ensure model robustness across multiple forest ecosystems. Application of the simulation model across multiple biomes has been informative in highlighting both similarities and differences in forest dynamics between biomes and forest types. For example, my results from Chapters 3 and 4 demonstrate that, despite the much higher diversity and complexity of tropical forests, stand structure can be simulated using the same input data used in simulating much simpler boreal stands. This highlights the key role of growth and mortality in shaping stand structure in forests globally.

However, I also note interesting differences between biomes, particularly in the simulation of stand-level mortality. In simulating forest stand structure in Quebec, I found that application of a growth-dependent mortality function was best able to reproduce stand dynamics, with strong evidence that mortality rates were highest in stems that had shown low growth rates in the previous year. In contrast, in the tropics, the best results were gained through use of a size-dependent mortality function. In tropical forests, I detected no strong stand-level growth-dependent mortality, and typically only weak patterns of stand-level size-dependent mortality, suggesting that in tropical forests high species diversity and the associated interspecific variation in mortality rates masks any strong stand-level trends. Modelling mortality at the stand-level may be sufficient to capture a large proportion of the variation in mortality in forests where species diversity is low or a small number of species are dominant, however in more diverse forests it could be informative to model mortality by functional group, or at a species- or genus- level where possible (Johnson et al., 2018; Rüger et al., 2020). In the case of my simulation approach, it would be possible to define functional groups based on species wood density, and to test whether modelling size- or growth-dependent mortality for individual functional groups improves model fit across different biomes. Because of the universality of the simulation approach, there is great potential to apply it in future cross-biome comparative analyses of forest dynamics and structural controls.

Finally, I suggest that this type of cross-biome approach can be valuable in addressing certain data limitations. Tree ring data was used to validate the simulation stand age estimates in Chapter 3, and indicated that simulated estimates of both the length of individual growth trajectories, and of the overall distribution of ages within the stand, are accurate for the Quebec dataset. In tropical

forests, lack of tree ring data means that there is limited data available on tree ages (e.g. Vieira et al., 2005), and so applying the simulation approach to these forests to generate estimates on tree and stand age could be of value. Beyond providing simple estimates of forest age, this could offer important insights into forest dynamics. For example, there is evidence that, following disturbance, the numbers of large trees take longer to recover than the numbers of smaller trees, suggesting that biomass recovery may be limited by the growth rate and establishment time of the largest trees (West et al., 2014; Vidal et al., 2016). As a result, recovery rates may be saturating, as observed in the simulation outputs in Chapter 4, making predictions of recovery times challenging to extrapolate from short-term data describing early recovery trajectories. Estimates of the growth trajectories and ages of the largest trees, generated from the simulation approach, would be useful in more accurately constraining predictions of forest recovery times, and helping to explain stand-level recovery dynamics.

5.2.3 Implications for future forest monitoring projects

My findings, particularly those presented in Chapter 4 of my thesis, will be of use in informing future forest monitoring approaches. The results from the simulated increases in mortality rates highlight the long timescales associated with forest responses to demographic rate change. Simulated response times to reach a new steady structure range between 118 and >350 years following the onset of increases in mortality rates, with longer response times associated with lower baseline demographic rates. There are long time-lags between the onset of increases in mortality rates and the effects of this on forest stand structure being fully realised: even in the fastest responding forests, it takes nearly 70 years af-

ter mortality rates stabilise for forest structure to equilibrate. Furthermore, for the slower-responding plot clusters, simulations suggest that it could take several years after the onset of increases in mortality rates for there to be a clear signal of declines in basal area or mean DBH. These results are corroborated by experience from long-term field studies; for example, Laurance et al. (2018) highlight that, following fragmentation, it took at least two decades for the full impacts on large tree abundance to become clear. Similarly, modelling of biomass changes within recent forest fragments suggest that it can take 50-100 years for a new biomass equilibrium to be reached follow disturbance (Pütz et al., 2011).

These findings highlight the importance of monitoring forests over sufficient time periods. Accurately capturing and characterising the chronic structural changes indicated in the simulation outputs will require plots to be monitored over many decades. This may be particularly important in fully capturing forest responses to more transient disturbances, such as periods of drought. Previous studies of forest responses to short-term perturbations, such as those associated with El Nino events, have often focussed on a monitoring period of approximately 2 years post-perturbation (e.g. Phillips et al., 2009; Bennett et al., 2021). However, if, as in the simulation outputs, structural responses are delayed or it takes time to detect them, short-term studies may fail to capture the full extent of forest responses, and underestimate the eventual impacts of disturbances. My results also suggest that understanding the intrinsic dynamics of the forest will be important in fully informing monitoring approaches. Changes may take longer to materialise in less dynamic forests, making a long-term view particularly crucial for fully capturing how these forests respond to change: finding no immediate evidence of directional change in these forests may simply be because they have not yet been monitored for sufficient periods. Extrapolation from short-term trends in these forests should

be done with great caution, as they are particularly unlikely to be representative of the long-term trajectory of the forests.

My thesis also highlights the value of forest monitoring approaches which integrate forest inventory data with tree ring data. Forest inventory data and tree ring data provide distinct, but complementary, information on tree growth dynamics: tree rings offer a longer term perspective on historical tree growth trajectories, while forest inventories provide data on a finer scale across a forest stand, and can generate data on current forest dynamics, including growth responses to disturbance or environmental change. This complementarity was valuable in validating the simulation approach in Chapter 3, in particular because use of the tree ring data enabled validation both of the individual growth trajectories, and of the stand-level outputs, including growth rates. This gave a useful insight into the accuracy of forest inventory data in capturing tree growth dynamics, as it showed that the annual growth estimates generated from forest censuses - even conducted at 10 year intervals - are consistent over long time periods with growth rates observed in the tree ring data. I suggest that there is potential to further integrate these data sources and extend this type of comparative approach. For example, there are sampling biases present in estimating demographic rates from tree ring and inventory data (e.g. Talbot et al., 2014; Duchesne et al., 2019); comparing estimates across two datasets from the same plot network could offer a new dimension to better understand these biases.

5.3.4 Implications for conservation and management of Amazonian forests

Amazonian forests face threats that extend well beyond the climate-driven demographic rate increases considered within this thesis, and include direct impacts from forest clearance, logging, fragmentation, and fire, which often have much more dramatic and rapid impacts on forests (Malhi et al., 2014). Conservation and management of Amazonian forests is therefore complex and challenging, as many interacting factors have to be considered.

The findings presented in my thesis have applications in informing conservation and management priorities across different Amazonian regions. My results indicate that the forests which are most vulnerable to increases in mortality rates are the less dynamic forests of the Guiana Shield and East-Central Amazon. These forests are strongly structured by variation in mortality rates (Chapter 2), and so show dramatic declines in basal area and the relative abundance of large stems in response to increases in mortality rates (Chapter 4). As these forests hold the highest biomass in the Amazon Basin, and support some of the largest tallest trees (Feldpausch et al., 2011), their high vulnerability has important implications for the carbon sink capacity of the Amazon as a whole; basal area declines in these regions are likely to lead to disproportionate absolute losses of biomass and carbon stocks (Chapter 4). As a result, protecting these forests from additional impacts should be a management priority. Although there is little that can be done on a local scale to reduce increases in mortality rates driven by global climate change, if forests can be buffered from more localised impacts, such as logging, fire, and fragmentation, mortality rate increases may be minimised, and forest resilience will be better maintained.

My results also suggest that the structural response of these forests to mortality rate increases may be slow compared to other forests across Amazonia (Chapter 4). Over short timescales, changes may be harder to detect compared with forests elsewhere in the Basin; however my results indicate that over longer timescales these forests are vulnerable to chronic declines in basal area (Chapter 4). Furthermore, these forests have intrinsically low growth rates, and so have long recovery times (Chapter 4), making them even more vulnerable to perturbations. This highlights the need for proactive approaches to forest conservation in these regions, as once impacts are detected forests may already be committed to much greater losses.

My findings also indicate that the more dynamic forests of the Western Amazon and Brazilian Shield have a high intrinsic potential for quick recovery times (Chapter 4). Because of their rapid, and potentially dramatic, structural responses to change, these forests may appear to have lost significant conservation and carbon storage value following disturbances, which may leave them vulnerable to further human impacts. Evidence from many countries worldwide shows that salvage logging or stand clearance is a common management practice in forests altered by natural disturbance, even where the ecosystem was previously protected (Lindenmayer and Laurance, 2017; Thorn et al., 2018). The simulation outputs presented in Chapter 4 predict short recovery times for these forests, suggesting that even highly disturbed forests in these regions may quickly recover biomass stocks. As a result, protection of these areas should still be prioritised.

5.2.5 Predicting the future of the tropical carbon sink

This thesis makes an important contribution to the literature surrounding our understanding of carbon sink dynamics in tropical forests. Our current understanding is that the carbon sink is declining as a result of increases in mortality rates (Brienen et al., 2015; Hubau et al., 2020). However, projections of future trajectories of the carbon sink are poorly constrained, with significant divergence among different model outputs (Padrón et al., 2022), and between model predictions and observed trends (Koch et al., 2021). The results presented in Chapter 4 suggest that declines in forest basal area are expected as a response to increases in mortality rates. This is expected to result in concurrent declines in forest biomass and a weakening of the carbon sink across Amazonian forests. Importantly, the simulated response of basal area and stand DBH to mortality increases show significant non-linearity, with the relationship between stand structural parameters and mortality rate approximately fitting an exponential decline function. This suggests that predictive approaches which apply linear extrapolations to observed trends (e.g. see Hubau et al., 2020), are unlikely to generate accurate estimates of future carbon sink dynamics.

Similarly, the results presented in Chapter 4 highlight the limitations of space-for-time approaches. Space-for-time substitutions are used to predict future ecological responses to climate change from current spatial patterns, and as such are offer a way to generate predictions where time-series data are unavailable (Lovell et al., 2023). While there is evidence that space-for-time approaches can be used to accurately infer future ecological change (Blois et al., 2013), my results illustrate the need for caution in drawing conclusions from these approaches. In Chapter 4, the results of the simulations show much greater declines in forest basal area for

a given increase in mortality rate than would be expected from observed spatial patterns. Here, extrapolation of spatial associations between mortality rates and stand structure would significantly underestimate structural change, particularly in the lowest mortality forests. This suggests that integration of observational data, experimental data or simulation and modelling outputs across both space and time could be highly beneficial (see Damgaard, 2019), in order to validate models spatially and temporally.

Previous projections of the carbon sink have aggregated trends at continental scales in order to extrapolate declines (e.g. Hubau et al., 2020). However, my results indicate that there is large spatial variation in the magnitude and speed of responses, which will be important to consider in projecting the future of the carbon sink. My results suggest that forests in the north-east of the Amazon basin are the most sensitive to increases in mortality rates, with these forests showing the greatest absolute declines in basal area for a given percentage increase in mortality rate. As these forests also have the highest biomass stocks in the basin (Johnson et al., 2016), declines in their capacity to hold biomass, and the associated losses of carbon stocks, could have a disproportionate effect on the carbon balance of Amazonian forests.

Furthermore, I find that forests in the Guiana Shield and East-Central Amazon are also slower to respond to increases in mortality rates. Although previous research has recognised that timelags between growth and mortality increases may be important in shaping the balance of the carbon sink (Brienen et al., 2020; Koch et al., 2021), studies have not yet incorporated spatial variation in temporal responses. This variation may be significant where extrapolations are made from current observations, as it suggests that declines in biomass may occur

non-linearly. The simulation results presented in Chapter 4 indicate that long-term declines would be detected more rapidly in areas of the southern and western Amazon; however, absolute declines in biomass are lower in these regions than elsewhere. These regions are unlikely to be representative of dynamics across the rest of Amazonia: if trends for the entire Amazon are projected from short-term changes in these regions, it could result in underestimates of carbon sink decline.

An additional factor to consider is the role of variation in growth rates. The potential impact of increasing growth rates in response to CO_2 fertilisation is poorly understood; while they may counteract the negative effects of mortality increases by increasing forest biomass accumulation (Terrer et al., 2019), the associated increases in overall stand turnover rates may prevent biomass accumulation and negate any carbon sink benefits (Brienen et al., 2020). In Chapter 2, I show that the relationship between stand growth rate and structural evenness varies according to forest type, with higher growth and mortality rates being associated with a more even stand structure and a higher proportion of large stems in dry forest, montane forest, and in the Brazilian Shield. In contrast, the opposite relationship is observed in the Guiana Shield and East-Central Amazon. This suggests that, while increases in stand turnover rates may have a negative effect on forest biomass in much of moist lowland Amazonia, there is the potential for a different response in dry forest, montane forests, and in the Brazilian Shield. Here, increases in growth rates may be more likely to drive increases in stand evenness, the frequency of large trees, and - by extension - stand biomass. The simulation approach I employed in Chapter 4 didn't incorporate any increases in growth rate, so I was unable to test for any variation in sensitivity to increases in growth rate within that analysis, however future work using this approach could be well placed to clarify spatial variation in increases in growth rates.

Finally, the results presented in this thesis highlight the importance of understanding the intrinsic resilience of forests as a key component of their responses to global change. To date, a lot of research has been focussed on understanding the impact of different environmental drivers on forest productivity and mortality; for example, quantifying the mortality impacts of drought (Phillips et al., 2010). While this is essential for accurately predicting forest responses, it is only part of the full picture. My findings show that forests may have very different intrinsic resilience to comparable mortality rate increases, such that similar drivers of mortality may have very different outcomes for biomass and forest carbon if forests have different underlying dynamics. As a result, accurate projections of changes in the carbon sink of tropical forests will rely both on accurate characterisation of drivers of change and their impacts on mortality rates, and on spatial data describing the intrinsic demographic dynamics of the forest system.

5.3 Final remarks

In this thesis, I have shown how demographic rates influence forest stand structure, using Amazonian forests as a case study. I showed that, across Amazonian forests, stand structure varies with growth and mortality rates, mediated by variation in climate, soils, and forest type. This suggests the potential for strong spatial variation in forest structural responses to projected increases in demographic rates. Using a simulation modelling approach, I showed that variation in mortality rates across Amazonia is associated with variation in the intrinsic resilience of forests, with significant implications for biomass stocks across the Amazon Basin. Future research needs to account for this variation in forest responses in order to better predict outcomes for the Amazonian carbon sink. The simulation approach has

great potential to be used in future research across biomes, and to be developed further to answer important questions about forest dynamics and responses to future environmental change.

References

Aleixo, I., Norris, D., Hemerik, L., Barbosa, A., Prata, E., Costa, F., and Poorter, L. (2019). Amazonian rainforest tree mortality driven by climate and functional traits.

Allen, C. D., Breshears, D. D., and McDowell, N. G. (2015). On underestimation of global vulnerability to tree mortality and forest die-off from hotter drought in the Anthropocene. *Ecosphere*, 6(8):1–55.

Álvarez-Dávila, E., Cayuela, L., González-Caro, S., Aldana, A. M., Stevenson, P. R., Phillips, O., Cogollo, Á., Peñuela, M. C., Von Hildebrand, P., Jiménez, E., Melo, O., Londoño-Vega, A. C., Mendoza, I., Velásquez, O., Fernández, F., Serna, M., Velázquez-Rua, C., Benítez, D., and Rey-Benayas, J. M. (2017). Forest biomass density across large climate gradients in northern South America is related to water availability but not with temperature. *PLoS ONE*, 12(3):1–16.

Alves, L. F., Vieira, S. A., Scaranello, M. A., Camargo, P. B., Santos, F. A., Joly, C. A., and Martinelli, L. A. (2010). Forest structure and live aboveground biomass variation along an elevational gradient of tropical Atlantic moist forest (Brazil). *Forest Ecology and Management*, 260(5):679–691.

Ameray, A., Cavard, X., and Bergeron, Y. (2023). Climate change may increase Quebec boreal forest productivity in high latitudes by shifting its current composition. *Frontiers in Forests and Global Change*, 6(February):1–19.

Anderson-Teixeira, K. J., Herrmann, V., Morgan, R. B., Bond-Lamberty, B., Cook-Patton, S. C., Ferson, A. E., Muller-Landau, H. C., and Wang, M. M. (2021). Carbon cycling in mature and regrowth forests globally.

Anderson-Teixeira, K. J., Mcgarvey, J. C., Muller-Landau, H. C., Park, J. Y., Gonzalez-Akre, E. B., Herrmann, V., Bennett, A. C., So, C. V., Bourg, N. A., Thompson, J. R., Mcmahon, S. M., and Mcshea, W. J. (2015). Size-related scaling of tree form and function in a mixed-age forest. *Functional Ecology*, 29(12):1587–1602.

Anderson-Teixeira, K. J., Wang, M. M., Mcgarvey, J. C., and Lebauer, D. S. (2016). Carbon dynamics of mature and regrowth tropical forests derived from a pantropical database (TropForC-db). *Global Change Biology*, 22(5):1690–1709.

Aragão, L. E., Poulter, B., Barlow, J. B., Anderson, L. O., Malhi, Y., Saatchi, S., Phillips, O. L., and Gloor, E. (2014). Environmental change and the carbon balance of Amazonian forests. *Biological Reviews*, 89(4):913–931.

Aragão, L. E. O., Malhi, Y., Roman-Cuesta, R. M., Saatchi, S., Anderson, L. O., and Shimabukuro, Y. E. (2007). Spatial patterns and fire response of recent Amazonian droughts. *Geophysical Research Letters*, 34(7):1–5.

Araujo, R. F., Chambers, J. Q., Celes, C. H. S., Muller-Landau, H. C., dos Santos, A. P. F., Emmert, F., Ribeiro, G. H., Gimenez, B. O., Lima, A. J., Campos, M. A., and Higuchi, N. (2020). Integrating high resolution drone imagery and forest inventory to distinguish canopy and understory trees and quantify their contributions to forest structure and dynamics. *PLoS ONE*, 15(12 December):1–16.

Asner, G. P., Anderson, C. B., Martin, R. E., Knapp, D. E., Tupayachi, R., Sinca, F., and Malhi, Y. (2014). Landscape-scale changes in forest structure and functional traits along an Andes-to-Amazon elevation gradient. *Biogeosciences*, 11(3):843–856.

Babst, F., Alexander, M. R., Szejner, P., Bouriaud, O., Klesse, S., Roden, J., Ciais, P., Poulter, B., Frank, D., Moore, D. J., and Trouet, V. (2014). A tree-ring perspective on the terrestrial carbon cycle. *Oecologia*, 176(2):307–322.

Bailey, R. L. and Dell, R. (1972). Quantifying Diameter Distributions with the Weibull Function. *Forest Sciences*, 19(2):97–104.

Baker, P. J. (2003). Tree age estimation for the tropics: A test from the southern Appalachians. *Ecological Applications*, 13(6):1718–1732.

Baker, T. R., Phillips, O. L., Malhi, Y., Almeida, S., Arroyo, L., Di Fiore, A., Erwin, T., Higuchi, N., Killeen, T. J., Laurance, S. G., Laurance, W. F., Lewis, S. L., Monteagudo, A., Neill, D. A., Núñez Vargas, P., Pitman, N. C., Silva, J. N. M., and Vásquez Martínez, R. (2004a). Increasing biomass in Amazonian forest plots. *Philosophical Transactions of the Royal Society B: Biological Sciences*, 359(1443):353–365.

Baker, T. R., Phillips, O. L., Malhi, Y., Almeidas, S., Arroyo, L., Di Fiore, A., Erwin, T. L., Killeen, T. J., Laurance, S. G., Laurance, W. F., Lewis, S. L., Lloyd, J., Monteagudo, A., Neill, D. A., Patino, S., Pitman, N. C. A., Silva, N., and Vasquez Martinez, R. (2004b). Variation in wood density determines spatial patterns in Amazonian forest biomass. *Global Change Biology*, 10:545–562.

Baker, T. R., Vela Díaz, D. M., Chama Moscoso, V., Navarro, G., Monteagudo, A., Pinto, R., Cangani, K., Fyllas, N. M., Lopez Gonzalez, G., Laurance, W. F., Lewis, S. L., Lloyd, J., ter Steege, H., Terborgh, J. W., and Phillips, O. L. (2016). Consistent, small effects of treefall disturbances on the composition and diversity of four Amazonian forests. *Journal of Ecology*, 104(2):497–506.

Baraloto, C., Rabaud, S., Molto, Q., Blanc, L., Fortunel, C., Hérault, B., Dávila, N., Mesones, I., Rios, M., Valderrama, E., and Fine, P. V. (2011). Disentangling stand and environmental correlates of aboveground biomass in Amazonian forests. *Global Change Biology*, 17(8):2677–2688.

Bastin, J. F., Barbier, N., Réjou-Méchain, M., Fayolle, A., Gourlet-Fleury, S., Maniatis, D., De Haulleville, T., Baya, F., Beeckman, H., Beina, D., Couteron, P., Chuyong, G., Dauby, G., Doucet, J. L., Droissart, V., Dufrêne, M., Ewango, C., Gillet, J. F., Gonmadje, C. H., Hart, T., Kavali, T., Kenfack, D., Libalah, M., Malhi, Y., Makana, J. R., Pélissier, R., Ploton, P., Serckx, A., Sonké, B., Stevart, T., Thomas, D. W., De Cannière, C., and Bogaert, J. (2015). Seeing Central African forests through their largest trees. *Scientific Reports*, 5:1–8.

Battipaglia, G., Zalloni, E., Castaldi, S., Marzaioli, F., and Valentini, R. (2015). Long Tree-Ring Chronologies Provide Evidence of Recent Tree Growth Decrease in a Central African Tropical Forest. pages 1–21.

Bechtold, W. A. and Patterson, P. L. (2005). The Enhanced Forest Inventory and Analysis Program — National Sampling Design and Estimation Procedures. *USDA General Technical Report*, SRS-80:85.

Becknell, J. M., Kissing Kucek, L., and Powers, J. S. (2012). Aboveground biomass in mature and secondary seasonally dry tropical forests: A literature review and global synthesis. *Forest Ecology and Management*, 276:88–95.

Bennett, A. C., Dargie, G. C., Cuni-Sanchez, A., Mukendi, J. T., Hubau, W., Mukinzi, J. M., Phillips, O. L., Malhi, Y., Sullivan, M. J., Cooper, D. L., Adu-Bredu, S., Affum-Baffoe, K., Amani, C. A., Banin, L. F., Beeckman, H., Begne, S. K., Bocko, Y. E., Boeckx, P., Bogaert, J., Brncic, T., Chezeaux, E., Clark, C. J., Daniels, A. K., de Haulleville, T., Kamdem, M. N. D., Doucet, J. L., Ondo, F. E., Ewango, C. E., Feldpausch, T. R., Foli, E. G., Gonmadje, C., Hall, J. S., Hardy, O. J., Harris, D. J., Ifo, S. A., Jeffery, K. J., Kearsley, E., Leal, M., Levesley, A., Makana, J. R., Lukasu, F. M., Medjibe, V. P., Mihindu, V., Moore, S., Begone, N. N., Pickavance, G. C., Poulsen, J. R., Reitsma, J., Sonké, B., Sunderland, T. C., Taedoumg, H., Talbot, J., Tuagben, D. S., Umunay, P. M., Verbeeck, H., Vleminckx, J., White, L. J., Woell, H., Woods, J. T., Zemagho, L., and Lewis, S. L. (2021). Resistance of African tropical forests to an extreme climate anomaly. *Proceedings of the National Academy of Sciences of the United States of America*, 118(21):1–12.

Bennett, A. C., Mcdowell, N. G., Allen, C. D., and Anderson-Teixeira, K. J. (2015). Larger trees suffer most during drought in forests worldwide. *Nature Plants*, 1(October):1–5.

Bergeron, Y. (2000). Species and stand dynamics in the mixed woods of Quebec's southern boreal forest. *Ecology*, 81(6):1500–1516.

Bin, Y., Ye, W., Muller-Landau, H. C., Wu, L., Lian, J., and Cao, H. (2012). Unimodal Tree Size Distributions Possibly Result from Relatively Strong Conservatism in Intermediate Size Classes. *PLoS ONE*, 7(12).

Bircher, N., Cailleret, M., and Bugmann, H. (2015). The agony of choice: Different empirical mortality models lead to sharply different future forest dynamics. *Ecological Applications*, 25(5):1303–1318.

Blois, J. L., Williams, J. W., Fitzpatrick, M. C., Jackson, S. T., and Ferrier, S. (2013). Space can substitute for time in predicting climate-change effects on biodiversity. *Proceedings of the National Academy of Sciences of the United States of America*, 110(23):9374–9379.

Botkin, D. B., Janak, J. F., and Wallis, J. R. (2010). Rationale, Limitations, and Assumptions of a Northeastern Forest Growth Simulator. *IBM Journal of Research and Development*, 16(2):101–116.

Boucher, Y., Arseneault, D., Sirois, L., and Blais, L. (2009). Logging pattern and landscape changes over the last century at the boreal and deciduous forest transition in Eastern Canada. *Landscape Ecology*, 24(2):171–184.

Brienen, R. J., Caldwell, L., Duchesne, L., Voelker, S., Barichivich, J., Baliva, M., Ceccantini, G., Di Filippo, A., Helama, S., Locosselli, G. M., Lopez, L., Piovesan, G., Schöngart, J., Villalba, R., and Gloor, E. (2020). Forest carbon sink neutralized by pervasive growth-lifespan trade-offs. *Nature Communications*, 11(1):1–10.

Brienen, R. J., Phillips, O. L., Feldpausch, T. R., Gloor, E., Baker, T. R., Lloyd, J., Lopez-Gonzalez, G., Monteagudo-Mendoza, A., Malhi, Y., Lewis, S. L., Vásquez Martinez, R., Alexiades, M., Álvarez Dávila, E., Alvarez-Loayza, P., Andrade, A., Aragaõ, L. E., Araujo-Murakami, A., Arets, E. J., Arroyo, L., Aymard C., G. A., Bánki, O. S., Baraloto, C., Barroso, J., Bonal, D., Boot, R. G., Camargo, J. L., Castilho, C. V., Chama, V., Chao, K. J., Chave, J., Comiskey, J. A., Cornejo Valverde, F., Da Costa, L., De Oliveira, E. A., Di Fiore, A., Erwin, T. L., Fauset, S., Forsthofer, M., Galbraith, D. R., Grahame, E. S., Groot, N., Hérault, B., Higuchi, N., Honorio Coronado, E. N., Keeling, H., Killeen, T. J., Laurance, W. F., Laurance, S., Licona, J., Magnussen, W. E., Marimon, B. S., Marimon-Junior, B. H., Mendoza, C., Neill, D. A., Nogueira, E. M., Núñez, P., Pallqui Camacho, N. C., Parada, A., Pardo-Molina, G., Peacock, J., Penã-Claros, M., Pickavance, G. C., Pitman, N. C., Poorter, L., Prieto, A., Quesada, C. A., Ramírez, F., Ramírez-Angulo, H., Restrepo, Z.,

Roopsind, A., Rudas, A., Salomaõ, R. P., Schwarz, M., Silva, N., Silva-Espejo, J. E., Silveira, M., Stropp, J., Talbot, J., Ter Steege, H., Teran-Aguilar, J., Terborgh, J., Thomas-Caesar, R., Toledo, M., Torello-Raventos, M., Umetsu, R. K., Van Der Heijden, G. M., Van Der Hout, P., Guimarães Vieira, I. C., Vieira, S. A., Vilanova, E., Vos, V. A., and Zagt, R. J. (2015). Long-term decline of the Amazon carbon sink. *Nature*, 519(7543):344–348.

Brienen, R. J. and Zuidema, P. A. (2006). Lifetime growth patterns and ages of Bolivian rain forest trees obtained by tree ring analysis. *Journal of Ecology*, 94(2):481–493.

Brienen, R. J., Zuidema, P. A., and During, H. J. (2006). Autocorrelated growth of tropical forest trees: Unraveling patterns and quantifying consequences. *Forest Ecology and Management*, 237(1-3):179–190.

Brienen, R. J., Zuidema, P. A., and Martínez-Ramos, M. (2010). Attaining the canopy in dry and moist tropical forests: Strong differences in tree growth trajectories reflect variation in growing conditions. *Oecologia*, 163(2):485–496.

Brienen, R. J. W., Schöngart, J., and Zuidema, P. A. (2016). Tree Rings in the Tropics: Insights into the Ecology and Climate Sensitivity of Tropical Trees BT - Tropical Tree Physiology: Adaptations and Responses in a Changing Environment. pages 439–461. Springer International Publishing, Cham.

Bugmann, H. (2001). A review of forest gap models. *Climatic Change*, 51:259–305.

Bugmann, H., Seidl, R., Hartig, F., Bohn, F., Brůna, J., Cailleret, M., François, L., Heinke, J., Henrot, A. J., Hickler, T., Hülsmann, L., Huth, A., Jacquemin, I., Kollas, C., Lasch-Born, P., Lexer, M. J., Merganič, J., Merganičová, K., Mette, T., Miranda, B. R., Nadal-Sala, D., Rammer, W., Rammig, A., Reineking, B., Roedig, E., Sabaté, S., Steinkamp, J., Suckow, F., Vacchiano, G., Wild, J., Xu, C., and Reyer, C. P. (2019). Tree mortality submodels drive simulated long-term forest dynamics: assessing 15 models from the stand to global scale. *Ecosphere*, 10(2).

Burkhart, H. E. (1971). Slash Pine Plantation Yield Estimates Based on Diameter Distribution: An Evaluation. *Forest Science*, 17(4):452–453.

Busing, R. T. (1991). A spatial model of forest dynamics. *Vegetatio*, 92(2):167–179.

Cailleret, M., Bircher, N., Hartig, F., Hülsmann, L., and Bugmann, H. (2020). Bayesian calibration of a growth-dependent tree mortality model to simulate the dynamics of European temperate forests. *Ecological Applications*, 30(1).

Cailleret, M., Jansen, S., Robert, E. M. R., Janda, P., Kane, J. M., Kharuk, V. I., Tognetti, R., and Jos, E. (2016). A synthesis of radial growth patterns preceding tree mortality. pages 1–16.

Caldwell, L. (2018). *Live fast, die young? A global analysis of the trade-off between tree growth rates and longevity*. PhD thesis, University of Leeds.

Camac, J. S., Condit, R., FitzJohn, R. G., McCalman, L., Steinberg, D., Westoby, M., Joseph Wright, S., and Falster, D. S. (2018). Partitioning mortality into growth-dependent and growth-independent hazards across 203 tropical tree species. *Proceedings of the National Academy of Sciences of the United States of America*, 115(49):12459–12464.

Caspersen, J. P., Vanderwel, M. C., Cole, W. G., and Purves, D. W. (2011). How stand productivity results from size- and competition-dependent growth and mortality. *PLoS ONE*, 6(12).

Chambers, J. Q., Negron-Juarez, R. I., Marra, D. M., Di Vittorio, A., Tews, J., Roberts, D., Ribeiro, G. H., Trumbore, S. E., and Higuchi, N. (2013). The steady-state mosaic of disturbance and succession across an old-growth central Amazon forest landscape. *Proceedings of the National Academy of Sciences of the United States of America*, 110(10):3949–3954.

Chave, J. (1999). Study of structural, successional and spatial patterns in tropical rain forests using TROLL, a spatially explicit forest model. *Ecological Modelling*, 124(2-3):233–254.

Chave, J., Andalo, C., Brown, S., Cairns, M. A., Chambers, J. Q., Eamus, D., Fölster, H., Fromard, F., Higuchi, N., Kira, T., Lescure, J. P., Nelson, B. W., Ogawa, H., Puig, H., Riéra, B., and Yamakura, T. (2005). Tree allometry and improved estimation of carbon stocks and balance in tropical forests. *Oecologia*, 145(1):87–99.

Chave, J., Condit, R., Muller-Landau, H. C., Thomas, S. C., Ashton, P. S., Bunyavejchewin, S., Co, L. L., Dattaraja, H. S., Davies, S. J., Esufali, S., Ewango, C. E., Feeley, K. J., Foster, R. B., Gunatilleke, N., Gunatilleke, S., Hall, P., Hart, T. B., Hernández, C., Hubbell, S. P., Itoh, A., Kiratiprayoon, S., LaFrankie, J. V., De Lao, S. L., Makana, J. R., Noor, M. N. S., Kassim, A. R., Samper, C., Sukumar, R., Suresh, H. S., Tan, S., Thompson, J., Tongco, M. D. C., Valencia, R., Vallejo, M., Villa, G., Yamakura, T., Zimmerman, J. K., and Losos, E. C. (2008). Assessing evidence for a pervasive alteration in tropical tree communities. *PLoS Biology*, 6(3):0455–0462.

Chave, J., Coomes, D., Jansen, S., Lewis, S. L., Swenson, N. G., and Zanne, A. E. (2009). Towards a worldwide wood economics spectrum. *Ecology Letters*, 12(4):351–366.

Chave, J., Piponiot, C., Maréchaux, I., de Foresta, H., Larpin, D., Fischer, F. J., Derroire, G., Vincent, G., and Hérault, B. (2020). Slow rate of secondary forest carbon accumulation in the Guianas compared with the rest of the Neotropics. *Ecological Applications*, 30(1):1–13.

Chave, J., Réjou-Méchain, M., Búrquez, A., Chidumayo, E., Colgan, M. S., Delitti, W. B., Duque, A., Eid, T., Fearnside, P. M., Goodman, R. C., Henry, M., Martínez-Yrízar, A., Mugasha, W. A., Muller-Landau, H. C., Mencuccini, M., Nelson, B. W., Ngomanda, A., Nogueira, E. M., Ortiz-Malavassi, E., Pélissier, R., Ploton, P., Ryan, C. M., Saldarriaga, J. G., and Vieilledent, G. (2014). Improved allometric models to estimate the aboveground biomass of tropical trees. *Global Change Biology*, 20(10):3177–3190.

Cole, L. E., Bhagwat, S. A., and Willis, K. J. (2014). Recovery and resilience of tropical forests after disturbance. *Nature Communications*, 5(May):1–7.

Cooke, B. J. and Lorenzetti, F. (2006). The dynamics of forest tent caterpillar outbreaks in Québec, Canada. *Forest Ecology and Management*, 226(1-3):110–121.

Coomes, D. A. and Allen, R. B. (2007). Mortality and Tree-Size Distributions in Natural Mixed-Age Forests. 95(1):27–40.

Coomes, D. A., Duncan, R. P., Allen, R. B., and Truscott, J. (2003). Disturbances prevent stem size-density distributions in natural forests from following scaling relationships. *Ecology Letters*, 6(11):980–989.

Cox, P. M., Pearson, D., Booth, B. B., Friedlingstein, P., Huntingford, C., Jones, C. D., and Luke, C. M. (2013). Sensitivity of tropical carbon to climate change constrained by carbon dioxide variability. *Nature*, 494(7437):341–344.

da Costa, A. C. L., Galbraith, D., Almeida, S., Portela, B. T. T., da Costa, M., de Athaydes Silva Junior, J., Braga, A. P., de Gonçalves, P. H., de Oliveira, A. A., Fisher, R., Phillips, O. L., Metcalfe, D. B., Levy, P., and Meir, P. (2010). Effect of 7 yr of experimental drought on vegetation dynamics and biomass storage of an eastern Amazonian rainforest. *New Phytologist*, 187(3):579–591.

Dalagnol, R., Wagner, F. H., Galvão, L. S., Streher, A. S., Phillips, O. L., Gloor, E., Pugh, T. A., Ometto, J. P., and Aragão, L. E. (2021). Large-scale variations in the dynamics of Amazon forest canopy gaps from airborne lidar data and opportunities for tree mortality estimates. *Scientific Reports*, 11(1):1–14.

Damgaard, C. (2019). A Critique of the Space-for-Time Substitution Practice in Community Ecology. *Trends in Ecology and Evolution*, 34(5):416–421.

de Avila, A. L., van der Sande, M. T., Dormann, C. F., Peña-Claros, M., Poorter, L., Mazzei, L., Ruschel, A. R., Silva, J. N., de Carvalho, J. O., and Bauhus, J. (2018). Disturbance intensity is a stronger driver of biomass recovery than remaining tree-community attributes in a managed Amazonian forest. *Journal of Applied Ecology*, 55(4):1647–1657.

de Castilho, C. V., Magnusson, W. E., de Araújo, R. N. O., Luizão, R. C., Luizão, F. J., Lima, A. P., and Higuchi, N. (2006). Variation in aboveground tree live biomass in a central Amazonian Forest: Effects of soil and topography. *Forest Ecology and Management*, 234(1-3):85–96.

de Paula, M. D., Costa, C. P. A., and Tabarelli, M. (2011). Carbon storage in a fragmented landscape of Atlantic forest: The role played by edge-affected habitats and emergent trees. *Tropical Conservation Science*, 4(3):349–358.

Dislich, C. and Huth, A. (2012). Modelling the impact of shallow landslides on forest structure in tropical montane forests. *Ecological Modelling*, 239:40–53.

Doughty, C. E., Metcalfe, D. B., Girardin, C. A., Amézquita, F. F., Cabrera, D. G., Huasco, W. H., Silva-Espejo, J. E., Araujo-Murakami, A., Da Costa, M. C., Rocha, W., Feldpausch, T. R., Mendoza, A. L., Da Costa, A. C., Meir, P., Phillips, O. L., and Malhi, Y. (2015). Drought impact on forest carbon dynamics and fluxes in Amazonia. *Nature*, 519(7541):78–82.

Duchesne, L., Houle, D., Ouimet, R., Caldwell, L., Gloor, M., and Brienen, R. (2019). Large apparent growth increases in boreal forests inferred from tree-rings are an artefact of sampling biases. *Scientific Reports*, 9(1):1–9.

Duchesne, L. and Ouimet, R. (2008). Population dynamics of tree species in southern Quebec, Canada: 1970-2005. *Forest Ecology and Management*, 255(7):3001–3012.

Duque, A., Peña, M. A., Cuesta, F., González-Caro, S., Kennedy, P., Phillips, O. L., Calderón-Loor, M., Blundo, C., Carilla, J., Cayola, L., Farfán-Ríos, W., Fuentes, A., Grau, R., Homeier, J., Loza-Rivera, M. I., Malhi, Y., Malizia, A., Malizia, L., Martínez-Villa, J. A., Myers, J. A., Osinaga-Acosta, O., Peralvo, M., Pinto, E., Saatchi, S., Silman, M., Tello, J. S., Terán-Valdez, A., and Feeley, K. J. (2021). Mature Andean forests as globally important carbon sinks and future carbon refuges. *Nature Communications*, 12(1):1–10.

Enquist, B. J., James H. Brown, and Geoffrey B. West (1998). Allometric scaling of plant energetics and population density. *Nature*, 395(September):163–165.

Enquist, B. J. and Niklas, K. J. (2001). Invariant scaling relations across tree-dominated communities. *Nature*, 410(6829):655–660.

Enquist, B. J., West, G. B., and Brown, J. H. (2009). Extensions and evaluations of a general quantitative theory of forest structure and dynamics. *Proceedings of the National Academy of Sciences of the United States of America*, 106(17):7046–7051.

Esquivel-Muelbert, A., Baker, T. R., Dexter, K. G., Lewis, S. L., Brienen, R. J., Feldpausch, T. R., Lloyd, J., Monteagudo-Mendoza, A., Arroyo, L., Álvarez-Dávila, E., Higuchi, N., Marimon, B. S., Marimon-Junior, B. H., Silveira, M., Vilanova, E., Gloor, E., Malhi, Y., Chave, J., Barlow, J., Bonal, D., Davila Cardozo, N., Erwin, T., Fauset, S., Hérault, B., Laurance, S., Poorter, L., Qie, L., Stahl, C., Sullivan, M. J., ter Steege, H., Vos, V. A., Zuidema, P. A., Almeida, E., Almeida de Oliveira, E., Andrade, A., Vieira, S. A., Aragão, L., Araujo-Murakami, A., Arets, E., Aymard C, G. A., Baraloto, C., Camargo, P. B., Barroso, J. G., Bongers, F., Boot, R., Camargo, J. L., Castro, W., Chama Moscoso, V., Comiskey, J., Cornejo Valverde, F., Lola da Costa, A. C., del Aguila Pasquel, J., Di Fiore, A., Fernanda Duque, L., Elias, F., Engel, J., Flores Llampazo, G., Galbraith, D., Herrera Fernández, R., Honorio Coronado, E., Hubau, W., Jimenez-Rojas, E., Lima, A. J. N., Umetsu, R. K., Laurance, W., Lopez-Gonzalez, G., Lovejoy, T., Aurelio Melo Cruz, O., Morandi, P. S., Neill, D., Núñez Vargas, P., Pallqui Camacho, N. C., Parada Gutierrez, A., Pardo, G., Peacock, J., Peña-Claros, M., Peñuela-Mora, M. C., Petronelli, P., Pickavance, G. C., Pitman, N., Prieto, A., Quesada, C., Ramírez-Angulo, H., Réjou-Méchain, M., Restrepo Correa, Z., Roopsind, A., Rudas, A., Salomão, R., Silva, N., Silva Espejo, J., Singh, J., Stropp, J., Terborgh, J., Thomas, R., Toledo, M., Torres-Lezama, A., Valenzuela Gamarra, L., van de Meer, P. J., van der Heijden, G., van der Hout, P., Vasquez Martinez, R., Vela, C., Vieira, I. C. G., and Phillips, O. L. (2019). Compositional response of Amazon forests to climate change. *Global Change Biology*, 25(1):39–56.

Esquivel-Muelbert, A., Phillips, O. L., Brienen, R. J., Fauset, S., Sullivan, M. J., Baker, T. R., Chao, K. J., Feldpausch, T. R., Gloor, E., Higuchi, N., Houwing-Duistermaat, J., Lloyd, J., Liu, H., Malhi, Y., Marimon, B., Marimon Junior, B. H., Monteagudo-Mendoza, A., Poorter, L., Silveira, M., Torre, E. V., Dávila, E. A., del Aguila Pasquel, J., Almeida, E., Loayza, P. A., Andrade, A., Aragão, L. E., Araujo-Murakami, A., Arets, E., Arroyo, L., Aymard C, G. A., Baisie, M., Baraloto, C., Camargo, P. B., Barroso, J., Blanc, L., Bonal, D., Bongers, F., Boot, R., Brown, F., Burban, B., Camargo, J. L., Castro, W., Moscoso, V. C., Chave, J., Comiskey, J., Valverde, F. C., da Costa, A. L., Cardozo, N. D., Di Fiore, A., Dourdain, A., Erwin, T., Llampazo, G. F., Vieira, I. C. G., Herrera, R., Honorio Coronado, E., Huamantupa-Chuquimaco, I., Jimenez-

Rojas, E., Killeen, T., Laurance, S., Laurance, W., Levesley, A., Lewis, S. L., Ladvocat, K. L. L. M., Lopez-Gonzalez, G., Lovejoy, T., Meir, P., Mendoza, C., Morandi, P., Neill, D., Nogueira Lima, A. J., Vargas, P. N., de Oliveira, E. A., Camacho, N. P., Pardo, G., Peacock, J., Peña-Claros, M., Peñuela-Mora, M. C., Pickavance, G., Pipoly, J., Pitman, N., Prieto, A., Pugh, T. A., Quesada, C., Ramirez-Angulo, H., de Almeida Reis, S. M., Rejou-Machain, M., Correa, Z. R., Bayona, L. R., Rudas, A., Salomão, R., Serrano, J., Espejo, J. S., Silva, N., Singh, J., Stahl, C., Stropp, J., Swamy, V., Talbot, J., ter Steege, H., Terborgh, J., Thomas, R., Toledo, M., Torres-Lezama, A., Gamarra, L. V., van der Heijden, G., van der Meer, P., van der Hout, P., Martinez, R. V., Vieira, S. A., Cayo, J. V., Vos, V., Zagt, R., Zuidema, P., and Galbraith, D. (2020). Tree mode of death and mortality risk factors across Amazon forests. *Nature Communications*, 11(1).

Farrior, C. E., Bohlman, S. A., Hubbell, S., and Pacala, S. W. (2016). Dominance of the suppressed: Power-law size structure in tropical forests. *Science*, 351(6269):155–157.

Fauset, S., Gloor, M., Fyllas, N. M., Phillips, O. L., Asner, G. P., Baker, T. R., Patrick Bentley, L., Brienen, R. J., Christoffersen, B. O., del Aguila-Pasquel, J., Doughty, C. E., Feldpausch, T. R., Galbraith, D. R., Goodman, R. C., Girardin, C. A., Honorio Coronado, E. N., Monteagudo, A., Salinas, N., Shenkin, A., Silva-Espejo, J. E., van der Heijden, G., Vasquez, R., Alvarez-Davila, E., Arroyo, L., Barroso, J. G., Brown, F., Castro, W., Cornejo Valverde, F., Davila Cardozo, N., Di Fiore, A., Erwin, T., Huamantupa-Chuquimaco, I., Núñez Vargas, P., Neill, D., Pallqui Camacho, N., Gutierrez, A. P., Peacock, J., Pitman, N., Prieto, A., Restrepo, Z., Rudas, A., Quesada, C. A., Silveira, M., Stropp, J., Terborgh, J., Vieira, S. A., and Malhi, Y. (2019). Individual-based modeling of amazon forests suggests that climate controls productivity while traits control demography. *Frontiers in Earth Science*, 7(April).

Fauset, S., Johnson, M. O., Gloor, M., Baker, T. R., Monteagudo M., A., Brienen, R. J., Feldpausch, T. R., Lopez-Gonzalez, G., Malhi, Y., Ter Steege, H., Pitman, N. C., Baraloto, C., Engel, J., Pétronelli, P., Andrade, A., Camargo, J. L. C., Laurance, S. G., Laurance, W. F., Chave, J., Allie, E., Vargas, P. N., Terborgh, J. W., Ruokolainen, K., Silveira, M., Aymard C., G. A., Arroyo, L., Bonal, D., Ramirez-Angulo, H., Araujo-Murakami, A., Neill, D., Hérault, B., Dourdain, A., Torres-Lezama, A., Marimon, B. S., Salomão, R. P., Comiskey, J. A., Réjou-Méchain, M., Toledo, M., Licona, J. C., Alarcón, A., Prieto, A., Rudas, A., Van Der Meer, P. J., Killeen, T. J., Marimon Junior, B. H., Poorter, L., Boot, R. G., Stergios, B., Torre, E. V., Costa, F. R., Levis, C., Schietti, J., Souza, P., Groot, N., Arets, E., Moscoso, V. C., Castro, W., Coronado, E. N., Peña-Claros, M., Stahl, C., Barroso, J., Talbot, J., Vieira, I. C. G., Van Der Heijden,

G., Thomas, R., Vos, V. A., Almeida, E. C., Davila, E. Á., Aragão, L. E., Erwin, T. L., Morandi, P. S., De Oliveira, E. A., Valadão, M. B., Zagt, R. J., Van Der Hout, P., Loayza, P. A., Pipoly, J. J., Wang, O., Alexiades, M., Cerón, C. E., Huamantupa-Chuquimaco, I., Di Fiore, A., Peacock, J., Camacho, N. C., Umetsu, R. K., De Camargo, P. B., Burnham, R. J., Herrera, R., Quesada, C. A., Stropp, J., Vieira, S. A., Steininger, M., Rodríguez, C. R., Restrepo, Z., Muelbert, A. E., Lewis, S. L., Pickavance, G. C., and Phillips, O. L. (2015). Hyperdominance in Amazonian forest carbon cycling. *Nature Communications*, 6:1–9.

Feeley, K. J., Joseph Wright, S., Nur Supardi, M. N., Kassim, A. R., and Davies, S. J. (2007). Decelerating growth in tropical forest trees. *Ecology Letters*, 10(6):461–469.

Feldpausch, T. R., Banin, L., Phillips, O. L., Baker, T. R., Lewis, S. L., Quesada, C. A., Affum-Baffoe, K., Arets, E. J., Berry, N. J., Bird, M., Brondizio, E. S., De Camargo, P., Chave, J., Djagbletey, G., Domingues, T. F., Drescher, M., Fearnside, P. M., França, M. B., Fyllas, N. M., Lopez-Gonzalez, G., Hladik, A., Higuchi, N., Hunter, M. O., Iida, Y., Salim, K. A., Kassim, A. R., Keller, M., Kemp, J., King, D. A., Lovett, J. C., Marimon, B. S., Marimon-Junior, B. H., Lenza, E., Marshall, A. R., Metcalfe, D. J., Mitchard, E. T., Moran, E. F., Nelson, B. W., Nilus, R., Nogueira, E. M., Palace, M., Patiño, S., Peh, K. S., Raventos, M. T., Reitsma, J. M., Saiz, G., Schrodt, F., Sonké, B., Taedoumg, H. E., Tan, S., White, L., Wöll, H., and Lloyd, J. (2011). Height-diameter allometry of tropical forest trees. *Biogeosciences*, 8(5):1081–1106.

Feldpausch, T. R., Lloyd, J., Lewis, S. L., Brienen, R. J., Gloor, M., Monteagudo Mendoza, A., Lopez-Gonzalez, G., Banin, L., Abu Salim, K., Affum-Baffoe, K., Alexiades, M., Almeida, S., Amaral, I., Andrade, A., Aragão, L. E., Araujo Murakami, A., Arets, E. J., Arroyo, L., Aymard C., G. A., Baker, T. R., Bánki, O. S., Berry, N. J., Cardozo, N., Chave, J., Comiskey, J. A., Alvarez, E., De Oliveira, A., Di Fiore, A., Djagbletey, G., Domingues, T. F., Erwin, T. L., Fearnside, P. M., França, M. B., Freitas, M. A., Higuchi, N., Honorio C., E., Iida, Y., Jiménez, E., Kassim, A. R., Killeen, T. J., Laurance, W. F., Lovett, J. C., Malhi, Y., Marimon, B. S., Marimon-Junior, B. H., Lenza, E., Marshall, A. R., Mendoza, C., Metcalfe, D. J., Mitchard, E. T., Neill, D. A., Nelson, B. W., Nilus, R., Nogueira, E. M., Parada, A., S.-H. Peh, K., Pena Cruz, A., Peñuela, M. C., Pitman, N. C., Prieto, A., Quesada, C. A., Ramírez, F., Ramírez-Angulo, H., Reitsma, J. M., Rudas, A., Saiz, G., Salomão, R. P., Schwarz, M., Silva, N., Silva-Espejo, J. E., Silveira, M., Sonké, B., Stropp, J., Taedoumg, H. E., Tan, S., Ter Steege, H., Terborgh, J., Torello-Raventos, M., Van Der Heijden, G. M., Vásquez, R., Vilanova, E., Vos, V. A., White, L.,

Willcock, S., Woell, H., and Phillips, O. L. (2012). Tree height integrated into pantropical forest biomass estimates. *Biogeosciences*, 9(8):3381–3403.

Feldpausch, T. R., Phillips, O. L., Brienen, R. J., Gloor, E., Lloyd, J., Lopez-Gonzalez, G., Monteagudo-Mendoza, A., Malhi, Y., Alarcón, A., Álvarez Dávila, E., Alvarez-Loayza, P., Andrade, A., Aragao, L. E., Arroyo, L., Aymard C., G. A., Baker, T. R., Baraloto, C., Barroso, J., Bonal, D., Castro, W., Chama, V., Chave, J., Domingues, T. F., Fauset, S., Groot, N., Honorio Coronado, E., Laurance, S., Laurance, W. F., Lewis, S. L., Licona, J. C., Marimon, B. S., Marimon-Junior, B. H., Mendoza Bautista, C., Neill, D. A., Oliveira, E. A., Oliveira dos Santos, C., Pallqui Camacho, N. C., Pardo-Molina, G., Prieto, A., Quesada, C. A., Ramírez, F., Ramírez-Angulo, H., Réjou-Méchain, M., Rudas, A., Saiz, G., Salomão, R. P., Silva-Espejo, J. E., Silveira, M., ter Steege, H., Stropp, J., Terborgh, J., Thomas-Caesar, R., van der Heijden, G. M., Vásquez Martinez, R., Vilanova, E., and Vos, V. A. (2016). Amazon forest response to repeated droughts. *Global Biogeochemical Cycles*, 30(7):964–982.

Fick, S. E. and Hijmans, R. J. (2017). WorldClim 2: new 1-km spatial resolution climate surfaces for global land areas. *International Journal of Climatology*, 37(12):4302–4315.

Fischer, F. J., Maréchaux, I., and Chave, J. (2019). Improving plant allometry by fusing forest models and remote sensing. *New Phytologist*, 223(3):1159–1165.

Fischer, R., Bohn, F., Dantas de Paula, M., Dislich, C., Groeneveld, J., Gutiérrez, A. G., Kazmierczak, M., Knapp, N., Lehmann, S., Paulick, S., Pütz, S., Rödig, E., Taubert, F., Köhler, P., and Huth, A. (2016). Lessons learned from applying a forest gap model to understand ecosystem and carbon dynamics of complex tropical forests. *Ecological Modelling*, 326:124–133.

ForestPlots.net, Blundo, C., Carilla, J., Grau, R., Malizia, A., Malizia, L., Osinaga-Acosta, O., Bird, M., Bradford, M., Catchpole, D., Ford, A., Graham, A., Hilbert, D., Kemp, J., Laurance, S., Laurance, W., Ishida, F. Y., Marshall, A., Waite, C., Woell, H., Bastin, J. F., Bauters, M., Beeckman, H., Boeckx, P., Bogaert, J., De Canniere, C., de Haulleville, T., Doucet, J. L., Hardy, O., Hubau, W., Kearsley, E., Verbeeck, H., Vleminckx, J., Brewer, S. W., Alarcón, A., Araujo-Murakami, A., Arets, E., Arroyo, L., Chavez, E., Fredericksen, T., Villaroel, R. G., Sibauty, G. G., Killeen, T., Licona, J. C., Lleigue, J., Mendoza, C., Murakami, S., Gutierrez, A. P., Pardo, G., Peña-Claros, M., Poorter, L., Toledo, M., Cayo, J. V., Viscarra, L. J., Vos, V., Ahumada, J., Almeida, E., Almeida, J., de Oliveira, E. A., da Cruz, W. A., de Oliveira, A. A., Carvalho, F. A., Obermuller, F. A., Andrade, A., Carvalho, F. A., Vieira, S. A., Aquino, A. C., Aragão, L., Araújo, A. C., Assis, M. A., Gomes, J. A. M. A., Baccaro,

F., de Camargo, P. B., Barni, P., Barroso, J., Bernacci, L. C., Bordin, K., de Medeiros, M. B., Broggio, I., Camargo, J. L., Cardoso, D., Carniello, M. A., Rochelle, A. L. C., Castilho, C., Castro, A. A. J. F., Castro, W., Ribeiro, S. C., Costa, F., de Oliveira, R. C., Coutinho, I., Cunha, J., da Costa, L., da Costa Ferreira, L., da Costa Silva, R., da Graça Zacarias Simbine, M., de Andrade Kamimura, V., de Lima, H. C., de Oliveira Melo, L., de Queiroz, L., de Sousa Lima, J. R., do Espírito Santo, M., Domingues, T., dos Santos Prestes, N. C., Carneiro, S. E. S., Elias, F., Eliseu, G., Emilio, T., Farrapo, C. L., Fernandes, L., Ferreira, G., Ferreira, J., Ferreira, L., Ferreira, S., Simon, M. F., Freitas, M. A., García, Q. S., Manzatto, A. G., Graça, P., Guilherme, F., Hase, E., Higuchi, N., Iguatemy, M., Barbosa, R. I., Jaramillo, M., Joly, C., Klipel, J., do Amaral, I. L., Levis, C., Lima, A. S., Dan, M. L., Lopes, A., Madeiros, H., Magnusson, W. E., dos Santos, R. M., Marimon, B., Junior, B. H. M., Grillo, R. M. M., Martinelli, L., Reis, S. M., Medeiros, S., Meira-Junior, M., Metzker, T., Morandi, P., do Nascimento, N. M., Moura, M., Müller, S. C., Nagy, L., Nascimento, H., Nascimento, M., Lima, A. N., de Araújo, R. O., Silva, J. O., Pansonato, M., Sabino, G. P., de Abreu, K. M. P., Rodrigues, P. J. F. P., Piedade, M., Rodrigues, D., Rodrigues Pinto, J. R., Quesada, C., Ramos, E., Ramos, R., Rodrigues, P., de Sousa, T. R., Salomão, R., Santana, F., Scaranello, M., Bergamin, R. S., Schietti, J., Schöngart, J., Schwartz, G., Silva, N., Silveira, M., Seixas, C. S., Simbine, M., Souza, A. C., Souza, P., Souza, R., Sposito, T., Junior, E. S., do Vale, J. D., Vieira, I. C. G., Villela, D., Vital, M., Xaud, H., Zanini, K., Zartman, C. E., Ideris, N. K. H., Metali, F. b. H., Salim, K. A., Saparudin, M. S., Serudin, R. M., Sukri, R. S., Begne, S., Chuyong, G., Djuikouo, M. N., Gonmadje, C., Simo-Droissart, M., Sonké, B., Taedoumg, H., Zemagho, L., Thomas, S., Baya, F., Saiz, G., Espejo, J. S., Chen, D., Hamilton, A., Li, Y., Luo, T., Niu, S., Xu, H., Zhou, Z., Álvarez-Dávila, E., Escobar, J. C. A., Arellano-Peña, H., Duarte, J. C., Calderón, J., Bravo, L. M. C., Cuadrado, B., Cuadros, H., Duque, A., Duque, L. F., Espinosa, S. M., Franke-Ante, R., García, H., Gómez, A., González-M., R., Idárraga-Piedrahíta, Á., Jimenez, E., Jurado, R., Oviedo, W. L., López-Camacho, R., Cruz, O. A. M., Polo, I. M., Paky, E., Pérez, K., Pijachi, A., Pizano, C., Prieto, A., Ramos, L., Correa, Z. R., Richardson, J., Rodríguez, E., Rodriguez M., G. M., Rudas, A., Stevenson, P., Chudomelová, M., Dancak, M., Hédl, R., Lhota, S., Svatek, M., Mukinzi, J., Ewango, C., Hart, T., Yakusu, E. K., Lisingo, J., Makana, J. R., Mbayu, F., Toirambe, B., Mukendi, J. T., Kvist, L., Nebel, G., Báez, S., Céron, C., Griffith, D. M., Andino, J. E. G., Neill, D., Palacios, W., Peñuela-Mora, M. C., Rivas-Torres, G., Villa, G., Demissie, S., Gole, T., Gonfa, T., Ruokolainen, K., Baisie, M., Bénédet, F., Betian, W., Bezard, V., Bonal, D., Chave, J., Droissart, V., Gourlet-Fleury, S., Hladik, A., Labrière, N., Naisso, P., Réjou-Méchain, M., Sist, P., Blanc, L., Burban, B.,

Derroire, G., Dourdain, A., Stahl, C., Bengone, N. N., Chezeaux, E., Ondo, F. E., Medjibe, V., Mihindou, V., White, L., Culmsee, H., Rangel, C. D., Horna, V., Wittmann, F., Adu-Bredu, S., Affum-Baffoe, K., Foli, E., Balinga, M., Roopsind, A., Singh, J., Thomas, R., Zagt, R., Murthy, I. K., Kartawinata, K., Mirmanto, E., Priyadi, H., Samsoedin, I., Sunderland, T., Yassir, I., Rovero, F., Vinceti, B., Hérault, B., Aiba, S. I., Kitayama, K., Daniels, A., Tuagben, D., Woods, J. T., Fitriadi, M., Karolus, A., Khoon, K. L., Majalap, N., Maycock, C., Nilus, R., Tan, S., Sitoe, A., Coronado G., I., Ojo, L., de Assis, R., Poulsen, A. D., Sheil, D., Pezo, K. A., Verde, H. B., Moscoso, V. C., Oroche, J. C. C., Valverde, F. C., Medina, M. C., Cardozo, N. D., de Rutte Corzo, J., del Aguila Pasquel, J., Llampazo, G. F., Freitas, L., Cabrera, D. G., Villacorta, R. G., Cabrera, K. G., Soria, D. G., Saboya, L. G., Rios, J. M. G., Pizango, G. H., Coronado, E. H., Huamantupa-Chuquimaco, I., Huasco, W. H., Aedo, Y. T. H., Peña, J. L. M., Mendoza, A. M., Rodriguez, V. M., Vargas, P. N., Ramos, S. C. P., Camacho, N. P., Cruz, A. P., Arevalo, F. R., Huaymacari, J. R., Rodriguez, C. R., Paredes, M. A. R., Bayona, L. R., del Pilar Rojas Gonzales, R., Peña, M. E. R., Revilla, N. S., Shareva, Y. C. S., Trujillo, R. T., Gamarra, L. V., Martinez, R. V., Arenas, J. V., Amani, C., Ifo, S. A., Bocko, Y., Boundja, P., Ekoungoulou, R., Hockemba, M., Nzala, D., Fofanah, A., Taylor, D., Bañares-de Dios, G., Cayuela, L., de la Cerda, Í. G., Macía, M., Stropp, J., Playfair, M., Wortel, V., Gardner, T., Muscarella, R., Rutishauser, E., Chao, K. J., Munishi, P., Bánki, O., Bongers, F., Boot, R., Fredriksson, G., Reitsma, J., ter Steege, H., van Andel, T., van de Meer, P., van der Hout, P., van Nieuwstadt, M., van Ulft, B., Veenendaal, E., Vernimmen, R., Zuidema, P., Zwerts, J., Akite, P., Bitariho, R., Chapman, C., Gerald, E., Leal, M., Mucunguzi, P., Abernethy, K., Alexiades, M., Baker, T. R., Banda, K., Banin, L., Barlow, J., Bennett, A., Berenguer, E., Berry, N., Bird, N. M., Blackburn, G. A., Brearley, F., Brienen, R., Burslem, D., Carvalho, L., Cho, P., Coelho, F., Collins, M., Coomes, D., Cuni-Sanchez, A., Dargie, G., Dexter, K., Disney, M., Draper, F., Duan, M., Esquivel-Muelbert, A., Ewers, R., Fadrique, B., Fauset, S., Feldpausch, T. R., França, F., Galbraith, D., Gilpin, M., Gloor, E., Grace, J., Hamer, K., Harris, D., Jeffery, K., Jucker, T., Kalamandeen, M., Klitgaard, B., Levesley, A., Lewis, S. L., Lindsell, J., Lopez-Gonzalez, G., Lovett, J., Malhi, Y., Marthews, T., McIntosh, E., Melgaço, K., Milliken, W., Mitchard, E., Moonlight, P., Moore, S., Morel, A., Peacock, J., Peh, K. S., Pendry, C., Pennington, R. T., de Oliveira Pereira, L., Peres, C., Phillips, O. L., Pickavance, G., Pugh, T., Qie, L., Riutta, T., Roucoux, K., Ryan, C., Sarkinen, T., Valeria, C. S., Spracklen, D., Stas, S., Sullivan, M., Swaine, M., Talbot, J., Taplin, J., van der Heijden, G., Vedovato, L., Willcock, S., Williams, M., Alves, L., Loayza, P. A., Arellano, G., Asa, C., Ashton, P., Asner, G., Brncic, T., Brown, F., Burnham, R., Clark, C., Comiskey, J., Damasco, G., Davies, S.,

Di Fiore, T., Erwin, T., Farfan-Rios, W., Hall, J., Kenfack, D., Lovejoy, T., Martin, R., Montiel, O. M., Pipoly, J., Pitman, N., Poulsen, J., Primack, R., Silman, M., Steininger, M., Swamy, V., Terborgh, J., Thomas, D., Umunay, P., Uriarte, M., Torre, E. V., Wang, O., Young, K., Aymard C., G. A., Hernández, L., Fernández, R. H., Ramírez-Angulo, H., Salcedo, P., Sanoja, E., Serrano, J., Torres-Lezama, A., Le, T. C., Le, T. T., and Tran, H. D. (2021). Taking the pulse of Earth's tropical forests using networks of highly distributed plots. *Biological Conservation*, 260(May).

Freund, C. A., Clark, K. E., Curran, J. F., Asner, G. P., and Silman, M. R. (2021). Landslide age, elevation and residual vegetation determine tropical montane forest canopy recovery and biomass accumulation after landslide disturbances in the Peruvian Andes. *Journal of Ecology*, (June):1–17.

Friend, A. D., Lucht, W., Rademacher, T. T., Keribin, R., Betts, R., Cadule, P., Ciais, P., Clark, D. B., Dankers, R., Falloon, P. D., Ito, A., Kahana, R., Kleidon, A., Lomas, M. R., Nishina, K., Ostberg, S., Pavlick, R., Peylin, P., Schaphoff, S., Vuichard, N., Warszawski, L., Wiltshire, A., and Woodward, F. I. (2014). Carbon residence time dominates uncertainty in terrestrial vegetation responses to future climate and atmospheric CO2. *Proceedings of the National Academy of Sciences of the United States of America*, 111(9):3280–3285.

Galbraith, D., Malhi, Y., Affum-Baffoe, K., Castanho, A. D., Doughty, C. E., Fisher, R. A., Lewis, S. L., Peh, K. S., Phillips, O. L., Quesada, C. A., Sonké, B., and Lloyd, J. (2013). Residence times of woody biomass in tropical forests.

Gloor, M., Gatti, L., Brienen, R., Feldpausch, T. R., Phillips, O. L., Miller, J., Ometto, J. P., Rocha, H., Baker, T., De Jong, B., Houghton, R. A., Malhi, Y., C. Aragão, L. E., Guyot, J. L., Zhao, K., Jackson, R., Peylin, P., Sitch, S., Poulter, B., Lomas, M., Zaehle, S., Huntingford, C., Levy, P., and Lloyd, J. (2012). The carbon balance of South America: A review of the status, decadal trends and main determinants. *Biogeosciences*, 9(12):5407–5430.

Gora, E. M. and Esquivel-Muelbert, A. (2021). Implications of size-dependent tree mortality for tropical forest carbon dynamics. *Nature Plants*, 7(4):384–391.

Gray, A., Brandeis, T., Shaw, J., McWilliams, W., and Miles, P. (2012). Forest Inventory and Analysis Database of the United States of America (FIA). *Biodiversity and Ecology*, 4:225–231.

Grondin, P., Brice, M.-H., Boulanger, Y., Morneau, C., Couillard, P.-L., Richard, P. J. H., Chalumeau, A., and Poirier, V. (2023). Ecological Classification in Forest Ecosystem Management: Links Between Current Practices and Future

Climate Change in a Québec Case Study BT - Boreal Forests in the Face of Climate Change: Sustainable Management. pages 219–246. Springer International Publishing, Cham.

Haddad, N. M., Brudvig, L. A., Clobert, J., Davies, K. F., Gonzalez, A., Holt, R. D., Lovejoy, T. E., Sexton, J. O., Austin, M. P., Collins, C. D., Cook, W. M., Damschen, E. I., Ewers, R. M., Foster, B. L., Jenkins, C. N., King, A. J., Laurance, W. F., Levey, D. J., Margules, C. R., Melbourne, B. A., Nicholls, A. O., Orrock, J. L., Song, D. X., and Townshend, J. R. (2015). Habitat fragmentation and its lasting impact on Earth's ecosystems. *Science Advances*, 1(2):1–10.

Hofhansl, F., Andersen, K. M., Fleischer, K., Fuchslueger, L., Rammig, A., Schaap, K. J., Valverde-Barrantes, O. J., and Lapola, D. M. (2016). Amazon forest ecosystem responses to elevated atmospheric Co2 and alterations in nutrient availability: Filling the gaps with model-experiment integration. *Frontiers in Earth Science*, 4(February):1–9.

Homeier, J., Breckle, S. W., Günter, S., Rollenbeck, R. T., and Leuschner, C. (2010). Tree diversity, forest structure and productivity along altitudinal and topographical gradients in a species-rich Ecuadorian montane rain forest. *Biotropica*, 42(2):140–148.

Homeier, J. and Leuschner, C. (2021). Factors controlling the productivity of tropical Andean forests: Climate and soil are more important than tree diversity. *Biogeosciences*, 18(4):1525–1541.

Hubau, W., Lewis, S. L., Phillips, O. L., Affum-Baffoe, K., Beeckman, H., Cuní-Sanchez, A., Daniels, A. K., Ewango, C. E., Fauset, S., Mukinzi, J. M., Sheil, D., Sonké, B., Sullivan, M. J., Sunderland, T. C., Taedoumg, H., Thomas, S. C., White, L. J., Abernethy, K. A., Adu-Bredu, S., Amani, C. A., Baker, T. R., Banin, L. F., Baya, F., Begne, S. K., Bennett, A. C., Benedet, F., Bitariho, R., Bocko, Y. E., Boeckx, P., Boundja, P., Brienen, R. J., Brncic, T., Chezeaux, E., Chuyong, G. B., Clark, C. J., Collins, M., Comiskey, J. A., Coomes, D. A., Dargie, G. C., de Haulleville, T., Kamdem, M. N. D., Doucet, J. L., Esquivel-Muelbert, A., Feldpausch, T. R., Fofanah, A., Foli, E. G., Gilpin, M., Gloor, E., Gonmadje, C., Gourlet-Fleury, S., Hall, J. S., Hamilton, A. C., Harris, D. J., Hart, T. B., Hockemba, M. B., Hladik, A., Ifo, S. A., Jeffery, K. J., Jucker, T., Yakusu, E. K., Kearsley, E., Kenfack, D., Koch, A., Leal, M. E., Levesley, A., Lindsell, J. A., Lisingo, J., Lopez-Gonzalez, G., Lovett, J. C., Makana, J. R., Malhi, Y., Marshall, A. R., Martin, J., Martin, E. H., Mbayu, F. M., Medjibe, V. P., Mihindou, V., Mitchard, E. T., Moore, S., Munishi, P. K., Bengone, N. N., Ojo, L., Ondo, F. E., Peh, K. S., Pickavance, G. C.,

Poulsen, A. D., Poulsen, J. R., Qie, L., Reitsma, J., Rovero, F., Swaine, M. D., Talbot, J., Taplin, J., Taylor, D. M., Thomas, D. W., Toirambe, B., Mukendi, J. T., Tuagben, D., Umunay, P. M., van der Heijden, G. M., Verbeeck, H., Vleminckx, J., Willcock, S., Wöll, H., Woods, J. T., and Zemagho, L. (2020). Asynchronous carbon sink saturation in African and Amazonian tropical forests. *Nature*, 579(7797):80–87.

Iida, Y., Kohyama, T. S., Swenson, N. G., Su, S. H., Chen, C. T., Chiang, J. M., and Sun, I. F. (2014a). Linking functional traits and demographic rates in a subtropical tree community: The importance of size dependency. *Journal of Ecology*, 102(3):641–650.

Iida, Y., Poorter, L., Sterck, F., Kassim, A. R., Potts, M. D., Kubo, T., and Kohyama, T. S. (2014b). Linking size-dependent growth and mortality with architectural traits across 145 co-occurring tropical tree species. *Ecology*, 95(2):353–363.

Iida, Y., Poorter, L., Sterck, F. J., Kassim, A. R., Kubo, T., Potts, M. D., and Kohyama, T. S. (2012). Wood density explains architectural differentiation across 145 co-occurring tropical tree species. *Functional Ecology*, 26(1):274–282.

Jiménez-Muñoz, J. C., Mattar, C., Barichivich, J., Santamaría-Artigas, A., Takahashi, K., Malhi, Y., Sobrino, J. A., and Schrier, G. V. D. (2016). Record-breaking warming and extreme drought in the Amazon rainforest during the course of El Niño 2015-2016.

Johnson, D. J., Needham, J., Xu, C., Massoud, E. C., Davies, S. J., Anderson-Teixeira, K. J., Bunyavejchewin, S., Chambers, J. Q., Chang-Yang, C. H., Chiang, J. M., Chuyong, G. B., Condit, R., Cordell, S., Fletcher, C., Giardina, C. P., Giambelluca, T. W., Gunatilleke, N., Gunatilleke, S., Hsieh, C. F., Hubbell, S., Inman-Narahari, F., Kassim, A. R., Katabuchi, M., Kenfack, D., Litton, C. M., Lum, S., Mohamad, M., Nasardin, M., Ong, P. S., Ostertag, R., Sack, L., Swenson, N. G., Sun, I. F., Tan, S., Thomas, D. W., Thompson, J., Umaña, M. N., Uriarte, M., Valencia, R., Yap, S., Zimmerman, J., McDowell, N. G., and McMahon, S. M. (2018). Climate sensitive size-dependent survival in tropical trees. *Nature Ecology and Evolution*, 2(9):1436–1442.

Johnson, M. O., Galbraith, D., Gloor, M., De Deurwaerder, H., Guimberteau, M., Rammig, A., Thonicke, K., Verbeeck, H., von Randow, C., Monteagudo, A., Phillips, O. L., Brienen, R. J., Feldpausch, T. R., Lopez Gonzalez, G., Fauset, S., Quesada, C. A., Christoffersen, B., Ciais, P., Sampaio, G., Kruijt, B., Meir, P., Moorcroft, P., Zhang, K., Alvarez-Davila, E., Alves de Oliveira, A., Amaral, I., Andrade, A., Aragao, L. E., Araujo-Murakami, A., Arets, E. J.,

Arroyo, L., Aymard, G. A., Baraloto, C., Barroso, J., Bonal, D., Boot, R., Camargo, J., Chave, J., Cogollo, A., Cornejo Valverde, F., Lola da Costa, A. C., Di Fiore, A., Ferreira, L., Higuchi, N., Honorio, E. N., Killeen, T. J., Laurance, S. G., Laurance, W. F., Licona, J., Lovejoy, T., Malhi, Y., Marimon, B., Marimon, B. H., Matos, D. C., Mendoza, C., Neill, D. A., Pardo, G., Peña-Claros, M., Pitman, N. C., Poorter, L., Prieto, A., Ramirez-Angulo, H., Roopsind, A., Rudas, A., Salomao, R. P., Silveira, M., Stropp, J., ter Steege, H., Terborgh, J., Thomas, R., Toledo, M., Torres-Lezama, A., van der Heijden, G. M., Vasquez, R., Guimarães Vieira, I. C., Vilanova, E., Vos, V. A., and Baker, T. R. (2016). Variation in stem mortality rates determines patterns of above-ground biomass in Amazonian forests: implications for dynamic global vegetation models. *Global Change Biology*, 22(12):3996–4013.

Kalamandeen, M., Gloor, E., Johnson, I., Agard, S., Katow, M., Vanbrooke, A., Ashley, D., Batterman, S. A., Ziv, G., Holder-Collins, K., Phillips, O. L., Brondizio, E. S., Vieira, I., and Galbraith, D. (2020). Limited biomass recovery from gold mining in Amazonian forests. *Journal of Applied Ecology*, 57(9):1730–1740.

Keeling, H. C. and Phillips, O. L. (2007). The global relationship between forest productivity and biomass. *Global Ecology and Biogeography*, 16(5):618–631.

Kobe, R. K. (1996). Intraspecific variation in sapling mortality and growth predicts geographic variation in forest composition. *Ecological Monographs*, 66(2):181–201.

Kobe, R. K., Pacala, S. W., Silander Jr, J. A., and Canham, C. D. (1995). Juvenile tree survivorship as a component of shade tolerance. *Ecological Applications*, 5(2):517–532.

Koch, A., Hubau, W., and Lewis, S. L. (2021). Earth System Models Are Not Capturing Present-Day Tropical Forest Carbon Dynamics. *Earth's Future*, 9(5):1–19.

Köhler, P. and Huth, A. (1998). The effects of tree species grouping in tropical rainforest modelling: Simulations with the individual-based model FORMIND. *Ecological Modelling*, 109(3):301–321.

Kohler, P. K. and Huth, A. (2004). Simulating growth dynamics in a south-east Asian rainforest threatened by recruitment shortage and tree harvesting. *Climatic Change*, 67:95–117.

Kohyama, T. (1993). Size-Structured Tree Populations in Gap-Dynamic Forest–The Forest Architecture Hypothesis for the Stable Coexistence of Species. *The Journal of Ecology*, 81(1):131.

Kohyama, T., Kubo, T., and Macklin, E. (2005). Effect of temporal autocorrelation on apparent growth rate variation in forest tree census data and an alternative distribution function of tree growth rate. *Ecological Research*, 20(1):11–15.

Kohyama, T., Suzuki, E., Partomihardjo, T., Yamada, T., and Kubo, T. (2003). Tree species differentiation in growth, recruitment and allometry in relation to maximum height in a Bornean mixed dipterocarp forest. *Journal of Ecology*, 91(5):797–806.

Kohyama, T. S. (1992). Size-Structured Multi-Species Model of Rain Forest Trees. *Functional Ecology*, 6(2):206–212.

Kohyama, T. S., Potts, M. D., Kohyama, T. I., Kassim, A. R., and Ashton, P. S. (2015). Demographic properties shape tree size distribution in a Malaysian rain forest. *American Naturalist*, 185(3):367–379.

Larson, A. J., Lutz, J. A., Donato, D. C., Freund, J. A., Swanson, M. E., HilleRisLambers, J., Sprugel, D. G., and Franklin, J. F. (2015). Spatial aspects of tree mortality strongly differ between young and old-growth forests. *Ecology*, 96(11):2855–2861.

Laurance, W. F., Camargo, J. L., Fearnside, P. M., Lovejoy, T. E., Williamson, G. B., Mesquita, R. C., Meyer, C. F., Bobrowiec, P. E., and Laurance, S. G. (2018). An Amazonian rainforest and its fragments as a laboratory of global change. *Biological Reviews*, 93(1):223–247.

Laurance, W. F., Camargo, J. L., Luizão, R. C., Laurance, S. G., Pimm, S. L., Bruna, E. M., Stouffer, P. C., Bruce Williamson, G., Benítez-Malvido, J., Vasconcelos, H. L., Van Houtan, K. S., Zartman, C. E., Boyle, S. A., Didham, R. K., Andrade, A., and Lovejoy, T. E. (2011). The fate of Amazonian forest fragments: A 32-year investigation. *Biological Conservation*, 144(1):56–67.

Laurance, W. F., Nascimento, H. E., Laurance, S. G., Andrade, A. C., Fearnside, P. M., Ribeiro, J. E., and Capretz, R. L. (2006). Rain forest fragmentation and the proliferation of successional trees. *Ecology*, 87(2):469–482.

Lebrija-Trejos, E., Pérez-García, E. A., Meave, J. A., Poorter, L., and Bongers, F. (2011). Environmental changes during secondary succession in a tropical dry forest in Mexico. *Journal of Tropical Ecology*, 27(5):477–489.

Lefcheck, J., Byrnes, J., and Grace, J. (2020). *piecewiseSEM: Piecewise Structural Equation Modeling*. R package version 2.1.2.

Lenth, R. V. (2021). *emmeans: Estimated Marginal Means, aka Least-Squares Means*. R package version 1.6.1.

Lewis, S. L., Lopez-Gonzalez, G., Sonké, B., Affum-Baffoe, K., Baker, T. R., Ojo, L. O., Phillips, O. L., Reitsma, J. M., White, L., Comiskey, J. A., Djuikouo K, M. N., Ewango, C. E., Feldpausch, T. R., Hamilton, A. C., Gloor, M., Hart, T., Hladik, A., Lloyd, J., Lovett, J. C., Makana, J. R., Malhi, Y., Mbago, F. M., Ndangalasi, H. J., Peacock, J., Peh, K. S., Sheil, D., Sunderland, T., Swaine, M. D., Taplin, J., Taylor, D., Thomas, S. C., Votere, R., and Wöll, H. (2009). Increasing carbon storage in intact African tropical forests. *Nature*, 457(7232):1003–1006.

Lewis, S. L., Phillips, O. L., Baker, T. R., Lloyd, J., Malhi, Y., Almeida, S., Higuchi, N., Laurance, W. F., Neill, D. A., Silva, J. N., Terborgh, J., Lezama, A. T., Martínez, R. V., Brown, S., Chave, J., Kuebler, C., Vargas, P. N., and Vinceti, B. (2004a). Concerted changes in tropical forest structure and dynamics: Evidence from 50 South American long-term plots. *Philosophical Transactions of the Royal Society B: Biological Sciences*, 359(1443):421–436.

Lewis, S. L., Phillips, O. L., Sheil, D., Vinceti, B., Baker, T. R., Brown, S., Graham, A. W., Higuchi, N., Hilbert, D. W., Laurance, W. F., Lejoly, J., Malhi, Y., Monteagudo, A., Vargas, P. N., Sonké, B., Nur Supardi, M. N., Terborgh, J. W., and Martínez, R. V. (2004b). Tropical forest tree mortality, recruitment and turnover rates: Calculation, interpretation and comparison when census intervals vary. *Journal of Ecology*, 92(6):929–944.

Lieberman, D., Lieberman, M., Hartshorn, G., and Peralta, R. (1985). Growth rates and age-size relationships of tropical wet forest trees in Costa Rica. *Journal of Tropical Ecology*, 1(2):97–109.

Lieberman, M. and Lieberman, D. (1985). Simulation of growth curves from periodic increment data. *Ecology*, 66(2):632–635.

Lima, R. A., Muller-Landau, H. C., Prado, P. I., and Condit, R. (2016). How do size distributions relate to concurrently measured demographic rates? Evidence from over 150 tree species in Panama. *Journal of Tropical Ecology*, 32(3):179–192.

Lindenmayer, D. B. and Laurance, W. F. (2017). The ecology, distribution, conservation and management of large old trees. *Biological Reviews*, 92(3):1434–1458.

Lopez-Gonzalez, G., Burkitt, M., Lewis, S., and Phillips, O. (2012). ForestPlots.net – managing permanent plot information across the tropics. *Biodiversity and Ecology*, 4(2007):95–103.

Lopez-Gonzalez, G., Lewis, S. L., Burkitt, M., Baker, T. R., and Phillips, O. L. (2009). ForestPlots.net Database.

Lopez-Gonzalez, G., Lewis, S. L., Burkitt, M., and Phillips, O. L. (2011). ForestPlots.net: A web application and research tool to manage and analyse tropical forest plot data. *Journal of Vegetation Science*, 22(4):610–613.

Lovell, R. S., Collins, S., Martin, S. H., Pigot, A. L., and Phillimore, A. B. (2023). Space-for-time substitutions in climate change ecology and evolution. *Biological Reviews*, 98(6):2243–2270.

Lutz, J. A., Furniss, T. J., Johnson, D. J., Davies, S. J., Allen, D., Alonso, A., Anderson-Teixeira, K. J., Andrade, A., Baltzer, J., Becker, K. M., Blomdahl, E. M., Bourg, N. A., Bunyavejchewin, S., Burslem, D. F., Cansler, C. A., Cao, K., Cao, M., Cárdenas, D., Chang, L. W., Chao, K. J., Chao, W. C., Chiang, J. M., Chu, C., Chuyong, G. B., Clay, K., Condit, R., Cordell, S., Dattaraja, H. S., Duque, A., Ewango, C. E., Fischer, G. A., Fletcher, C., Freund, J. A., Giardina, C., Germain, S. J., Gilbert, G. S., Hao, Z., Hart, T., Hau, B. C., He, F., Hector, A., Howe, R. W., Hsieh, C. F., Hu, Y. H., Hubbell, S. P., Inman-Narahari, F. M., Itoh, A., Janík, D., Kassim, A. R., Kenfack, D., Korte, L., Král, K., Larson, A. J., Li, Y. D., Lin, Y., Liu, S., Lum, S., Ma, K., Makana, J. R., Malhi, Y., McMahon, S. M., McShea, W. J., Memiaghe, H. R., Mi, X., Morecroft, M., Musili, P. M., Myers, J. A., Novotny, V., de Oliveira, A., Ong, P., Orwig, D. A., Ostertag, R., Parker, G. G., Patankar, R., Phillips, R. P., Reynolds, G., Sack, L., Song, G. Z. M., Su, S. H., Sukumar, R., Sun, I. F., Suresh, H. S., Swanson, M. E., Tan, S., Thomas, D. W., Thompson, J., Uriarte, M., Valencia, R., Vicentini, A., Vrška, T., Wang, X., Weiblen, G. D., Wolf, A., Wu, S. H., Xu, H., Yamakura, T., Yap, S., and Zimmerman, J. K. (2018). Global importance of large-diameter trees. *Global Ecology and Biogeography*, 27(7):849–864.

Malhi, Y., Doughty, C. E., Goldsmith, G. R., Metcalfe, D. B., Girardin, C. A., Marthews, T. R., del Aguila-Pasquel, J., Aragão, L. E., Araujo-Murakami, A., Brando, P., da Costa, A. C., Silva-Espejo, J. E., Farfán Amézquita, F., Galbraith, D. R., Quesada, C. A., Rocha, W., Salinas-Revilla, N., Silvério, D., Meir, P., and Phillips, O. L. (2015). The linkages between photosynthesis, productivity, growth and biomass in lowland Amazonian forests. *Global Change Biology*, 21(6):2283–2295.

Malhi, Y., Gardner, T. A., Goldsmith, G. R., Silman, M. R., and Zelazowski, P. (2014). Tropical forests in the anthropocene.

Malhi, Y., Girardin, C. A., Goldsmith, G. R., Doughty, C. E., Salinas, N., Metcalfe, D. B., Huaraca Huasco, W., Silva-Espejo, J. E., del Aguilla-Pasquell, J., Farfán Amézquita, F., Aragão, L. E., Guerrieri, R., Ishida, F. Y., Bahar, N. H., Farfan-Rios, W., Phillips, O. L., Meir, P., and Silman, M. (2017). The variation

of productivity and its allocation along a tropical elevation gradient: a whole carbon budget perspective. *New Phytologist*, 214(3):1019–1032.

Malhi, Y., Phillips, O. L., Lloyd, J., Baker, T., Wright, J., Almeida, S., Arroyo, L., Frederiksen, T., Grace, J., Higuchi, N., Killeen, T., Laurance, W. F., Leaño, C., Lewis, S., Meir, P., Monteagudo, A., Neill, D., Núñez Vargas, P., Panfil, S. N., Patiño, S., Pitman, N., Quesada, C. A., Rudas-Ll., A., Salomão, R., Saleska, S., Silva, N., Silveira, M., Sombroek, W. G., Valencia, R., Vásquez Martínez, R., Vieira, I. C., and Vinceti, B. (2002). An international network to monitor the structure, composition and dynamics of Amazonian forests (RAINFOR). *Journal of Vegetation Science*, 13(3):439–450.

Malhi, Y., Wood, D., Baker, T. R., Wright, J., Phillips, O. L., Cochrane, T., Meir, P., Chave, J., Almeida, S., Arroyo, L., Higuchi, N., Killeen, T. J., Laurance, S. G., Laurance, W. F., Lewis, S. L., Monteagudo, A., Neill, D. A., Vargas, P. N., Pitman, N. C., Quesada, C. A., Salomão, R., Silva, J. N. M., Lezama, A. T., Terborgh, J., Martínez, R. V., and Vinceti, B. (2006). The regional variation of aboveground live biomass in old-growth Amazonian forests. *Global Change Biology*, 12(7):1107–1138.

Maréchaux, I. and Chave, J. (2017). An individual-based forest model to jointly simulate carbon and tree diversity in Amazonia: description and applications. *Ecological Monographs*, 87(4):632–664.

Marimon, B. S., Marimon-Junior, B. H., Feldpausch, T. R., Oliveira-Santos, C., Mews, H. A., Lopez-Gonzalez, G., Lloyd, J., Franczak, D. D., de Oliveira, E. A., Maracahipes, L., Miguel, A., Lenza, E., and Phillips, O. L. (2014). Disequilibrium and hyperdynamic tree turnover at the forest-cerrado transition zone in southern Amazonia. *Plant Ecology and Diversity*, 7(1-2):281–292.

Meakem, V., Tepley, A. J., Gonzalez-Akre, E. B., Herrmann, V., Muller-Landau, H. C., Wright, S. J., Hubbell, S. P., Condit, R., and Anderson-Teixeira, K. J. (2018). Role of tree size in moist tropical forest carbon cycling and water deficit responses. *New Phytologist*, 219(3):947–958.

(MFFP), M. d. F. d. l. F. e. d. P. (2019). Bilan quinquennal de l'aménagement durable des forêts 2013-2018 - Superficies touchées par la récolte. Technical report.

Millar, C. I. and Stephenson, N. L. (2015). Temperate forest health in an era of emerging megadisturbance.

Ministère des Forêts, d. l. F. e. d. P. M. (2016). Norme d'inventaire écoforestier, placettes-échantillons permanentes, édition 2016. Technical report, Gouverne-

ment du Québec, Ministère des Forêts, de la Faune et des Parcs, Direction des inventaires forestiers.

Ministère des Ressources naturelles et des Forêts (MRNF) (2022). Placette-échantillon permanente [dataset].

Moonlight, P. W., Banda-R, K., Phillips, O. L., Dexter, K. G., Pennington, R. T., Baker, T. R., C. de Lima, H., Fajardo, L., González-M., R., Linares-Palomino, R., Lloyd, J., Nascimento, M., Prado, D., Quintana, C., Riina, R., Rodríguez M., G. M., Maria Villela, D., Aquino, A. C. M. M., Arroyo, L., Bezerra, C., Tadeu Brunello, A., Brienen, R. J. W., Cardoso, D., Chao, K., Cotta Coutinho, Í. A., Cunha, J., Domingues, T., Espírito Santo, M. M., Feldpausch, T. R., Ferreira Fernandes, M., Goodwin, Z. A., Jiménez, E. M., Levesley, A., Lopez-Toledo, L., Marimon, B., Miatto, R. C., Mizushima, M., Monteagudo, A., Soelma Beserra de Moura, M., Murakami, A., Neves, D., Nicora Chequín, R., César de Sousa Oliveira, T., Almeida de Oliveira, E., P. de Queiroz, L., Pilon, A., Marques Ramos, D., Reynel, C., Rodrigues, P. M. S., Santos, R., Särkinen, T., Fernando da Silva, V., Souza, R. M. S., Vasquez, R., and Veenendaal, E. (2020). Expanding tropical forest monitoring into Dry Forests: The DRYFLOR protocol for permanent plots. *PLANTS, PEOPLE, PLANET*, 3(3):295–300.

Moorcroft, P. R., Hurtt, G. C., and Pacala, S. W. (2001). A method for scaling vegetation dynamics: The ecosystem demography model (ED). *Ecological Monographs*, 71(4):557–586.

Moore, J. R., Argles, A. P., Zhu, K., Huntingford, C., and Cox, P. M. (2020). Validation of demographic equilibrium theory against tree-size distributions and biomass density in Amazonia. *Biogeosciences*, 17(4):1013–1032.

Morin, X., Fahse, L., Scherer-Lorenzen, M., and Bugmann, H. (2011). Tree species richness promotes productivity in temperate forests through strong complementarity between species. *Ecology Letters*, 14(12):1211–1219.

Moser, J. W. and Hall, O. F. (1969). Deriving Growth and Yield Functions for Uneven-Aged Forest Stands. *Forest Science*, 15(2):183–188.

Muller-Landau, H. C., Condit, R. S., Chave, J., Thomas, S. C., Bohlman, S. A., Bunyavejchewin, S., Davies, S., Foster, R., Gunatilleke, S., Gunatilleke, N., Harms, K. E., Hart, T., Hubbell, S. P., Itoh, A., Kassim, A. R., LaFrankie, J. V., Lee, H. S., Losos, E., Makana, J. R., Ohkubo, T., Sukumar, R., Sun, I. F., Nur Supardi, M. N., Tan, S., Thompson, J., Valencia, R., Muñoz, G. V., Wills, C., Yamakura, T., Chuyong, G., Dattaraja, H. S., Esufali, S., Hall, P., Hernandez, C., Kenfack, D., Kiratiprayoon, S., Suresh, H. S., Thomas, D.,

Vallejo, M. I., and Ashton, P. (2006a). Testing metabolic ecology theory for allometric scaling of tree size, growth and mortality in tropical forests. *Ecology Letters*, 9(5):575–588.

Muller-Landau, H. C., Condit, R. S., Harms, K. E., Marks, C. O., Thomas, S. C., Bunyavejchewin, S., Chuyong, G., Co, L., Davies, S., Foster, R., Gunatilleke, S., Gunatilleke, N., Hart, T., Hubbell, S. P., Itoh, A., Kassim, A. R., Kenfack, D., LaFrankie, J. V., Lagunzad, D., Lee, H. S., Losos, E., Makana, J. R., Ohkubo, T., Samper, C., Sukumar, R., Sun, I. F., Nur Supardi, M. N., Tan, S., Thomas, D., Thompson, J., Valencia, R., Vallejo, M. I., Muñoz, G. V., Yamakura, T., Zimmerman, J. K., Dattaraja, H. S., Esufali, S., Hall, P., He, F., Hernandez, C., Kiratiprayoon, S., Suresh, H. S., Wills, C., and Ashton, P. (2006b). Comparing tropical forest tree size distributions with the predictions of metabolic ecology and equilibrium models. *Ecology Letters*, 9(5):589–602.

Muller-Landau, H. C., Cushman, K. C., Arroyo, E. E., Martinez Cano, I., Anderson-Teixeira, K. J., and Backiel, B. (2021). Patterns and mechanisms of spatial variation in tropical forest productivity, woody residence time, and biomass.

Murphy, P. G. and Lugo, A. E. (1986). Ecology of tropical dry forest. *Annual review of ecology and systematics. Vol. 17*, pages 67–88.

Muscolo, A., Bagnato, S., Sidari, M., and Mercurio, R. (2014). A review of the roles of forest canopy gaps.

Nascimento, H. E. and Laurance, W. F. (2004). Biomass dynamics in amazonian forest fragments. *Ecological Applications*, 14(4 SUPPL.).

Nascimento, H. E., Laurance, W. F., Condit, R., Laurance, S. G., D'Angelo, S., and Andrade, A. C. (2005). Demographic and life-history correlates for Amazonian trees. *Journal of Vegetation Science*, 16(6):625.

Navarro, L., Morin, H., Bergeron, Y., and Girona, M. M. (2018). Changes in spatiotemporal patterns of 20th century spruce budworm outbreaks in eastern Canadian boreal forests. *Frontiers in Plant Science*, 9(December):1–15.

Nepstad, D. C., Tohver, I. M., David, R., Moutinho, P., and Cardinot, G. (2007). Mortality of large trees and lianas following experimental drought in an amazon forest. *Ecology*, 88(9):2259–2269.

Newnham, R. M. (1964). *The development of a stand model for Douglas fir*. PhD thesis, University of British Colombia.

Numata, S., Yasuda, M., Okuda, T., Kachi, N., and Nur Supardi, M. N. (2006). Canopy gap dynamics of two different forest stands in a Malaysian lowland rain forest. *Journal of Tropical Forest Science*, 18(2):109–116.

Oliver, T. H., Heard, M. S., Isaac, N. J., Roy, D. B., Procter, D., Eigenbrod, F., Freckleton, R., Hector, A., Orme, C. D. L., Petchey, O. L., Proença, V., Raffaelli, D., Suttle, K. B., Mace, G. M., Martín-López, B., Woodcock, B. A., and Bullock, J. M. (2015). Biodiversity and Resilience of Ecosystem Functions. *Trends in Ecology and Evolution*, 30(11):673–684.

Pacala, S. W., Canham, C. D., Saponara, J., Silander, J. A., Kobe, R. K., and Ribbens, E. (1996). Forest models defined by field measurements: estimation, error analysis and dynamics. *Ecological Monographs*, 66(1):1–43.

Pacala, S. W., Canham, C. D., and Silander, J. A. (1993). Forest models defined by field measurements: I. The design of a northeastern forest simulator. *Canadian Journal of Forest Research*, 23(10):1980–1988.

Padrón, R. S., Gudmundsson, L., Liu, L., Humphrey, V., and Seneviratne, S. I. (2022). Drivers of intermodel uncertainty in land carbon sink projections. *Biogeosciences*, 19(23):5435–5448.

Pan, Y., Birdsey, R. A., Fang, J., Houghton, R., Kauppi, P. E., Kurz, W. A., Phillips, O. L., Shvidenko, A., Lewis, S. L., Canadell, J. G., Ciais, P., Jackson, R. B., Pacala, S. W., McGuire, A. D., Piao, S., Rautiainen, A., Sitch, S., Hayes, D., Richard, A., Pekka, E., Werner, A., Oliver, L., Simon, L., Josep, G., Robert, B., Stephen, W., and David, A. (2011). A large and persistent carbon sink in the world's forests. *Science*, 333(August):988–993.

Pan, Y., Birdsey, R. A., Phillips, O. L., and Jackson, R. B. (2013). The Structure, Distribution, and Biomass of the World's Forests. *Annual Review of Ecology, Evolution, and Systematics*, 44(1):593–622.

Peng, C., Ma, Z., Lei, X., Zhu, Q., Chen, H., Wang, W., Liu, S., Li, W., Fang, X., and Zhou, X. (2011). A drought-induced pervasive increase in tree mortality across Canada's boreal forests. *Nature Climate Change*, 1(9):467–471.

Pennington, R. T., Lavin, M., and Oliveira-Filho, A. (2009). Woody plant diversity, evolution, and ecology in the tropics: Perspectives from seasonally dry tropical forests. *Annual Review of Ecology, Evolution, and Systematics*, 40:437–457.

Phillips, O. L., Aragão, L. E. O. C., Lewis, S. L., Fisher, J. B., Lloyd, J., López-gonzález, G., Malhi, Y., Monteagudo, A., Peacock, J., Quesada, C. A., Heijden, G. V. D., Almeida, S., Amaral, I., Arroyo, L., Aymard, G., Baker, T. R., Bánki,

O., Blanc, L., Bonal, D., Brando, P., Chave, J., Cristina, Á., Oliveira, A. D., Cardozo, N. D., Czimczik, C. I., Feldpausch, T. R., Freitas, M. A., Gloor, E., Higuchi, N., Jiménez, E., Lloyd, G., Meir, P., Mendoza, C., Morel, A., Neill, D. A., Nepstad, D., Patiño, S., Peñuela, M. C., Prieto, A., Ramírez, F., Schwarz, M., Silva, J., Silveira, M., Thomas, A. S., Steege, H., Stropp, J., Vásquez, R., Zelazowski, P., Dávila, E. A., Andelman, S., Andrade, A., Chao, K.-j., Erwin, T., Fiore, A. D., C, E. H., Keeling, H., Killeen, T. J., Laurance, W. F., Cruz, A. P., Pitman, N. C. A., Vargas, P. N., Ramírez-angulo, H., Rudas, A., and Salamão, R. (2009). Drought sensitivity of the Amazon Rainforest. *Science*, 323(March):1344–1347.

Phillips, O. L., Baker, T. R., Arroyo, L., Higuchi, N., Killeen, T. J., Laurance, W. F., Lewis, S. L., Lloyd, J., Malhi, Y., Monteagudo, A., Neill, D. A., Nüñez Vargas, P., Silva, J. N., Terborgh, J., Vásquez Martínez, R., Alexiades, M., Almeida, S., Brown, S., Chave, J., Comiskey, J. A., Czimczik, C. I., Di Fiore, A., Erwin, T., Kuebler, C., Laurance, S. G., Nascimento, H. E., Olivier, J., Palacios, W., Patiño, S., Pitman, N. C., Quesada, C. A., Saldias, M., Torres Lezama, A., and Vinceti, B. (2004). Pattern and process in Amazon tree turnover, 1976-2001. *Philosophical Transactions of the Royal Society B: Biological Sciences*, 359(1443):381–407.

Phillips, O. L., Baker, T. R., Chao, K., Jimenez, E., Lewis, S. L., Lloyd, J., Peacock, J., Lopez-Gonzalez, G., and Feldpausch, T. R. (2014). RAINFOR - Tree Field Work Database Codes.

Phillips, O. L., Baker, T. R., Feldpausch, T. R., and Brienen, R. J. (2021). RAINFOR Field Manual for Plot Establishment and Remeasurement. Technical report.

Phillips, O. L., Brienen, R. J., Gloor, E., Baker, T. R., Lloyd, J., Lopez-Gonzalez, G., Monteagudo-Mendoza, A., Malhi, Y., Lewis, S. L., Vásquez Martinez, R., Alexiades, M., Álvarez Dávila, E., Alvarez-Loayza, P., Andrade, A., Aragão, L. E., Araujo-Murakami, A., Arets, E. J., Arroyo, L., Aymard, G. A., Bánki, O. S., Baraloto, C., Barroso, J., Bonal, D., Boot, R. G., Camargo, J. L., Castilho, C. V., Chama, V., Chao, K. J., Chave, J., Comiskey, J. A., Valverde, F. C., da Costa, L., de Oliveira, E. A., Di Fiore, A., Erwin, T. L., Fauset, S., Forsthofer, M., Galbraith, D. R., Grahame, E. S., Groot, N., Hérault, B., Higuchi, N., Honorio Coronado, E. N., Keeling, H., Killeen, T. J., Laurance, W. F., Laurance, S., Licona, J., Magnusson, W. E., Marimon, B. S., Marimon-Junior, B. H., Mendoza, C., Neill, D. A., Nogueira, E. M., Núñez, P., Pallqui Camacho, N. C., Parada, A., Pardo-Molina, G., Peacock, J., Peña-Claros, M., Pickavance, G. C., Pitman, N. C., Poorter, L., Prieto, A., Quesada, C. A., Ramírez, F., Ramírez-Angulo, H., Restrepo, Z., Roopsind, A., Rudas, A., Sa-

lomão, R. P., Schwarz, M., Silva, N., Silva-Espejo, J. E., Silveira, M., Stropp, J., Talbot, J., ter Steege, H., Teran-Aguilar, J., Terborgh, J., Thomas-Caesar, R., Toledo, M., Torello-Raventos, M., Umetsu, K., van der Heijden, G. M., van der Hout, P., Guimarães Vieira, I. C., Vieira, S. A., Vilanova, E., Vos, V. A., Zagt, R. J., Alarcon, A., Amaral, I., Camargo, P. P., Brown, I. F., Blanc, L., Burban, B., Cardozo, N., Engel, J., de Freitas, M. A., de Oliveira, A., Fredericksen, T. S., Ferreira, L., Hinojosa, N. T., Jimenez, E., Lenza, E., Mendoza, C., Mendoza Polo, I., Peña Cruz, A., Peñuela, M. C., Petronelli, P., Singh, J., Maquirino, P., Serano, J., Sota, A., Oliveira dos Santos, C., Ybarnegaray, J., and Ricardo, J. (2017). Carbon uptake by mature Amazon forests has mitigated Amazon nations' carbon emissions. *Carbon Balance and Management*, 12(1):1–9.

Phillips, O. L., Heijden, G. V. D., Lewis, S. L., Lo, G., Lloyd, J., Malhi, Y., Monteagudo, A., Almeida, S., Da, E. A., Andelman, S., Andrade, A., Arroyo, L., Aymard, G., Baker, T. R., Costa, L., Feldpausch, T. R., Fisher, J. B., Fyllas, N. M., Freitas, M. A., Jime, E., Keeling, H., Tim, J., Gloor, E., Higuchi, N., Lovett, J. C., Meir, P., Mendoza, C., Morel, A., Nu, P., Prieto, A., Quesada, C. A., Peh, K. S.-h., Pen, A., Schwarz, M., and Silva, J. (2010). Drought–mortality relationships for tropical forests. *New Phytologist*, 187:631–646.

Phillips, O. L., Malhi, Y., Higuchi, N., Laurance, W. F., Núñez, P. V., Vásquez, R. M., Laurance, S. G., Ferreira, L. V., Stern, M., Brown, S., and Grace, J. (1998). Changes in the carbon balance of tropical forests: Evidence from long-term plots. *Science*, 282(5388):439–442.

Poorter, L., Bongers, F., Aide, T. M., Almeyda Zambrano, A. M., Balvanera, P., Becknell, J. M., Boukili, V., Brancalion, P. H., Broadbent, E. N., Chazdon, R. L., Craven, D., De Almeida-Cortez, J. S., Cabral, G. A., De Jong, B. H., Denslow, J. S., Dent, D. H., DeWalt, S. J., Dupuy, J. M., Durán, S. M., Espírito-Santo, M. M., Fandino, M. C., César, R. G., Hall, J. S., Hernandez-Stefanoni, J. L., Jakovac, C. C., Junqueira, A. B., Kennard, D., Letcher, S. G., Licona, J. C., Lohbeck, M., Marín-Spiotta, E., Martínez-Ramos, M., Massoca, P., Meave, J. A., Mesquita, R., Mora, F., Munõz, R., Muscarella, R., Nunes, Y. R., Ochoa-Gaona, S., De Oliveira, A. A., Orihuela-Belmonte, E., Peña-Claros, M., Pérez-Garciá, E. A., Piotto, D., Powers, J. S., Rodríguez-Velázquez, J., Romero-Pérez, I. E., Ruíz, J., Saldarriaga, J. G., Sanchez-Azofeifa, A., Schwartz, N. B., Steininger, M. K., Swenson, N. G., Toledo, M., Uriarte, M., Van Breugel, M., Van Der Wal, H., Veloso, M. D., Vester, H. F., Vicentini, A., Vieira, I. C., Bentos, T. V., Williamson, G. B., and Rozendaal, D. M. (2016). Biomass resilience of Neotropical secondary forests. *Nature*, 530(7589):211–214.

Poorter, L., van der Sande, M. T., Arets, E. J., Ascarrunz, N., Enquist, B.,

Finegan, B., Licona, J. C., Martínez-Ramos, M., Mazzei, L., Meave, J. A., Muñoz, R., Nytch, C. J., de Oliveira, A. A., Pérez-García, E. A., Prado-Junior, J., Rodríguez-Velázques, J., Ruschel, A. R., Salgado-Negret, B., Schiavini, I., Swenson, N. G., Tenorio, E. A., Thompson, J., Toledo, M., Uriarte, M., van der Hout, P., Zimmerman, J. K., and Peña-Claros, M. (2017). Biodiversity and climate determine the functioning of Neotropical forests. *Global Ecology and Biogeography*, 26(12):1423–1434.

Poorter, L., Wright, S. J., Paz, H., Ackerly, D. D., Condit, R., Ibarra-Manríquez, G., Harms, K. E., Licona, J. C., Martínez-Ramos, M., Mazer, S. J., Muller-Landau, H. C., Peña-Claros, M., Webb, C. O., and Wright, I. J. (2008). Are functional traits good predictors of demographic rates? Evidence from five neotropical forests. *Ecology*, 89(7):1908–1920.

Pütz, S., Groeneveld, J., Alves, L. F., Metzger, J. P., and Huth, A. (2011). Fragmentation drives tropical forest fragments to early successional states: A modelling study for Brazilian Atlantic forests. *Ecological Modelling*, 222(12):1986–1997.

Qie, L., Lewis, S. L., Sullivan, M. J., Lopez-Gonzalez, G., Pickavance, G. C., Sunderland, T., Ashton, P., Hubau, W., Abu Salim, K., Aiba, S. I., Banin, L. F., Berry, N., Brearley, F. Q., Burslem, D. F., Dančák, M., Davies, S. J., Fredriksson, G., Hamer, K. C., Hédl, R., Kho, L. K., Kitayama, K., Krisnawati, H., Lhota, S., Malhi, Y., Maycock, C., Metali, F., Mirmanto, E., Nagy, L., Nilus, R., Ong, R., Pendry, C. A., Poulsen, A. D., Primack, R. B., Rutishauser, E., Samsoedin, I., Saragih, B., Sist, P., Slik, J. W., Sukri, R. S., Svátek, M., Tan, S., Tjoa, A., Van Nieuwstadt, M., Vernimmen, R. R., Yassir, I., Kidd, P. S., Fitriadi, M., Ideris, N. K. H., Serudin, R. M., Abdullah Lim, L. S., Saparudin, M. S., and Phillips, O. L. (2017). Long-term carbon sink in Borneo's forests halted by drought and vulnerable to edge effects. *Nature Communications*, 8(1).

Quesada, C. A., Lloyd, J., Schwarz, M., Patiño, S., Baker, T. R., Czimczik, C., Fyllas, N. M., Martinelli, L., Nardoto, G. B., Schmerler, J., Santos, A. J., Hodnett, M. G., Herrera, R., Luizão, F. J., Arneth, A., Lloyd, G., Dezzeo, N., Hilke, I., Kuhlmann, I., Raessler, M., Brand, W. A., Geilmann, H., Filho, J. O., Carvalho, F. P., Filho, R. N., Chaves, J. E., Cruz, O. F., Pimentel, T. P., and Paiva, R. (2010). Variations in chemical and physical properties of Amazon forest soils in relation to their genesis. *Biogeosciences*, 7(5):1515–1541.

Quesada, C. A., Phillips, O. L., Schwarz, M., Czimczik, C. I., Baker, T. R., Patiño, S., Fyllas, N. M., Hodnett, M. G., Herrera, R., Almeida, S., Alvarez Dávila, E., Arneth, A., Arroyo, L., Chao, K. J., Dezzeo, N., Erwin, T., Di Fiore, A., Higuchi, N., Honorio Coronado, E., Jimenez, E. M., Killeen, T., Lezama, A. T.,

Lloyd, G., Löpez-González, G., Luizão, F. J., Malhi, Y., Monteagudo, A., Neill, D. A., Núñez Vargas, P., Paiva, R., Peacock, J., Peñuela, M. C., Peña Cruz, A., Pitman, N., Priante Filho, N., Prieto, A., Ramírez, H., Rudas, A., Salomão, R., Santos, A. J., Schmerler, J., Silva, N., Silveira, M., Vásquez, R., Vieira, I., Terborgh, J., and Lloyd, J. (2012). Basin-wide variations in Amazon forest structure and function are mediated by both soils and climate. *Biogeosciences*, 9(6):2203–2246.

R Core Team (2020). *R: A Language and Environment for Statistical Computing*. R Foundation for Statistical Computing, Vienna, Austria.

Reich, P. B. (2014). The world-wide ' fast – slow ' plant economics spectrum : a traits manifesto. pages 275–301.

Ripley, B. (2021). *MASS: Support Functions and Datasets for Venables and Ripley's MASS*. R package version 7.3-54.

Rödig, E., Cuntz, M., Heinke, J., Rammig, A., and Huth, A. (2017). Spatial heterogeneity of biomass and forest structure of the Amazon rain forest: Linking remote sensing, forest modelling and field inventory. *Global Ecology and Biogeography*, 26(11):1292–1302.

Rödig, E., Cuntz, M., Rammig, A., Fischer, R., Taubert, F., and Huth, A. (2018). The importance of forest structure for carbon fluxes of the Amazon rainforest. *Environmental Research Letters*, 13(5).

Rozendaal, D. M. and Chazdon, R. L. (2015). Demographic drivers of tree biomass change during secondary succession in northeastern Costa Rica. *Ecological Applications*, 25(2):506–516.

Rüger, N., Condit, R., Dent, D. H., DeWalt, S. J., Hubbell, S. P., Lichstein, J. W., Lopez, O. R., Wirth, C., and Farrior, C. E. (2020). Demographic trade-offs predict tropical forest dynamics. *Science*, 368(6487):165–168.

Rüger, N., Huth, A., Hubbell, S. P., and Condit, R. (2011). Determinants of mortality across a tropical lowland rainforest community. *Oikos*, 120(7):1047–1056.

Rüger, N., Williams-Linera, G., Kissling, W. D., and Huth, A. (2008). Long-term impacts of fuelwood extraction on a tropical montane cloud forest. *Ecosystems*, 11(6):868–881.

Rüger, N., Wirth, C., Wright, S. J., and Condit, R. (2012). Functional traits explain light and size response of growth rates in tropical tree species.

Rutishauser, E., Hérault, B., Baraloto, C., Blanc, L., Descroix, L., Sotta, E. D., Ferreira, J., Kanashiro, M., Mazzei, L., D'Oliveira, M. V., De Oliveira, L. C., Peña-Claros, M., Putz, F. E., Ruschel, A. R., Rodney, K., Roopsind, A., Shenkin, A., Da Silva, K. E., De Souza, C. R., Toledo, M., Vidal, E., West, T. A., Wortel, V., and Sist, P. (2015). Rapid tree carbon stock recovery in managed Amazonian forests.

Sato, H., Itoh, A., and Kohyama, T. (2007). SEIB-DGVM: A new Dynamic Global Vegetation Model using a spatially explicit individual-based approach. *Ecological Modelling*, 200(3-4):279–307.

Schramski, J. R., Dell, A. I., Grady, J. M., Sibly, R. M., and Brown, J. H. (2015). Metabolic theory predicts whole-ecosystem properties. *Proceedings of the National Academy of Sciences of the United States of America*, 112(8):2617–2622.

Segura, G., Balvanera, P., Durán, E., and Pérez, A. (2002). Tree community structure and stem mortality along a water availability gradient in a Mexican tropical dry forest. *Plant Ecology*, 169(2):259–271.

Shifley, S. R., He, H. S., Lischke, H., Wang, W. J., Jin, W., Gustafson, E. J., Thompson, J. R., Thompson, F. R., Dijak, W. D., and Yang, J. (2017). The past and future of modeling forest dynamics: from growth and yield curves to forest landscape models. *Landscape Ecology*, 32(7):1307–1325.

Shugart, H. H., Wang, B., Fischer, R., Ma, J., Fang, J., Yan, X., Huth, A., and Armstrong, A. H. (2018). Gap models and their individual-based relatives in the assessment of the consequences of global change. *Environmental Research Letters*, 13(3).

Silva, C. V., Aragão, L. E., Barlow, J., Espirito-Santo, F., Young, P. J., Anderson, L. O., Berenguer, E., Brasil, I., Brown, I. F., Castro, B., Farias, R., Ferreira, J., França, F., Graça, P. M., Kirsten, L., Lopes, A. P., Salimon, C., Scaranello, M. A., Seixas, M., Souza, F. C., and Xaud, H. A. (2018). Drought-induced Amazonian wildfires instigate a decadal-scale disruption of forest carbon dynamics. *Philosophical Transactions of the Royal Society B: Biological Sciences*, 373(1760).

Spracklen, D. V. and Righelato, R. (2014). Tropical montane forests are a larger than expected global carbon store. *Biogeosciences*, 11(10):2741–2754.

Stephenson, N. L., Van Mantgem, P. J., Bunn, A. G., Bruner, H., Harmon, M. E., O'Connell, K. B., Urban, D. L., and Franklin, J. F. (2011). Causes and implications of the correlation between forest productivity and tree mortality rates. *Ecological Monographs*, 81(4):527–555.

Sullivan, M. J. P., Lewis, S. L., Affum-baffoe, K., Castilho, C., Sanchez, A. C., Ewango, C. E. N., Hubau, W., Marimon, B., Monteagudo-mendoza, A., Qie, L., Martinez, R. V., Baker, T. R., Brienen, R. J. W., Feldpausch, T. R., Galbraith, D., Gloor, M., Malhi, Y., Aiba, S.-i., Alexiades, M. N., Almeida, E. C., Oliveira, E. A. D., Loayza, P. A., Andrade, A., Vieira, S. A., Araujo-murakami, A., Arets, E. J. M. M., Arroyo, L., Ashton, P., C, G. A., Banin, L. F., Baraloto, C., Barlow, J., Barroso, J., Batterman, S. A., Beeckman, H., Begne, S. K., Bennett, A. C., Berenguer, E., Berry, N., Blanc, L., Boeckx, P., Bogaert, J., Bonal, D., Bongers, F., Bradford, M., Brearley, F. Q., Brncic, T., Brown, F., Burban, B., Castro, W., Ribeiro, S. C., Moscoso, V. C., Chezeaux, E., Clark, C. J., Souza, F. C. D., Collins, M., Comiskey, J. A., Valverde, F. C., Medina, M. C., Danc, M., Dargie, G. C., Davies, S., Cardozo, N. D., Haulleville, T. D., Medeiros, M. B. D., Fiore, A. D., Doucet, J.-l., Droissart, V., Duque, L. F., Ekoungoulou, R., Elias, F., Erwin, T., Esquivel-muelbert, A., Fauset, S., Ferreira, J., Llampazo, G. F., Foli, E., Ford, A., Gilpin, M., Hall, J. S., Hamer, K. C., Hamilton, A. C., Harris, D. J., Hart, T. B., Herault, B., Herrera, R., Higuchi, N., Hladik, A., Huamantupa-chuquimaco, I., Huasco, W. H., Jeffery, K. J., Jimenez-rojas, E., Kalamandeen, M., Kearsley, E., Umetsu, R. K., Kho, L. K., Killeen, T., Kitayama, K., Klitgaard, B., Koch, A., Laurance, W., Laurance, S., Leal, M. E., Levesley, A., Lima, A. J. N., Lisingo, J., Lopes, A. P., Lopez-gonzalez, G., Lovejoy, T., Lovett, J. C., Lowe, R., Magnusson, W. E., Malumbres-olarte, J., Marshall, A. R., Marthews, T., Matias, S., Reis, D. A., Maycock, C., Mendoza, C., Metali, F., Mihindou, V., Milliken, W., Mitchard, E. T. A., Morandi, P. S., Mossman, H. L., Nagy, L., Nascimento, H., Neill, D., Nilus, R., Palacios, W., Camacho, N. P., Peacock, J., Pendry, C., Pickavance, G. C., Pipoly, J., Pitman, N., Playfair, M., Poorter, L., Poulsen, J. R., Poulsen, A. D., Preziosi, R., Prieto, A., Primack, R. B., Reitsma, J., Correa, Z. R., Sousa, T. R. D., Bayona, L. R., Roopsind, A., Rutishauser, E., Salim, K. A., Schietti, J., Sheil, D., Silva, R. C., Espejo, J. S., Valeria, C. S., Silveira, M., Simo-droissart, M., Simon, M. F., Singh, J., Carlos, Y., Shareva, S., Stahl, C., Stropp, J., Sukri, R., Sunderland, T., Swaine, M. D., Swamy, V., Taedoumg, H., Talbot, J., Taplin, J., Taylor, D., Steege, H., Terborgh, J., Thomas, R., Thomas, S. C., Torres-lezama, A., Umunay, P., Gamarra, L. V., Heijden, G. V. D., Hout, P. V. D., Meer, P. V. D., Nieuwstadt, M. V., Verbeeck, H., Vernimmen, R., Vicentini, A., Torre, E. V., Vleminckx, J., Vos, V., Wang, O., White, L. J. T., Willcock, S., Woods, J. T., Wortel, V., Young, K., Zagt, R., Zemagho, L., Zuidema, P. A., Zwerts, J. A., and Phillips, O. L. (2020). Long-term thermal sensitivity of Earth ' s tropical forests. 874(May):869–874.

Tabarelli, M., Lopes, A. V., and Peres, C. A. (2008). Edge-effects Drive Tropical Forest Fragments Towards an Early-Successional System. *Biotropica*, 40(6):657–661.

Talbot, J., Lewis, S. L., Lopez-Gonzalez, G., Brienen, R. J., Monteagudo, A., Baker, T. R., Feldpausch, T. R., Malhi, Y., Vanderwel, M., Araujo Murakami, A., Arroyo, L. P., Chao, K. J., Erwin, T., van der Heijden, G., Keeling, H., Killeen, T., Neill, D., Núñez Vargas, P., Parada Gutierrez, G. A., Pitman, N., Quesada, C. A., Silveira, M., Stropp, J., and Phillips, O. L. (2014). Methods to estimate aboveground wood productivity from long-term forest inventory plots. *Forest Ecology and Management*, 320:30–38.

Tavares, J. V., Oliveira, R. S., Mencuccini, M., Signori-Müller, C., Pereira, L., Diniz, F. C., Gilpin, M., Marca Zevallos, M. J., Salas Yupayccana, C. A., Acosta, M., Pérez Mullisaca, F. M., Barros, F. d. V., Bittencourt, P., Jancoski, H., Scalon, M. C., Marimon, B. S., Oliveras Menor, I., Marimon, B. H., Fancourt, M., Chambers-Ostler, A., Esquivel-Muelbert, A., Rowland, L., Meir, P., Lola da Costa, A. C., Nina, A., Sanchez, J. M., Tintaya, J. S., Chino, R. S., Baca, J., Fernandes, L., Cumapa, E. R., Santos, J. A. R., Teixeira, R., Tello, L., Ugarteche, M. T., Cuellar, G. A., Martinez, F., Araujo-Murakami, A., Almeida, E., da Cruz, W. J. A., del Aguila Pasquel, J., Aragão, L., Baker, T. R., de Camargo, P. B., Brienen, R., Castro, W., Ribeiro, S. C., Coelho de Souza, F., Cosio, E. G., Davila Cardozo, N., da Costa Silva, R., Disney, M., Espejo, J. S., Feldpausch, T. R., Ferreira, L., Giacomin, L., Higuchi, N., Hirota, M., Honorio, E., Huaraca Huasco, W., Lewis, S., Flores Llampazo, G., Malhi, Y., Monteagudo Mendoza, A., Morandi, P., Chama Moscoso, V., Muscarella, R., Penha, D., Rocha, M. C., Rodrigues, G., Ruschel, A. R., Salinas, N., Schlickmann, M., Silveira, M., Talbot, J., Vásquez, R., Vedovato, L., Vieira, S. A., Phillips, O. L., Gloor, E., and Galbraith, D. R. (2023). Basin-wide variation in tree hydraulic safety margins predicts the carbon balance of Amazon forests. *Nature*, 617(May).

Ter Steege, H., Pitman, N. C., Phillips, O. L., Chave, J., Sabatier, D., Duque, A., Molino, J. F., Prévost, M. F., Spichiger, R., Castellanos, H., Von Hildebrand, P., and Vásquez, R. (2006). Continental-scale patterns of canopy tree composition and function across Amazonia. *Nature*, 443(7110):444–447.

Terrer, C., Jackson, R. B., Prentice, I. C., Keenan, T. F., Kaiser, C., Vicca, S., Fisher, J. B., Reich, P. B., Stocker, B. D., Hungate, B. A., Peñuelas, J., McCallum, I., Soudzilovskaia, N. A., Cernusak, L. A., Talhelm, A. F., Van Sundert, K., Piao, S., Newton, P. C., Hovenden, M. J., Blumenthal, D. M., Liu, Y. Y., Müller, C., Winter, K., Field, C. B., Viechtbauer, W., Van Lissa, C. J., Hoosbeek, M. R., Watanabe, M., Koike, T., Leshyk, V. O., Polley, H. W., and Franklin, O. (2019). Nitrogen and phosphorus constrain the CO2 fertilization of global plant biomass.

Thomas, R. Q., Kellner, J. R., Clark, D. B., and Peart, D. R. (2013). Low mortality in tall tropical trees. *Ecology*, 94(4):920–929.

Thorn, S., Bässler, C., Brandl, R., Burton, P. J., Cahall, R., Campbell, J. L., Castro, J., Choi, C. Y., Cobb, T., Donato, D. C., Durska, E., Fontaine, J. B., Gauthier, S., Hebert, C., Hothorn, T., Hutto, R. L., Lee, E. J., Leverkus, A. B., Lindenmayer, D. B., Obrist, M. K., Rost, J., Seibold, S., Seidl, R., Thom, D., Waldron, K., Wermelinger, B., Winter, M. B., Zmihorski, M., and Müller, J. (2018). Impacts of salvage logging on biodiversity: A meta-analysis.

van Bellen, S., Garneau, M., and Bergeron, Y. (2010). Impact of climate change on forest fire severity and consequences for carbon stocks in boreal forest stands of Quebec, Canada: A synthesis. *Fire Ecology*, 6(3):16–44.

van der Sande, M. T., Peña-Claros, M., Ascarrunz, N., Arets, E. J., Licona, J. C., Toledo, M., and Poorter, L. (2017). Abiotic and biotic drivers of biomass change in a Neotropical forest. *Journal of Ecology*, 105(5):1223–1234.

Van Mantgem, P. J., Stephenson, N. L., Byrne, J. C., Daniels, L. D., Franklin, J. F., Fulé, P. Z., Harmon, M. E., Larson, A. J., Smith, J. M., Taylor, A. H., and Veblen, T. T. (2009). Widespread increase of tree mortality rates in the Western United States. *Science*, 323(5913):521–524.

Vanclay, J. K. (1989). A growth model for north Queensland rainforests. *Forest Ecology and Management*, 27(3-4):245–271.

Vidal, E., West, T. A., and Putz, F. E. (2016). Recovery of biomass and merchantable timber volumes twenty years after conventional and reduced-impact logging in Amazonian Brazil. *Forest Ecology and Management*, 376:1–8.

Vieira, S., Trumbore, S., Camargo, P. B., Selhorst, D., Chambers, J. Q., Higuchi, N., and Martinelli, L. A. (2005). Slow growth rates of Amazonian trees: Consequences for carbon cycling. *Proceedings of the National Academy of Sciences of the United States of America*, 102(51):18502–18507.

Vilanova, E., Ramírez-Angulo, H., Torres-Lezama, A., Aymard, G., Gámez, L., Durán, C., Hernández, L., Herrera, R., van der Heijden, G., Phillips, O. L., and Ettl, G. J. (2018). Environmental drivers of forest structure and stem turnover across Venezuelan tropical forests. *PLoS ONE*, 13(6):1–27.

West, T. A., Vidal, E., and Putz, F. E. (2014). Forest biomass recovery after conventional and reduced-impact logging in Amazonian Brazil. *Forest Ecology and Management*, 314(2014):59–63.

Wyckoff, P. H. and Clark, J. S. (2000). Predicting tree mortality from diameter growth: A comparison of maximum likelihood and Bayesian approaches. *Canadian Journal of Forest Research*, 30(1):156–167.

Xu, P., Zhou, T., Yi, C., Luo, H., Zhao, X., Fang, W., Gao, S., and Liu, X. (2018). Impacts of water stress on forest recovery and its interaction with canopy height. *International Journal of Environmental Research and Public Health*, 15(6).

Yamamoto, S.-i. (2000). Forest Gap Dynamics and Tree Regeneration. *Journal of Forest Research*, 5(4):223–229.

Yu, K., Smith, W. K., Trugman, A. T., Condit, R., Hubbell, S. P., Sardans, J., Peng, C., Zhu, K., Peñuelas, J., Cailleret, M., Levanic, T., Gessler, A., Schaub, M., Ferretti, M., and Anderegg, W. R. (2019). Pervasive decreases in living vegetation carbon turnover time across forest climate zones. *Proceedings of the National Academy of Sciences of the United States of America*, 116(49):24662–24667.

Zhao, M. and Running, S. W. (2010). Drought-Induced Reduction in Global Terrestrial Net Primary Production from 2000 Through 2009. *Science*, 329(5994):940–943.